



universität  
wien

# DISSERTATION

Titel der Dissertation

Influence of tylophorine and *Peucedanum ostruthium* on  
vascular smooth muscle cell proliferation

angestrebter akademischer Grad

Doktor der Naturwissenschaften (Dr. rer.nat.)

Verfasserin / Verfasser: Helge Joa

Dissertationsgebiet (lt. Studienblatt): Doktoratsstudium der Naturwissenschaften Molekulare Biologie

Betreuerin / Betreuer: Univ.-Prof. Dr. Verena M Dirsch

Wien, im Januar 2011



**Gewidmet, meinen Eltern**



## Abstract

Atherosclerosis is the primary cause of coronary artery disease, one of the major causes of death in the western world. Proliferation of vascular smooth muscle cells and subsequent alteration of the vessel wall is one of the major events in atherosclerosis and restenosis.

The aim of the study was to investigate a) tylophorine, a phenanthroindolizidine alkaloid, which was shown to inhibit tumor cell proliferation, with regard to its influence on cell proliferation, mitogenic signalling pathways and/or the cell cycle in primary rat aortic vascular smooth muscle cells (VSMC) and human umbilical vein smooth muscle cells (HUVSMC) and b) a plant extract of *Peucedanum ostruthium* on its anti-proliferative activity in VSMC and its active substance.

In this study we show that tylophorine inhibits PDGF-induced proliferation of VSMCs in the G0/G1-phase of the cell cycle. Tylophorine does not affect the major early PDGF-triggered signalling events. We found, however, a fast down regulation of cyclin D1 below control levels in response to tylophorine. This decrease in cyclin D1 levels is not due to a transcriptional inhibition of the cyclin D1 gene since mRNA levels of cyclin D1 are unaffected. Further analyses reveal that cyclin D1 is down-regulated by proteasomal degradation. Consistent results were obtained for HUVSMC treated with tylophorine. Therefore, tylophorine has a unique action of inhibiting proliferating smooth muscle cells by enhancing the degradation of cyclin D1.

Furthermore, the analysis of 7 major coumarin compounds, contained in the DCM-extract of *Peucedanum ostruthium*, revealed that ostruthin is the only active substance which inhibits the proliferation of VSMC. Thus, we identified the anti-proliferative principle of the *Peucedanum ostruthium* extract and uncovered a novel bioactivity for ostruthin.



## Zusammenfassung

Atherosklerose ist die Hauptursache für die Erkrankung der Herzkranzgefäße, eine der bedeutenden Todesursachen in der westlichen Welt. Die Proliferation von glatten Gefäßmuskelzellen und die damit verbundene Gefäßveränderung sind die wichtigsten Vorgänge bei Atherosklerose und Restenose.

Das Ziel der Studie war es a) Tylophorine, ein Phenanthroindolizidinalkaloid, das für seine Tumorzellproliferation hemmende Aktivität bekannt ist, im Hinblick auf seine Einflüsse auf die Zellproliferation, mitogene Signalwege und/oder dem Zellzyklus von primären Gefäßmuskelzellen der Ratte (VSMC), sowie glatten Gefäßmuskelzellen der menschlichen Nabelschnurvene (HUVSMC), zu untersuchen. Weiterhin sollte b) ein Pflanzenextrakt von *Peucedanum ostruthium* auf seine antiproliferative Wirkung an glatten Gefäßmuskelzellen (VSMC) analysiert, sowie die für seine Aktivität verantwortliche Substanz bestimmt werden.

In dieser Studie zeigen wir, dass Tylophorine die PDGF-induzierte Proliferation von VSMC in der G1-Phase des Zellzyklus hemmt. Dabei werden die wichtigsten, von PDGF-induzierten Signalwege durch Tylophorine nicht beeinflusst. Weiterhin fanden wir heraus, dass Tylophorine den Cyclin D1 - Gehalt der Zelle schnell herunterreguliert. Die Abnahme der Cyclin D1 Level wird nicht durch transkriptionelle Hemmung erreicht, da die mRNA-Level von Cyclin D1 unbeeinflusst bleiben. Weitere Analysen ergaben, dass die Herunterregulierung von Cyclin D1 durch proteasomalen Abbau bedingt ist. Damit übereinstimmende Ergebnisse konnten auch für Tylophorine behandelte HUVSMC erzielt werden. Daher besitzt Tylophorine einen einzigartigen Wirkungsmechanismus, um proliferierende glatte Gefäßmuskelzellen zu hemmen, der sich durch einen schnellen proteasomalen Abbau von Cyclin D1 auszeichnet.

Weiterhin ergab die Analyse der 7 wichtigsten, der Klasse der Coumarine zugehörigen Inhaltsstoffe des DCM-Extrakt von *Peucedanum ostruthium*, lediglich eine auf VSMC antiproliferativ wirksame Substanz – Ostruthin. Wir haben also das antiproliferative Prinzip des *Peucedanum ostruthium* Extrakts herausgefunden und eine neue Bioaktivität für Ostruthin gefunden.





## **1. CONTENTS**

|  |           |
|--|-----------|
| <b>1. CONTENTS .....</b>   | <b>9</b>  |
| <b>2. INTRODUCTION .....</b>   | <b>15</b> |
| <b>2.1. Atherosclerosis .....</b>  | <b>16</b> |
| 2.1.1. Pathology of atherosclerosis .....                                | 16        |
| 2.1.2. The role of VSMC in atherosclerosis .....                         | 17        |
| <b>2.2. Restenosis .....</b>   | <b>18</b> |
| 2.2.1. Pathology of restenosis .....                                     | 18        |
| 2.2.2. The role of VSMC in restenosis .....                              | 19        |
| 2.2.3. Surgical treatments of atherosclerotic stenosis .....             | 19        |
| 2.2.4. Stenting .....  | 20        |
| 2.2.5. Pharmacological inhibitors in drug eluting stents .....           | 20        |
| <b>2.3. VSMC migration .....</b>   | <b>22</b> |
| 2.3.1. Migratory stimuli for VSMC .....                                  | 23        |
| 2.3.2. Signaling cascades in VSMC migration .....                        | 23        |
| <b>2.4. VSMC proliferation .....</b>                                     | <b>24</b> |
| 2.4.1. VSM cell cycle regulation .....                                   | 24        |
| 2.4.2. Cell cycle phases .....   | 24        |
| 2.4.3. Cyclins, CDK and CKI .....  | 25        |
| 2.4.4. Important G1-phase regulators .....                               | 26        |
| 2.4.4.1. Cyclin D1 .....   | 26        |
| 2.4.4.2. p21 .....   | 27        |
| 2.4.5. Regulation of cyclin and CKI degradation .....                    | 28        |
| <b>2.5. PDGF signaling .....</b>   | <b>29</b> |
| 2.5.1. PDGF receptor activation .....                                    | 30        |
| 2.5.2. Early events in PDGFR signaling .....                             | 31        |
| 2.5.3. Signaling cascades downstream of the PDGF receptor .....          | 31        |
| 2.5.4. PDGF signaling in vascular disease .....                          | 33        |
| <b>2.6. Investigated natural products and medicinal plants .....</b>     | <b>33</b> |
| 2.6.1. <i>Tylophora indica</i> - source and traditional use .....        | 33        |
| 2.6.1.1. Chemical structure of tylophorine .....                         | 34        |
| 2.6.1.2. Tylophorine and cancer .....                                    | 35        |
| 2.6.1.3. Tylophorine analogues and their possible mechanism of action .. | 36        |

|  |           |
|--|-----------|
| 2.6.2. <i>Peucedanum ostruthium</i> .....                            | 36        |
| 2.6.2.1. Traditional use .....                                       | 36        |
| 2.6.2.2. Source .....  | 36        |
| <b>2.7. Aims of the study .....</b>                                  | <b>37</b> |
| <b>3. MATERIALS AND METHODS.....</b>                                 | <b>38</b> |
| <b>3.1. Materials.....</b>   | <b>39</b> |
| 3.1.1. Chemicals.....  | 39        |
| 3.1.2. Buffers and solutions.....                                    | 39        |
| 3.1.3. Cell culture media and reagents.....                          | 44        |
| 3.1.4. Technical equipment .....                                     | 46        |
| 3.1.5. Software .....  | 46        |
| <b>3.2. Methods.....</b>   | <b>47</b> |
| 3.2.1. Cell culture .....  | 47        |
| 3.2.1.1. Vascular Smooth Muscle Cell Isolation and Cultivation ..... | 47        |
| 3.2.1.1.1. Isolation.....  | 47        |
| 3.2.1.1.2. Cultivation of VSMC.....                                  | 48        |
| 3.2.1.1.3. Storage.....  | 48        |
| 3.2.1.1.4. Smooth muscle alpha-actin staining.....                   | 48        |
| 3.2.2. SDS gel electrophoresis and western blot analysis.....        | 49        |
| 3.2.2.1. Whole cell protein lysate .....                             | 49        |
| 3.2.2.2. Protein quantification.....                                 | 49        |
| 3.2.2.3. SDS-PAGE .....  | 50        |
| 3.2.2.4. Western blotting and detection .....                        | 50        |
| 3.2.3. Cell cycle analysis by flow cytometry .....                   | 51        |
| 3.2.3.1. Propidium iodide staining .....                             | 51        |
| 3.2.3.2. BrdU/7-AAD staining with flow cytometry.....                | 52        |
| 3.2.3.3. Annexin V-FITC staining .....                               | 53        |
| 3.2.3.4. Mitotracker green staining.....                             | 54        |
| 3.2.4. Proliferation assays .....                                    | 54        |
| 3.2.4.1. Crystal violet staining .....                               | 54        |
| 3.2.4.2. 5-Bromo-2-deoxyuridine (BrdU) assay.....                    | 55        |
| 3.2.4.3. Resazurin conversion assay.....                             | 55        |

|   |               |
|---|---------------|
| 3.2.5. RNA isolation and real-time qPCR analysis .....                    | 56            |
| 3.2.5.1. RNA isolation .....  | 56            |
| 3.2.5.2. Reverse transcription.....                                       | 57            |
| 3.2.5.3. Quantitative real-time PCR.....                                  | 57            |
| 3.2.6. Transfection of VSMC.....  | 57            |
| 3.2.6.1. Fugene HD .....  | 58            |
| 3.2.6.2. Amaxa® .....   | 58            |
| 3.2.6.3. Analysis of VSMC transfection.....                               | 59            |
| 3.2.7. Transfection of HEK cells.....                                     | 59            |
| 3.2.8. Wound healing assay .....  | 60            |
| 3.2.9. Saphenous vein model .....   | 60            |
| 3.2.10. Statistical analysis.....   | 61            |
| <br><b>4. RESULTS.....</b>  | <br><b>62</b> |
| <b>4.1. Characterization of Vascular Smooth Muscle Cells .....</b>        | <b>63</b>     |
| <b>4.2. Impact of tylophorine on VSMC proliferation .....</b>             | <b>63</b>     |
| 4.2.1. Inhibition of VSMC proliferation (crystal violet staining) .....   | 63            |
| 4.2.2. Inhibition of VSMC proliferation (DNA-synthesis).....              | 64            |
| 4.2.3. Accumulation of VSMC in G1-phase.....                              | 65            |
| 4.2.4. Tylophorine does not induce apoptosis .....                        | 66            |
| 4.2.5. Tylophorine is not an S-phase, but a true G0/G1-arrestor .....     | 67            |
| <b>4.3. Influence of tylophorine on signaling cascades .....</b>          | <b>69</b>     |
| 4.3.1. Early PDGF-BB-induced signaling events .....                       | 69            |
| 4.3.2. Role of NFκB in PDGF-BB signaling.....                             | 70            |
| 4.3.2.1. NFκB-Luciferase reporter gene assay.....                         | 71            |
| 4.3.2.2. Tylophorine has no influence on IκBα levels .....                | 73            |
| <b>4.4. Cyclin D1 is down-regulated by tylophorine.....</b>               | <b>74</b>     |
| <b>4.5. Influence of mitogens on cyclin D1 expression levels.....</b>     | <b>77</b>     |
| <b>4.6. Influence of tylophorine on cyclin A.....</b>                     | <b>76</b>     |
| <b>4.7 No influence of tylophorine on CDK4, but p21 expression levels</b> | <b>77</b>     |
| <b>4.8. No effect of tylophorine on total p53 expression levels .....</b> | <b>79</b>     |
| <b>4.9. Mechanism of cyclin D1 and p21 degradation .....</b>              | <b>79</b>     |
| 4.9.1. No effect of tylophorine on cyclin D1 and p21 mRNA levels.....     | 80            |

|  |            |
|--|------------|
| 4.9.2. Proteasome-dependent cyclin D1 degradation .....                                  | 81         |
| <b>4.10. Tylophorine has a comparable effect on HUVSMC .....</b>                         | <b>82</b>  |
| <b>4.11. Pepchip kinase array - p53 phosphorylation on serine 9.....</b>                 | <b>84</b>  |
| 4.11.1. Confirmation of kinase array results.....  | 85         |
| 4.11.1.1. Effect of tylophorine on p53 serine 9 .....                                    | 85         |
| 4.11.1.2. Effect on other p53 phosphorylation sites .....                                | 86         |
| <b>4.12. Tylophorine inhibits HUVSMC proliferation.....</b>                              | <b>86</b>  |
| <b>4.13. Tylophorine increases the mitochondrial mass .....</b>                          | <b>90</b>  |
| <b>4.14. Effect of tylophorine on “cycling” VSMC .....</b>                               | <b>90</b>  |
| <b>4.15. Migration of VSMC – Wound healing assay .....</b>                               | <b>91</b>  |
| <b>4.16. Inhibition of neointimal thickening.....</b>                                    | <b>92</b>  |
| <b>4.17. Plant extracts and natural compounds as anti-proliferative<br/>drugs .....</b>  | <b>93</b>  |
| 4.17.1. Screening of plant extracts.....   | 93         |
| 4.17.2. Impact of <i>Peucedanum ostruthium</i> on VSMC .....                             | 94         |
| 4.17.2.1. Inhibition of VSMC proliferation .....   | 94         |
| 4.17.2.2. The extract contains 7 major coumarins.....                                    | 95         |
| 4.17.2.3. Effect of the major compounds .....  | 98         |
| 4.17.2.4. Activity of structural related furano-/coumarins.....                          | 99         |
| 4.17.2.5. Ostruthin inhibits DNA-synthesis .....   | 100        |
| <b>5. DISCUSSION .....</b>   | <b>101</b> |
| 5.1. Anti-proliferative activity of tylophorine and its molecular<br>mode of action..... | 102        |
| 5.2. <i>Peucedanum ostruthium</i> and its major coumarins.....                           | 111        |
| <b>6. REFERENCES.....</b>  | <b>113</b> |
| <b>7. APPENDIX .....</b>   | <b>136</b> |
| 7.1. Abbreviations .....   | 137        |
| 7.2. Supplementary data.....   | 141        |
| 7.2.1. Pepsan results .....  | 141        |
| 7.2.2. Chemical structures of coumarins .....  | 143        |

|  |            |
|--|------------|
| <b>7.3. Publications.....</b>          | <b>146</b> |
| <b>7.4. Poster Presentations .....</b> | <b>146</b> |
| <b>7.5. Curriculum Vitae.....</b>      | <b>147</b> |
| <b>7.6. Acknowledgements .....</b>     | <b>148</b> |

## **2. INTRODUCTION**

## 2. INTRODUCTION

### 2.1. Atherosclerosis

#### 2.1.1. Pathology of atherosclerosis

Cardiovascular disease (CVD) is the leading mortal disease worldwide in the developed societies (Murray CJ et al., 1997). The combination of an unhealthy life-style, genetic susceptibility and increased lifespan is the common bases for atherosclerosis (Lusis AJ et al., 2000).

Under normal physiological conditions the endothelium is a selective permeable barrier between blood and tissues. The important physical force acting on endothelial cells (EC) is fluid shear stress, which is able to change EC morphology. In the tubular regions of arteries, where the blood flow is laminar, EC are ellipsoid in shape and aligned in the direction of blood flow. In areas where flow is disturbed and oscillatory, for example in arterial branching or curvature, EC have polygonal shapes and no particular orientation. These regions have an increased permeability to macromolecules such as low-density lipoproteins (LDL) as well as platelets and blood monocytes and are preferential sites for lesion formation (Gimbrone MA et al., 1999).

Accumulation of LDL in the sub-endothelial matrix is the initiating event in atherosclerosis development followed by modification of LDL via oxidation to produce oxLDL. Only this oxidized LDL is rapidly taken up by macrophages to generate so called foam cells - cholesterol-filled macrophages, which are found in early lesions of atherosclerosis (Glass CK and Witztum JL, 2001).

Activated leukocytes produce a plethora of inflammatory mediators which promote vascular smooth muscle cells (VSMC) proliferation and migration (Ross R et al., 1999; Rivard A and Andre's V et al., 2000; Dzau et al. 2002). Upon enrichment of lipid-rich necrotic debris and migration of VSMC from the medial layer of the artery, the lesion is advancing to "fatty streaks" (Navab et al., 1996; Steinberg and Witztum, 1999). Further, accumulation of VSMC and VSMC-derived extracellular matrix consisting of a growing mass of extracellular lipid, mostly cholesterol and its ester, generates a fibrous plaque.



Rupture or erosion of the lesion leads to thrombus formation resulting in myocardial infarction or stroke. Figure 1 depicts the initiation and progression of atherosclerosis.

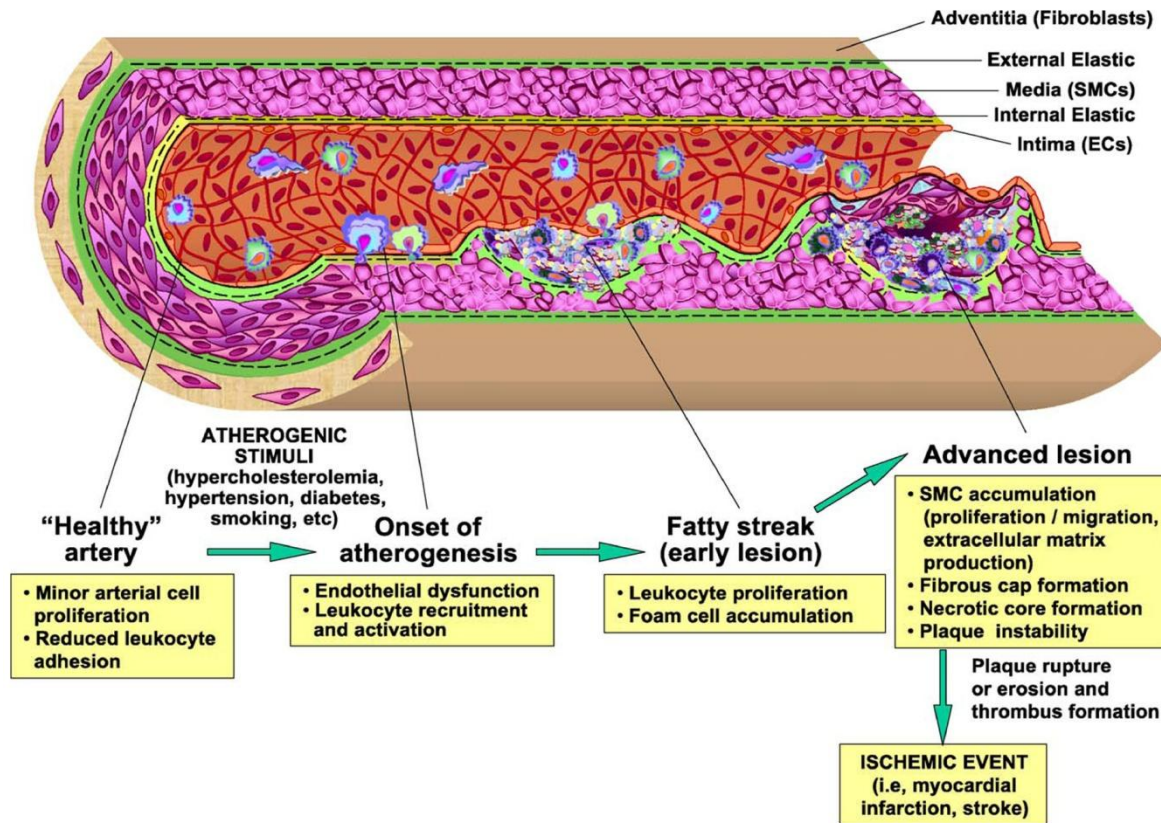


**Figure 1.** Initiation and progression of atherosclerosis. The cartoon illustrates different stages of atheroma progression. At the onset of atherogenesis is the endothelial dysfunction, followed by the formation of a fatty streak, which can further lead to the advanced lesion; Here, the proliferation/migration of smooth muscle cells play the most important role. This lesion is vulnerable to rupture and can narrow the vessel. Figure from Andrés V (2004).

### 2.1.2. The role of VSMC in atherosclerosis

In the vasculature, VSMC can be found in two different shapes – the “contractile” and the “synthetic”. Intimal SMCs differ significantly from medial SMCs and have unique atherogenic properties essential for the initiation of plaques (Mosse PR et al., 1985). Human medial SMCs express proteins involved in the contractile function of the cell, whereas those SMCs found in the intima have a higher proliferative index, and a greater synthetic capacity for extracellular matrix, cytokines and proteases (Campbell, 1994; Worth NF 2001). Furthermore, SMCs can switch between the “contractile” and

“synthetic” phenotype in response to atherogenic stimuli including cytokines (Corjay MH et al., 1989; Hautmann MB et al., 1997; Li X et al., 1997), extracellular matrix (Hedin U et al., 1998; Thyberg J et al., 1989), lipids (Pidkovka NA et al., 2007), shear stress (Reusch P et al., 1996), and reactive oxygen species (Su B et al., 2001). This “phenotypic switching” facilitates many of the pathogenic roles of SMCs due to changes in SMC functions. SMCs of the “synthetic” phenotype migrate and proliferate more promptly than “contractile” SMCs and synthesize up to 25 to 46 times more collagen (Marra DE et al., 2000; Dzau VJ et al., 2002).

Mechanism relevant for cell proliferation and migration are also involved in the growth of vascular obstructive lesions during restenosis post-angioplasty, graft atherosclerosis and transplant vasculopathy.

## 2. Restenosis

### 2.2.1. Pathology of restenosis

Restenosis is the healing response of the arterial wall to mechanical injury. It consists of vessel remodeling and neointimal hyperplasia. The latter is characterized by smooth muscle migration/proliferation and extracellular matrix deposition.

The arterial remodeling can be characterized as a continuous spectrum of changes in vascular dimension (Schwartz et al, 1998). For example, lumen deterioration in nonstented coronary arteries can lead to negative remodeling (vessel shrinkage) (Di Mario C et al., 1995; Mintz G et al., 1996). Here, adventitial myofibroblasts may play an important role. They are capable of collagen synthesis and tissue contraction (Staab ME et al., 1997; Labinaz M et al., 1997). A protective effect might occur through the association between enhanced inflammation and vessel enlargement (Costa MA et al., 2001).

But remodeling does not occur after stenting (Dussaillant G et al., 1995; Costa MA et al., 2000). Bare-metal stents prevent vessel shrinkage (elastic recoil and negative remodeling). The vessel narrowing occurs due to induction of an

enhanced neointimal hyperplasia response. This enhanced proliferative response has been the focus of pharmacological prevention of restenosis and led to the development of drug eluting stents (DES).

### 2.2.2. The role of VSMC in restenosis

Atherosclerotic stenosis necessitates arterial reconstruction procedures, including percutaneous transluminal coronary (balloon) angioplasty (PTCA), coronary artery bypass (Zargham R et al., 2008) and stenting. After the surgical treatments with or without stenting, restenosis occurs. VSMC play a vital role in this process.

Whereas in healthy vessels VSMC are in a differentiated resting state, they dedifferentiate to the 'synthetic' phenotype after encountering distinct cytokines or growth factors such as PDGF.

PTCA, coronary artery bypass and stenting lead to endothelial dysfunction and cause an inflammatory state of the vessel. This initiates the VSMC hyperproliferation and migration driven by chemotactic stimuli. These processes result in the formation of a neointima mainly composed of VSMC, which subsequently deposit huge amounts of extracellular matrix (Kraitzer A., 2008). These events are followed by accumulation of other cell types like myofibroblasts and smooth muscle progenitor cells (Zargham R et al., 2008)

### 2.2.3. Surgical treatments of atherosclerotic stenosis

Opening of obstructed coronary arteries is often treated by PTCA. But this method of revascularization is limited by thrombosis at the site of angioplasty and elastic recoil, as well as VSMC growth in response to the balloon-induced injury that results in neointimal formation (Cooper Woods T et al., 2004).

Further, obstructed coronary arteries are routinely treated by operative myocardial revascularization - coronary artery bypass grafting (CABG). The success of this approach depends on the frequently used saphenous vein grafts

in CABG (Reisinger U et al., 2009) and the loss of patency due to thrombosis, and intimal hyperplasia leading to vein graft restenosis.

### 2.2.4. Stenting

The incidence of restenosis after PTCA, stenting and coronary artery bypass is highly independent of the used method (Zargham R et al., 2008). It occurs up to 20% after bypass surgery (Griffiths H, 2004) and up to 40% within 6 months after percutaneous transluminal angioplasty (Schillinger M et al., 2003). Stenting has not significantly improved the patency rate (Cheng S et al., 2003). Drug eluting stents (DES), first approved already 2003 by the FDA, seemed to be promising in prevention of restenosis. But on the one hand not all patients are responsive to the drugs used as coating agents like rapamycin or taxol (Cooper Woods T, 2004) and on the other hand there might be an increased risk for thrombosis with these coating agents (Maisel WH et al., 2007). Therefore restenosis still remains the major problem of any type of coronary interventions.

### 2.2.5. Pharmacological inhibitors in drug eluting stents

Stent applications are limited by the frequent occurrence of restenosis due to smooth muscle cell proliferation leading to neointimal hyperplasia and surgical lesion revascularization. Coated stents with drugs that target smooth muscle cell proliferation reduce in-stent restenosis.

Rapamycin and numerous agents, including the antineoplastic drug taxol, inhibit VSMC proliferation and migration (Jayaraman T and Marks AR, 1993; Marx SO et al., 1995; Poon M et al., 1996; Gallo R et al., 1999).

Rapamycin is a macrocyclic lactone, which has a major intracellular receptor - the immunophilin FKBP12 (FK506 binding protein). The rapamycin-FKBP12 complex binds to the mammalian target of rapamycin (mTOR) (Sabers CJ et al., 1999), blocks cell-cycle progression at the G1-to-S transition in VSMC

(Mita MM et al., 2003; Marx SO et al., 1995) by increase of the cyclin-dependent kinase inhibitor p27<sup>Kip1</sup> expression. The specific mechanism underlying this effect is however unclear. Rapamycin also has further cellular effects that might contribute to its ability to prevent restenosis. The inhibition of mTOR by rapamycin-FKBP12 leads to inhibition of phosphorylation of p70S6K and the initiation factor 4E (eIF-4E) binding protein, 4E-BP1 (Hidalgo M and Rowinsky EK, 2000; Burnett PE et al., 1998). These two pathways may contribute to the modulation of cellular proliferation, but the precise mechanism how rapamycin prevents restenosis remains to be determined (Rosner D et al., 2005).

In several clinical studies it could be demonstrated that stents coated with rapamycin lead to a reduction of in-stent restenosis compared to bare metal stents (BMS) (Morice MC et al., 2002; Leon MB et al., 2003; Sousa JE et al., 2003). Also several rapamycin analogues, like everolimus (Grube E et al., 2004) zotarolimus (Fajadet J et al., 2006) or biolimus (Chevalier B et al., 2007) were effectively tested for the use in DES. But, these devices have the potential to increase inflammatory and thrombogenic responses and to associate also with the polymers used for the delivery of antirestenotic agents, which may have life-threatening consequences (Virmani R et al., 2002).

Taxol, which is also used as coating agent in DES, stabilizes the microtubule assembly and inhibits thereby the proliferation of cells. Through this mechanism taxol induces its anti-restenotic effects (Schiff PB et al., 1979; Schiff PB and Horwitz SB, 1980). Microtubules are polymers assembled from tubulin dimers, which are in a dynamic equilibrium of assembly and disassembly, regulated according to cell-cycle phase. They are a component of the mitotic spindle apparatus and play a role in migration, cell shape maintenance and growth-factor signaling (Dugina VB et al., 1995; Rosette C et al., 1995; Rosania GR and Swanson JA, 1996). Taxol binds to the beta-tubulin subunit in the microtubule and promotes its polymerization. This shifts the equilibrium between microtubules and the tubulin dimers toward assembly. Bundles of disorganized microtubules are formed at all phases of the cell cycle and therefore preventing M-phase progression. This mechanism interrupts the

cell division (Schiff PB and Horwitz SB, 1980; Rowinsky EK et al., 1988; De Brabander M et al., 1981).

In several clinical studies it could be demonstrated that taxol-eluting stents prevent of in-stent restenosis to a higher percentage than BMS (Columbo A, 2002; Tanabe K et al., 2003). But, there is also a report with insignificant difference in restenosis rates between taxol-eluting stents and BMS (Lansky AJ et al., 2004).

Novel approaches are needed to improve the safety and efficacy of DES. One of the main components that determines the performance of a stent is the active drug. Here, is a lot of space for further improvements and new candidate compound identification.

### **2.3. VSMC migration**

In response to pathological stimuli, VSMC switch from the contractile to a proliferative and migratory phenotype. This switching is necessary under normal physiological conditions for wound healing and during development in order to allow the growth of new vessels. Under pathophysiological conditions, however, it contributes to atherosclerosis or restenosis (Lundberg MS and Crow MT, 1999).

Receptor tyrosine kinases (RTKs) and G protein-coupled receptors (GPCRs) regulate via multiple signaling pathways the actin cytoskeleton polymerization and depolymerization. Trimeric G proteins, small G proteins, lipid kinases, Calcium-dependent protein kinases, ROCK, and MAPKs are key signaling molecules (Abedi H and Zachary I, 1995; Bornfeldt KE et al., 1995).

To migrate, VSMC extend lamellipodia via actin polymerization toward the stimulus. Then the trailing edge needs to detach by degradation of focal contacts. This action is followed by generation of force by myosin II in the cell body to move the cell forward. The therefore needed actin polymerization is coordinated by several actin-binding proteins, such as WAVE, WASP and the

actin-related protein 2/3 (ARP2/3) complex, which become activated by the small G proteins Rho, Rac, and Cdc42 (Gerthoffer WT, 2007).

VSMC accomplish their migration along concentration gradients of soluble chemicals or matrix components through cell polarization, cytoskeletal, and focal contact remodeling and traction forces.

### 2.3.1. Migratory stimuli for VSMC

A wide variety of growth factors and cytokines have been linked to VSMC migration. VSMC respond to soluble factors such as cytokines and move along a gradient of varying adhesiveness due to different components of the ECM like integrins (Gerthoffer WT, 2007). Also, physical factors like shear stress influence VSMC migration. The best studied and most potent chemoattractant for VSMC of these factors is PDGF-BB (Bornfeldt KE et al., 1994; Hughes AD et al., 1996).

### 2.3.2. Signaling cascades in VSMC migration

In response to different pro-migratory stimuli including PDGF-BB, Rac-1 and Cdc42 members of the p21 activated protein kinase (PAK) family are activated. The PAKs can stabilize or destabilize actin as well as microtubules and are essential for the formation of lamellipodia (Tien Y and Autieri M, 2006). Furthermore, activation of Rac and cdc42 leads to nucleation and the formation of new actin filaments via the Wiskott–Aldrich syndrome protein (WASP) and WASP-family verprolin-homologous protein (WAVE) (Takenawa T and Suetsugu S, 2007). Myosin II is activated by PAK or Calcium/calmodulin (CaM)–myosin light chain kinase (MLCK) (Webb DJ et al. 2002; Vicente-Manzanares M et al., 2005). Nevertheless every increase in myoplasmic  $\text{Ca}^{2+}$  concentration will activate MLCK and myosin II.  $\text{Ca}^{2+}$  oscillations were observed during PDGF-stimulated cell migration (Scherberich A et al., 2000) and MLCK inhibitors block VSMC migration (Kishi H et al., 2000; Nakayama

M et al., 2005). Further,  $\text{Ca}^{2+}$ -independent activation of myosin II can occur through activation of RhoA and ROCK.

## **2.4. VSMC proliferation**

### **2.4.1. VSM cell cycle regulation**

Vascular proliferation contributes to cellular processes such as inflammation, matrix alterations as well as the pathophysiology of in-stent restenosis and vein bypass graft failure. A strategy for the treatment of these conditions is to inhibit VSMC proliferation by specific targeting of the cell cycle regulation of VSMC.

### **2.4.2. Cell cycle phases**

When VSMC are stimulated with growth factors, they enter G1- from G0-phase. In the gap phase 1 (G1-phase), the cell assembles the factors which are necessary for DNA replication. Only during this G0 to S interval, cell cycle progression depends on growth factors. In case cells become serum-starved during the S to G2/M-phase interval, they continue to cycle until the completion of mitosis. If they are not exposed to growth factors again they exit into the G0 state afterwards (Pardee AB, 1989). In S-phase the DNA synthesis occurs. After DNA replication is completed, the cells enter another gap phase (G2). In this phase the cell prepares for mitosis (M). Between G1 - S and G2 - M interphases restriction points ensure correct cell cycle progression (Elledge SJ, 1996).

Each phase of the cell cycle is tightly controlled by many regulatory mechanisms. The regulatory proteins controlling the cell-cycle progression belong to the family of cyclins, cyclin dependent kinases (CDK), CDK inhibitors (CKI) and the tumor-suppressor gene products p53 and retinoblastoma protein (Dzau VJ et al., 2002).



### 2.4.3. Cyclins, CDK and CKI

CDKs form holoenzymes with the regulatory cyclins and coordinate the different cell cycle phases (Koepp DM et al., 1997). The activity of the phase-specific cyclin-CDK complex is regulated by modifying the threonine and tyrosine phosphorylation status and up and down regulation of cyclin levels. This is necessary for specific and correct progression through the cell cycle. CDK are ubiquitously expressed throughout the cell cycle. Their activity is regulated by the limited expression of cyclins. Transition through the G1-phase of the cell cycle requires increasing accumulation of cyclin D-CDK4 and cyclin E-CDK2 complexes (Sherr CJ, 1995). The subsequent G2-M-phase transition is regulated by cyclin A-CDK2 and cyclin B-CDK1 complexes (Fig. 2). Furthermore, the cell cycle progression is regulated by cyclin-dependent kinase inhibitors (CKI). The family of CKI includes the CIP/KIP members p21Cip1, p27Kip1, and p57Kip2, which inhibit several CDK (Sherr CJ and Roberts JM, 1995 and 1999). These CKI bind to CDK and prevent their activation. Further, the cell cycle progression is modulated by transcription factors. Activation of p53 induces the expression of the CKI p21CIP1 and thus inhibits the activity of the G1 cyclin-CDK complexes, leading to a G1-phase arrest (Levine AJ, 1997). The transcription factors of the E2F family control the gene expression of proteins important for S-phase entry and cell cycle regulation (Sherr CJ, 1995). During quiescence, E2F members are in complexes with retinoblastoma protein (RB) and inactive. Mitogenic stimulation leads to hyperphosphorylation of the retinoblastoma protein by the cyclin D-CDK4 and cyclin E-CDK2 complexes and to dissociation from E2F. Then, E2F activates the expression of genes such as those encoding cyclins E, cyclin A and CDK1.

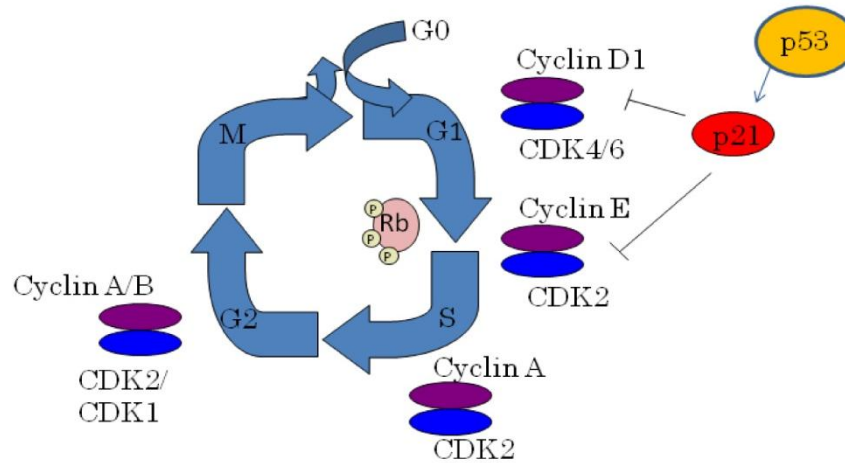


**Figure 2:** CDKs form holoenzymes with cyclins and coordinate the different cell cycle phases. Transition through the G1-phase of the cell cycle requires increasing accumulation of cyclin D-CDK4 and cyclin E-CDK2 complexes. The S-phase is regulated by cyclin A-CDK2 complexes. The subsequent G2-M-phase transition is regulated by cyclin A-CDK2 and cyclin B-CDK1 complexes. Furthermore, the cell cycle progression is regulated by cyclin-dependent kinase inhibitors like the depicted p21Cip1 which inhibit cyclin D1-CDK4 complexes. p21 itself is the mediator of p53 induced growth suppression.

#### 2.4.4. Important G1-phase regulators

D type cyclins are known to be mitogenic sensors that pass on signals to the cell cycle machinery (Sherr CJ and Roberts JM, 1999). They will be presented together with the CKI p21 in the following chapter.

##### 2.4.4.1. Cyclin D1

Cyclin D1 is expressed as a response to many mitogenic signals. Its expression forces the cell to pass from G0- to G1-phase and to start proliferation (Sherr CJ, 1995 and 1996). After mitogenic stimulation, the mRNA levels of cyclin D1 and correspondingly also the cyclin D1 expression levels increase. Cyclin D1 mRNA levels as well as cyclin D1 expression levels are highly regulated after

induction. As already stated before, cyclin D1 is the regulatory subunit of CDK4 or 6, and is necessary for the transition from the G1 to S phase by mediating the phosphorylation of RB, the gatekeeper of the G1 phase. As long as mitogenic stimulation is present the induction of cyclin D1 continues throughout the G1-phase of the cell cycle. For the transition to S phase, cyclin D1 is exported from the nucleus to the cytoplasm. This export is dependent on phosphorylation of cyclin D1 at threonine (Thr)-286 by glycogen synthase kinase-3 (GSK-3) and the nuclear exportin CRM1. Then, cyclin D1 is degraded via proteolysis by the 26S proteasome (Alt JR et al., 2000; Perez-Roger I et al., 1999; Sherr CJ and Roberts JM, 1999; Diehl JA et al., 1997 and 1998). The mechanism of cyclin D1 degradation will be explained in section 2.5.5.

#### 2.4.4.2. p21

The cyclin D-CDK complex contains additionally p21 (Zhang H et al., 1994) also known as Cip1, Sdi1, Cap20, and Waf1 (Harper JW et al., 1993; el-Deiry WS et al., 1993; Xiong Y et al., 1992; Gu Y et al., 1993; Noda A et al., 1994). p21 also associates with cyclin E-CDK2, cyclin A-CDK2, and cyclin B-CDK1 complexes, and inhibits these CDK (Harper JW et al., 1993 and 1995). Association of p21 with cyclin D-CDK4/6 inhibits RB phosphorylation and induces cell cycle arrest in G1-phase. Furthermore, p21 is a target gene of the p53 tumor suppressor, and mediates p53-dependent cell cycle arrest in response to DNA damage (el-Deiry WS et al., 1993). Overall, p21 is a negative regulator that keeps cells in G0-phase (Li Y et al., 1994) or stops the cell cycle in G1-phase by association and inactivation of E2F (Afshari CA et al., 1996). However, p21 is not just a cyclin-CDK inhibitor; in a certain amount it is required for normal cell cycle progression. p21 stabilizes and promotes active cyclin-CDK complex formation in a dose-dependent manner (Philipp J et al., 1999; LaBaer J et al., 1997; Besson A and Yong VW, 2000; Weiss RH et al., 2000).

During S phase, PCNA is necessary for the formation of the DNA replication complex and therefore interacts with DNA polymerase  $\delta$  (pol $\delta$ ) (Prelich G and

Stillman B, 1988; Kelman Z, 1997). p21 is able to block the ability of PCNA to activate pol $\delta$  by competing with pol $\delta$  on the same binding site of PCNA, leading to a DNA replication block and intra-S-phase arrest (Oku T et al., 1998; Li R et al., 1994; Waga S et al., 1994).

#### 2.4.5. Regulation of cyclin and CKI degradation

Mitogen-initiated signals regulate the trafficking and the proteolysis of cyclin D1 (Diehl JA et al., 1997 and 1998). The phosphorylation site of cyclin D1, the specific threonine residue (Thr-286) located near its C-terminus, needs to be phosphorylated by Glycogen Synthase Kinase-3 $\beta$  (GSK-3 $\beta$ ) for cyclin D1 polyubiquitination and its nuclear export. The activity of GSK-3 $\beta$  is modulated by the Ras, PI-3K, Akt pathway (Klinghoffer RA et al., 1996; Rodriguez-Viciano P et al., 1996; Franke TF et al., 1997). GSK-3 $\beta$  can be modulated by phosphorylation on serine 9 leading to decreased catalytic activity (Stambolic V and Woodgett JR, 1994). The modulation of cyclin D1 via this pathway is important for G1-phase progression.

After polyubiquitination and nuclear export, cyclin D1 is degraded by the 26 S proteasome. For the specific recognition and further degradation of cyclin D1, ubiquitin-ligases are necessary (Guo Y et al., 2005). The ubiquitin-ligases involved in this process under normal physiological conditions are still unknown. At least, after DNA damage, recent publications show that there are several E3 ubiquitin-ligases involved in cyclin D1 degradation such as FBXO31 (Santra MK et al., 2009) or FBX4 (Jia L and Sun Y; 2009).

p21 is targeted for proteasomal degradation during cell cycle by several E3 ligases, including SCF<sup>SKP2</sup>, CRL4(Cdt2) and APC/CCdc20 (Amador V et al., 2007; Bornstein G et al., 2003; Kim Y et al., 2008; Wang W et al., 2005; Yu ZK et al., 2007). For degradation, p21 needs to be phosphorylated at S130 and gets afterwards ubiquitylated and further processed by the proteasome (Coulombe P et al., 2004). Furthermore, p21 is also degraded in an ubiquitin-independent manner (Sheaff RJ et al., 2000; Chen X et al., 2004), which is mediated by Mdm2 (Jin Y et al., 2003; Zhang Z et al., 2004). Therefore, p21 is degraded

by ubiquitin-dependent and -independent pathways, although the exact involved regulatory mechanisms are unknown.

## 2.5. PDGF signaling

Platelet-derived growth factors (PDGFs) are mitogens acting on many cell types like fibroblasts or smooth muscle cells. The family of PDGFs is composed of four different polypeptide chains, PDGF-A, PDGF-B, PDGF-C and PDGF-D, encoded by four different genes. These PDGF chains can assemble into five different dimeric isoforms - PDGF-AA, PDGFAB, PDGF-BB, PDGF-CC and PDGF-DD (Fredriksson L et al., 2004). PDGF-BB has been shown to be by far the most potent stimulus for VSMC migration and proliferation (Andrae J et al., 2008).

All the PDGFs share a similar structure with a typical growth factor domain which is involved in dimerization of the two subunits, receptor binding and receptor activation. The growth factor domain has a length of around 100 amino acid residues and is also called PDGF/VEGF homology domain. This structural motive is also found in the family of VEGF-related growth factors (Joukov V et al., 1997) in many different organisms (Duchek P et al., 2001; Yamazaki Y et al., 2003). Further, the PDGFs have an accessory amino acid sequence found in the N- or C-terminus. It is involved in the regulation of the biological properties of these factors. For example, PDGF-A and PDGF-B have sequences involved in the binding to the extracellular matrix (LaRochelle WJ et al., 1991; Östman A et al., 1991). The PDGFs and their receptors are usually expressed in different cell types. During embryonic development PDGF-A is produced by the epithelial cells and its PDGFR- $\alpha$  is expressed by mesenchymal cells (Orr-Urtreger A and Lonai P, 1992). PDGF-B and PDGFR- $\beta$  are mainly expressed in the developing vasculature. PDGF-B is produced by endothelial cells, and PDGFR- $\beta$  is expressed by pericytes and vascular smooth muscle cells (Hellström M et al. 1999). During murine embryogenesis, PDGF-C is expressed in many cell types, like cardiomyocytes and vascular smooth muscle cells (Aase K et al., 2002), PDGF-D in the metanephric mesenchyme and PDGF-B in

endothelial cells (Bergsten E et al., 2001). In human primary vascular cells, PDGF-C is found in coronary artery vascular smooth muscle cells and PDGF-D in umbilical vein cells (Uutela M et al. 2001).

#### 2.5.1. PDGF receptor activation

The tyrosine kinase receptors of the PDGFs are activated by ligand-induced dimerization or oligomerization (Heldin CH et al., 1998). The PDGF isoforms have two receptor binding epitopes and bind two receptor molecules simultaneously (Fretto LJ et al. 1993; Herren B et al., 1993). But the receptors are able to bind different chains. Whereas the  $\alpha$ -receptor binds both A- and B-chains, the  $\beta$ -receptor binds only the B-chain with high affinity. Therefore, the different PDGF combinations activate different receptor dimers. PDGF-AA leads to  $\alpha\alpha$ -receptor dimerization, PDGF-AB to  $\alpha\alpha$ - or  $\alpha\beta$ -receptor dimers and PDGF-BB induces  $\alpha\alpha$ ,  $\alpha\beta$  or  $\beta\beta$  combinations (Bishayee S et al., 1989; Heldin CH et al., 1989; Seifert RA et al., 1989; Kanakaraj P et al., 1991). For vascular smooth muscle cells it is known that they do not possess PDGF- $\alpha$ -receptors (Inui H et al., 1993). The existence of the other possible dimers PDGF-AC or PDGF-AD cannot be excluded but have not been described so far *in vitro* or *in vivo* (Tallquist M and Kazlauskas A, 2004).

The PDGF-induced receptor dimerization leads to conformational changes of the kinase domains. They approach each other and enable mutual phosphorylation on tyrosine residues. For the PDGFR- $\beta$  receptor it is Y857 and for the PDGFR- $\alpha$  receptor it is Y849 (Kazlauskas A, 2008). This autophosphorylation leads to further activation of several kinase domains at the receptor which are able to phosphorylate several target proteins (Kazlauskas A, 2008).

In general, interactions between components in the different signaling pathways are necessary for the intracellular transduction of signals. Specific domains, like Src homology 2 (SH2) domains and phosphotyrosine binding (PTB) domains exert this interaction by recognition of phosphorylated tyrosine residues. There are also other domains like SH3 domains recognizing proline-

rich regions (PH) domains. Furthermore, PDZ domains recognize C-terminal valine residue (Pawson T and Scott JD, 1997).

### 2.5.2. Early events in PDGF receptor signaling

Signal transduction molecules like the Src family of tyrosine kinases, phosphatidylinositol 3P kinase (PI3K), Src kinase, phospholipase C- $\gamma$  (PLC- $\gamma$ ), the tyrosine phosphatase SHP-2, GTPase activating protein (GAP) for Ras, signal transducers and activators of transcription (Stats) and several other molecules bind to different phosphorylation sites in the PDGF  $\alpha$ - and  $\beta$ -receptors. This binding of different SH2 domain molecules is specific (Songyang Z et al., 1993).

### 2.5.3. Signaling cascades downstream of the PDGF receptor

PDGF receptor activation leads to further recruitment and activation of the signaling molecules mentioned above. This in turn activates a complex network driving many different signaling cascades contributing to different cellular responses such as cell proliferation, motility and cell differentiation.

Important signal transduction pathways belong to the Src, MAPK, PI3K and (Jak)/STAT pathway and will be discussed in the following:

The Src family of tyrosine kinases is important in the mitogenic response to PDGF (Bromann PA et al., 2004; Twamley-Stein GM et al., 1993; Roche S et al., 1995). The Src tyrosine kinase activity is regulated by the phosphorylation status of Y416 and Y530. Src becomes activated by phosphorylation of Y416 and dephosphorylation of Y530 (Bjorge JD et al., 2000). Further, PDGF-induced and Src mediated DNA synthesis seems to be linked to the transcription factor c-Myc, which participates in G1-to S-phase transition (Barone MV and Courtneidge SA, 1995). The Src-mediated transcriptional

activation of c-Myc, includes the transcription factor STAT3 (Bowman T et al., 2001) and the tumor suppressor p53 (Broome MA and Courtneidge SA, 2000). For the activation of the mitogens-activated protein kinase (MAPK)-pathways, the activation of Ras is essential. The PDGFR- $\beta$  regulates the activation of Ras by direct or indirect binding of the Grb2/Sos1 complex which results in phosphorylation of the MAPK kinase kinase (MKKK), leading to MKK activation (MEK 1/2) (Avruch J et al., 1994), which in turn phosphorylates the MAPK extracellular signal-regulated kinases (Erk1/2). The serine/threonine kinases Erk1/2 translocate to the nucleus and activate the protein kinase p90 ribosomal S6 kinase/(MAPK)-activated protein kinase-1a (Dalby KN et al., 1998; Frödin M and Gammeltoft S, 1999). This activates immediate early genes relevant for the cell cycle (c-fos, c-myc and c-jun), followed by cell cycle progression and proliferation (Murphy LO and Blenis J, 2006; Murphy LO et al., 2004; Kortenjann M et al., 1994). Additionally to Erk1/2, there are several more MAPKs activated by PDGF through the MKKK pathway particularly the p38MAPKs and the c-Jun NH2-terminal kinases (JNKs).

The major downstream effector of PI3K is the serine/threonine kinase Akt. PI3K is activated by recruitment to the PDGF-receptor via its regulatory subunit p85 and leads to PI(3,4,5)P3 production. The latter molecule serves as anchor and causes the translocation of Akt to the inner membrane, recruits PDK1 and PDK2, which in turn phosphorylate Akt on T308 and S473 (Kandel ES and Hay N, 1999; Fresno Vara JA et al., 2004). Then, Akt is able to modulate functions of several proteins involved in the regulation of cell cycle progression and proliferation. One substrate of Akt is the glycogen synthase kinase-3 (GSK-3), which inactivates proteins like c-Myc and cyclin D or leads to their degradation. Hence, Akt phosphorylates the CDK inhibitors p21Cip1 and p27Kip1 and leads to repression of their inhibitory effects on cell cycle progression (Cantley LC, 2002).

STAT3 belongs to the Janus kinase (Jak)/STAT pathway and can also be responsible for the induction of cell cycle progression and anti-apoptotic effects (Lim CP and Cao X, 1999). STAT3 can be activated by PDGF and plays an important role in the G1-/S-phase transition through the expression of the immediate early gene c-myc, the up regulation of cyclin D1, cyclin A and the



down regulation of CDK inhibitors p21Cip1 and p27Kip1 (Yu H and Jove R, 2004; Hirano T et al., 2000).

#### 2.5.4. PDGF signaling in vascular disease

During the development of atherosclerosis and restenosis, several cytokines and growth factors are important like tumor necrosis factor- $\alpha$  (TNF- $\alpha$ ), interferon- $\gamma$  (IFN- $\gamma$ ), PDGF, transforming growth factor- $\beta$  (TGF- $\beta$ ) and insulin-like growth factor-I (IGF-I) (Tedgui A and Mallat Z, 2006). But, as already mentioned above, PDGF-BB is the most potent stimulus for both, proliferation and migration of VSMC and extracellular matrix production (Andrae J et al., 2008). This indicates an active role of PDGF in the tissue remodeling during the progression of atherosclerosis and restenosis. In addition, it was shown, at least in animal models, that the selective inhibition of PDGF-induced signaling cascades inhibits neointima formation (Dong LH et al., 2010).

### 2.6. Investigated natural products and medicinal plants

A promising strategy for the treatment of atherosclerosis and restenosis is to inhibit VSMC proliferation by targeting specific the cell cycle regulation of VSMC. For the identification of such cell cycle specific inhibitors, natural products represent a rich source. They could provide new promising lead structures acting by novel molecular mechanisms.

#### 2.6.1. *Tylophora indica* - source and traditional use

*Tylophora indica* (Asclepiadaceae), also known as *Tylophora asthmatica*, is a perennial climbing plant native to the forests of eastern and southern India. As reviewed by Chemler SR in 2001, it was included as an official drug in the Bengal pharmacopoeia of 1884. This indigenous medicinal plant was

traditionally used for the treatment of various ailments like asthma as well as bronchitis, rheumatism and dysentery. Investigations of the pharmacological properties have confirmed the anti-asthmatic effects of *Tylophora indica* leaf extracts (Shivpuri DN et al. 1972). Currently the *Tylophora indica* extract is marketed by several pharmaceutical companies as anti-asthmatic herbal drug. The plant contains several phenanthroindolizidine alkaloids (Gellert E., 1982). The major alkaloid is tylophorine and was first isolated from *Tylophora indica* in 1935. It has been reported to have anti-inflammatory (Gopalakrishnan C et al. 1979 and 1980), immunosuppressive (Ganguly T and Sainis KB, 2001) and anti-leukemic (Gellert E., 1982) properties. Further, an anti-tumor activity for tylophorine was published by Donaldson et al. in 1968.

In addition, *Tylophora indica* contains several more structurally-related similar alkaloids, like tylophorinidine, (+)-septicine and (+)-isotylocrebrine.

#### 2.6.1.1. Chemical structure of tylophorine

The structure including the stereochemistry of tylophorine was reported in 1960 by Govindachari and colleagues. Tylophorine is a 2,3,6,7-tetramethoxyphen-anthro-(9,10,6',7')-indolizidine alkaloid (Fig. 3). It was first reported to have the (S)-stereochemistry; later revision led to the (R) conformation (Buckley TF and Rapoport H, 1983).

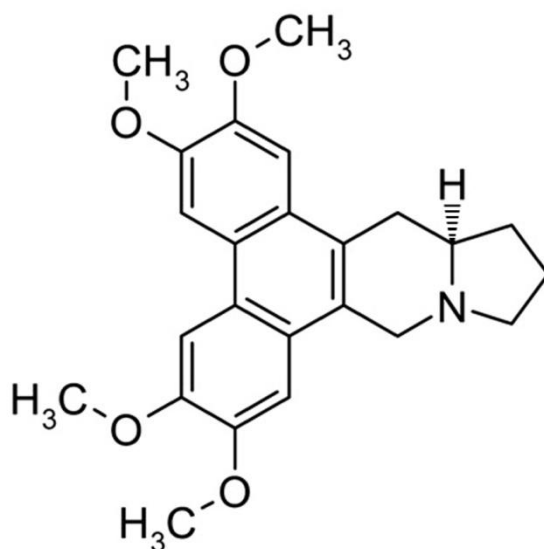


**Figure 3.** Chemical structure of (-)-R-tylophorine.

#### 2.6.1.2. Tylophorine and cancer

As mentioned above, *Tylophora* alkaloids were known for its anti-leukemia properties since the 1960s. Tylocrebrine was tested in clinic trials in 1966 and failed due to central nervous system toxicity. Therefore, these alkaloids were not used for further anti-cancer drug development. Later, tylophorine was tested in animal models. (R)-Tylophorine was non-toxic in rats up to a dose of 500 mg/kg (Gopalakrishnan C et al., 1979), and non-toxic in hamsters up to 60 mg/kg (Bhutani KK et al., 1987). CNS toxicity has been observed in rats at high doses of (R)-tylophorine (Gopalakrishnan C et al., 1979).

Tylophorine regained popularity again in the last decade. It was then used as the lead structure for the development of novel anti-proliferative analogs effective against several cancer cell lines (Staerk D et al., 2002; Gao W et al., 2004). Tylophorine ((+)-S-tylophorine) exerts potent growth-inhibitory effects on HepG2, a human hepatocellular carcinoma cell line, and KB, a human nasopharyngeal carcinoma cell line. The tylophorine analogs exhibit potent cytotoxic activity against a broad range of human cancer cells, like A549 (lung cancer cell line), ZR-751 (breast cancer cell line), DU-145 (prostate cancer cell

line), KB (nasopharyngeal cancer cell line), and KB-Vin (multidrug resistant KB subline) (Wei L et al., 2007).

#### 2.6.1.3. Tylophorine analogues and their possible mechanism of action

For tylophorine, especially the (+)-S-tylophorine, there are already several investigations performed on cancer cell lines. (+)-S-tylophorine significantly inhibits activator protein-1, cAMP response element and nuclear factor  $\kappa$ B (NF- $\kappa$ B) mediated transcription (Gao W et al., 2004). Furthermore, tylophorine is able to arrest HepG2, HONE-1 (epithelial tumor cell line), and NUGC-3 (stomach cancer cells) carcinoma cells in G1-phase of the cell cycle by down regulation of cyclin A2 expression (Wu CM et al., 2009). However, the exact mechanism of action of tylophorine is still unknown.

### 2.6.2. *Peucedanum ostruthium*

#### 2.6.2.1. Traditional use

Extracts from plants traditionally used against inflammatory indications were tested on their ability to inhibit VSMC proliferation. In the frame of this ongoing screening, done in big part by the diploma student Thomas Nakel, a highly active hit was found, the DCM-extract from *Peucedanum ostruthium* rhizomes.

#### 2.6.2.2. Source

*Peucedanum* species have a long history of usage in the Austrian traditional medicine. Especially the rhizomes of *Peucedanum ostruthium* have been traditionally used for inflammatory diseases since ancient times. Furthermore, anti-inflammatory action of *Peucedanum ostruthium* root extract has recently

been demonstrated in vivo upon oral administration to rats that were subjected to carrageenan-induced paw edema (Hiermann A and Schantl D, 1998).

## **2.7. Aims of the study**

Cardiovascular disease (CVD) is the leading mortal disease worldwide in the developed societies (Murray CJ et al., Lancet, 1997). Proliferation of vascular smooth muscle cells (VSMC) contributes to atherosclerosis and restenosis. For the VSMC-mediated vessel narrowing processes, mitogen-induced cell division is essential and PDGF-BB is one the most important mitogenic factors to induce VSMC proliferation.

Natural products are often a rich source for the identification of new lead structures and novel molecular mechanisms. Consequently we selected a compound which already demonstrated a promising activity profile in cancer cells – tylophorine.

We examined if tylophorine (I) possesses anti-proliferative activity in rat and human smooth muscle cells, (II) interferes with key cell cycle regulatory proteins and (III) further aimed to confirm the discovered effects in human saphenous veins in culture. The unique activity that we observed suggests tylophorine as a promising lead for the development of pharmaceuticals targeting vasculo-proliferative disorders, such as restenosis or atherosclerosis.

Further, we examined a plant extract from the roots of *Peucedanum ostruthium*, a traditionally used medicinal plant with anti-inflammatory properties, for a putative anti-proliferative activity in rat aortic VSMC.

### **3. MATERIALS AND METHODS**

### 3. Materials and methods

#### 3.1. Materials

##### 3.1.1. Chemicals

All chemicals were obtained from Sigma Aldrich (St. Louis, MO, USA), Fluka (Buchs, Switzerland) or Carl Roth (Karlsruhe, Germany) unless otherwise stated.

Tylophorine was initially provided by Prof. Proksch (University of Duesseldorf, Department of Pharmaceutical Biology), but for further studies bought from Alexis Biochemicals (Switzerland).

##### 3.1.2. Buffers and solutions

###### Blotting buffer 5 X

|                   |            |
|-------------------|------------|
| TRIS-base         | 15.17 g    |
| Glycine           | 72.9 g     |
| dH <sub>2</sub> O | ad 1000 ml |

###### Complete™ 25 X

(Roche Diagnostics, Penzberg, Germany)

one tablet

|                   |      |
|-------------------|------|
| dH <sub>2</sub> O | 2 ml |
|-------------------|------|

###### Coumaric acid (stock solution)

|                 |          |
|-----------------|----------|
| p-Coumaric acid | 0.15 g   |
| DMSO            | ad 10 ml |

###### Crystal violet solution

|                  |             |
|------------------|-------------|
| Crystal violet   | 0.5 % (m/v) |
| in 20 % methanol |             |

Digestion buffer

|                       |           |
|-----------------------|-----------|
| Collagenase (246U/mg) | 0.1 g     |
| HEPES                 | 0.24 g    |
| Ascorbic acid         | 0.005 g   |
| Gentamicin sulphate   | 0.005 g   |
| BSA                   | 0.1 g     |
| Ham's F12 medium      | ad 100 ml |

ECL

|                                      |        |
|--------------------------------------|--------|
| dH <sub>2</sub> O                    | 4.5 ml |
| TRIS-base, 1 M pH 8.5                | 0.5 ml |
| Luminol (stock solution)             | 25 µl  |
| p-Coumaric acid (stock solution)     | 11 µl  |
| H <sub>2</sub> O <sub>2</sub> (30 %) | 3.0 µl |

Electrophoresis buffer 5 X

|            |            |
|------------|------------|
| TRIS-base  | 15.0 g     |
| Glycine    | 72.0 g     |
| SDS        | 5.0 g      |
| Aqua dest. | ad 1000 ml |

Ethanol/sodium citrate solution

|                      |            |
|----------------------|------------|
| Sodium citrate 0.1 M | 50 % (v/v) |
| in ethanol           |            |

FACS buffer pH 7.37

|                                  |        |
|----------------------------------|--------|
| NaCl                             | 8.12 g |
| KH <sub>2</sub> PO <sub>4</sub>  | 0.26 g |
| Na <sub>2</sub> HPO <sub>4</sub> | 2.35 g |
| KCl                              | 0.28 g |
| LiCl                             | 0.43 g |
| NaN <sub>3</sub>                 | 0.20 g |
| Na <sub>2</sub> EDTA             | 0.36 g |



|                   |            |
|-------------------|------------|
| dH <sub>2</sub> O | ad 1000 ml |
|-------------------|------------|

HBS buffer pH 7.05

|  |        |
|--|--------|
| NaCl   | 280 mM |
| KCl  | 10 mM  |
| Na <sub>2</sub> HPO <sub>4</sub> · 2H <sub>2</sub> O | 1.5 mM |
| Dextrose   | 12 mM  |
| HEPES  | 50 mM  |
| adjust to pH 7.05                                    |        |

HBSS buffer pH 7.4

|  |            |
|--|------------|
| NaCl                                   | 8.18 mg    |
| KCl                                    | 400 mg     |
| Na <sub>2</sub> HPO <sub>4</sub>       | 19.75 mg   |
| KH <sub>2</sub> PO <sub>4</sub>        | 50 mg      |
| CaCl <sub>2</sub> x 2 H <sub>2</sub> O | 180 mg     |
| MgSO <sub>4</sub>                      | 97.5 mg    |
| Glucose                                | 1000 mg    |
| HEPES                                  | 4760 mg    |
| dH <sub>2</sub> O                      | ad 1000 ml |

HFS-buffer (Hypotonic fluorochrome solution)

|                       |             |
|-----------------------|-------------|
| Sodium citrate        | 0.1 % (w/v) |
| Triton X-100 (in PBS) | 0.1 % (v/v) |

Luminol (stock solution)

|         |          |
|---------|----------|
| Luminol | 0.44 g   |
| DMSO    | ad 10 ml |

Lysis buffer (stock solution)

|       |       |
|-------|-------|
| HEPES | 50 mM |
| NaCl  | 50 mM |

|   |                      |
|---|----------------------|
| NaF   | 50 mM                |
| Na <sub>4</sub> P <sub>2</sub> O <sub>7</sub> x 10 H <sub>2</sub> O | 10mM                 |
| EDTA  | 5 mM                 |
| Na <sub>3</sub> VO <sub>4</sub>                                     | 1 mM                 |
|   | in dH <sub>2</sub> O |

The reagents were dissolved in 325 ml H<sub>2</sub>O (4°C), adjusted to pH 7.5 with NaOH and filled up to a final volume of 430 ml.

#### PBS pH 7.4

|                                  |            |
|----------------------------------|------------|
| NaCl                             | 7.2 g      |
| Na <sub>2</sub> HPO <sub>4</sub> | 1.48 g     |
| KH <sub>2</sub> PO <sub>4</sub>  | 0.43 g     |
| dH <sub>2</sub> O                | ad 1000 ml |

#### PMSF

|                       |       |
|-----------------------|-------|
| PMSF (in isopropanol) | 0.1 M |
|-----------------------|-------|

#### Resolving gel 10 %

|                   |         |
|-------------------|---------|
| PAA solution 30 % | 5 ml    |
| TRIS-base pH 8.0  | 3.75 ml |
| SDS 10 %          | 0.15 ml |
| dH <sub>2</sub> O | 6.1 ml  |
| TEMED             | 15 µl   |
| APS 10 %          | 75 µl   |

#### Sample buffer for RNA gel (10 X)

|                   |        |
|-------------------|--------|
| Bromphenol blue   | 4.0 mg |
| dH <sub>2</sub> O | 5.0 ml |
| Glycerol          | 5.0 ml |

#### SDS sample buffer (stock solution)

|                                 |         |
|---------------------------------|---------|
| TRIS-HCl solution, 0.5 M pH 6.8 | 37.5 ml |
| SDS                             | 6.0 g   |

|                   |            |
|-------------------|------------|
| Glycerol          | 30.0 ml    |
| Bromophenol blue  | 15.0 mg    |
| dH <sub>2</sub> O | ad 1000 ml |

#### Stacking gel

|                   |          |
|-------------------|----------|
| PAA solution 30 % | 0.64 ml  |
| TRIS-HCl pH 6.8   | 0.375 ml |
| SDS 10 %          | 37.5 µl  |
| Aqua dest         | 2.62 ml  |
| TEMED             | 7.5 µl   |
| APS 10 %          | 37.5 µl  |

#### TBE (10 X)

|                   |            |
|-------------------|------------|
| Tris base         | 108 g      |
| Boric acid        | 55 g       |
| EDTA 0.5 M pH 8.0 | 40 ml      |
| dH <sub>2</sub> O | ad 1000 ml |

#### TBS-T pH 8.0

|                                   |            |
|-----------------------------------|------------|
| TRIS-base                         | 3.0 g      |
| NaCl                              | 11.1 g     |
| Tween-20 (add after adjusting pH) | 1 ml       |
| dH <sub>2</sub> O                 | ad 1000 ml |

#### Trypsin/EDTA in PBS

|         |        |
|---------|--------|
| Trypsin | 0.05 % |
| EDTA    | 0.02 % |

### 3.1.3. Cell culture media and reagents

|  |  |
|--|--|
| Calf serum   | Lonza Group Ltd. (Basel, Switzerland)  |
| Complete protease inhibitor  | Roche Diagnostics (Basel, Switzerland) |
| Collagenase II   | Invitrogen (Carlsbad, CA, USA)         |
| DMSO   | Fluka (Buchs, Switzerland)             |
| Dulbecco's Modified Eagle Medium (DMEM)  |  |
| 4.5 g/L glucose, w/o L-glutamine   | Lonza Group Ltd. (Basel, Switzerland)  |
| Ham's F-12 medium  | Invitrogen (Carlsbad, CA, USA)         |
| L-glutamine 200 mM   | Lonza Group Ltd. (Basel, Switzerland)  |
| Penicillin/streptomycin mixture<br>(10,000 U/ml potassium penicillin/<br>10,000 µg/ml streptomycin sulphate) | Lonza Group Ltd. (Basel, Switzerland)  |
| Recombinant human PDGF-BB  | Bachem (Weil am Rhein, Germany)        |
| Trypsin (1:250)  | Invitrogen (Carlsbad, CA, USA)         |

#### Growth medium

|                         |                    |
|-------------------------|--------------------|
| DMEM                    | 500 ml             |
| Calf Serum (CS)         | 10 %               |
| Penicillin/Streptomycin | 100 U/ml/100 µg/ml |
| L-glutamine             | 2 mM               |

#### Starving medium

|                         |                    |
|-------------------------|--------------------|
| DMEM                    | 500 ml             |
| Calf Serum (CS)         | 0.1 %              |
| Penicillin/Streptomycin | 100 U/ml/100 µg/ml |
| L-glutamine             | 2 mM               |

#### Freeze medium

|                 |        |
|-----------------|--------|
| DMEM            | 8.0 ml |
| Calf Serum (CS) | 2.0 ml |
| DMSO            | 1.1 ml |

Primary Antibodies

| Target                                      | Source | Dilution  | Provider                           |
|---|--------|-----------|------------------------------------|
| ACTIVE-JNK®                                 | rabbit | pc 1:1000 | Promega (Madison, USA)             |
| α-smooth muscle-actin-FITC                  | mouse  | mc 1:250  | Sigma Aldrich (St. Louis, USA)     |
| α-tubulin                                   | mouse  | mc 1:1000 | Santa Cruz (Santa Cruz, USA)       |
| c-Myc                                       | rabbit | pc 1:1000 | New England Biolabs (Beverly, USA) |
| Cyclin D1                                   | mouse  | mc 1:1000 | New England Biolabs (Beverly, USA) |
| Retinoblastoma protein-S <sup>807/811</sup> | rabbit | pc 1:1000 | New England Biolabs (Beverly, USA) |
| phospho Akt S <sup>473</sup>                | rabbit | pc 1:1000 | New England Biolabs (Beverly, USA) |
| phospho Erk1/2 Y <sup>202/204</sup>         | rabbit | pc 1:1000 | New England Biolabs (Beverly, USA) |
| phospho p38 Y <sup>180/182</sup>            | rabbit | pc 1:1000 | New England Biolabs (Beverly, USA) |
| phospho STAT3 Y <sup>705</sup>              | rabbit | pc 1:1000 | New England Biolabs (Beverly, USA) |

Secondary, HRP-linked antibodies

|            |      |        |                                    |
|------------|------|--------|------------------------------------|
| mouse IgG  | goat | 1:2500 | Upstate (Charlottesville, USA)     |
| rabbit IgG | goat | 1:2500 | New England Biolabs (Beverly, USA) |

Antibodies were diluted as stated above in TBS-T and prepared with 5 % BSA or 5 % milk powder.

Used kits

|   |   |
|---|---|
| Cell Proliferation ELISA, BrdU (chemiluminescent) | Roche Diagnostics GmbH (Basel, Switzerland) |
| FITC BrdU Flow Kit                                | BD Biosciences Pharmingen (San Diego, USA)  |

Miscellaneous material

|                                  |  |
|----------------------------------|--|
| 96-well Microplates              | Greiner bio-one (Frickenhause, Germany)  |
| Cell scraper                     | Greiner bio-one (Frickenhause, Germany)  |
| Gel blotting paper               | Whatman plc (Kent, UK)                   |
| Precision Plus Protein™ Standard | BIO-RAD Laboratories (Hercules, CA, USA) |

|   |  |
|---|--|
| PVDF Membrane (0.2 $\mu$ m)             | BIO-RAD Laboratories (Hercules, CA, USA) |
| Serological Pipettes                    | Sarstedt GmbH (Nümbrecht, Germany)       |
| Tissue Culture Dishes (6 cm, 10 cm)     | Greiner bio-one (Frickenhausen, Germany) |
| Tissue Culture Flask 75 cm <sup>2</sup> | Sarstedt GmbH (Nümbrecht, Germany)       |

### 3.1.4. Technical equipment

|                                      |  |
|--------------------------------------|--|
| Digital SLR Camera E-330             | Olympus Europa GmbH (Hamburg, Germany)           |
| FACSCalibur™                         | BD Biosciences Pharmingen (San Diego, CA, USA)   |
| Fluorescence Microscope BX51         | Olympus Europa GmbH (Hamburg, Germany)           |
| Galaxy Mini Microcentrifuge          | VWR International Inc. (West Chester, PA, USA)   |
| HERAcell™ 150 Incubator              | Thermo Fisher Scientific Inc. (Waltham, CA, USA) |
| Heraeus™ B15 Incubator               | Thermo Fisher Scientific Inc. (Waltham, CA, USA) |
| Heraeus™ Fresco™ Centrifuge          | Thermo Fisher Scientific Inc. (Waltham, USA)     |
| HERAsafe™ KS Workbench               | Thermo Fisher Scientific Inc. (Waltham, USA)     |
| LAS-3000™ Luminescent Image Analyzer | Fujifilm (Tokyo, Japan)                          |
| Light Microscope CKX31               | Olympus Europa GmbH (Hamburg, Germany)           |
| Mini-PROTEAN™ 3 Cell                 | BIO-RAD Laboratories (Hercules, USA)             |
| Mini Trans-Blot™                     | BIO-RAD Laboratories (Hercules, USA)             |
| Power Pac™ HC power supply           | BIO-RAD Laboratories (Hercules, USA)             |
| Power supply Power Pac™ HC           | BIO-RAD Laboratories (Hercules, USA)             |
| RCT basic Magnetic Stirrer           | IKA™ Laboratory equipment (Staufen, Germany)     |
| Tecan GENios™ Pro                    | Tecan Sunrise™ Tecan (Mannedorf, Switzerland)    |
| Vibrax VXR basic Shaker              | IKA™ Laboratory equipment (Staufen, Germany)     |
| Vi-Cell™ XR Cell Viability Analyzer  | Beckman Coulter (Fullerton, USA)                 |
| Vortex Shaker                        | VWR International Inc. (West Chester, USA)       |

### 3.1.5. Software

|                        |                                       |
|------------------------|---------------------------------------|
| AIDA™ version 4.06     | Raytest GmbH (Straubenhardt, Germany) |
| Image Reader LAS-3000™ | Version 2.0 Fujifilm (Tokyo, Japan)   |
| Vi-Cell™ XR 2.03       | Beckman Coulter (Fullerton, USA)      |

## **3.2. Methods**

### **3.2.1. Cell culture**

#### 3.2.1.1. Vascular Smooth Muscle Cell Isolation and Cultivation

Vascular smooth muscle cells (VSMC) from thoracic aortas of Sprague-Dawley rats were kindly provided by Kathy K. Griendling (Emory University, Atlanta, USA). These cells were used in all experiments elaborating rat aortic VSMC. Human umbilical vein smooth muscle cells (HUVSMC) were kindly provided by David Bernhard (Allgemeines Krankenhaus, Vienna, Austria).

##### 3.2.1.1.1. Isolation

Besides the provided VSMC from KK Griendling, further VSMC were isolated from thoracic aortas of Fischer rats to learn the isolation procedure. The method was done as follows:

The aortas were cut out from rats and placed in PBS, cleaned from connective tissue and then cut longitudinally. After that the aortas were incubated for 15 min at 37 °C in digestion buffer (Ham's F-12 medium supplemented with 253 U/ml collagenase II, 10 mM HEPES, 0.28 mM ascorbic acid, and 0.1% bovine serum albumin). The adventitia and the endothelium were scrapped off and the aortas were dissected, followed by a second incubation in digestion buffer at 37 °C for 3 h to complete the enzymatic digestion. Hereupon the cells were harvested by centrifugation (10 min, 1100 rpm, 25°C) and then seeded with growth medium (Dulbecco's modified Eagle's medium supplemented with 2 mM L-glutamine, 100 U/ml penicillin, 100 µg/ml streptomycin, and 10% calf serum) in a 25 cm<sup>2</sup> flask. To verify the cells as VSMC they were incubated with a monoclonal anti- $\alpha$ -smooth muscle actin FITC-conjugated antibody (1:250 dilution, Sigma) and analyzed by fluorescence microscopy.

#### 3.2.1.1.2. Cultivation of VSMC

VSMC were grown at 37 °C and 5 % CO<sub>2</sub> in DMEM containing 2 mM glutamine, 100 U/ml penicillin/100 µg/ml streptomycin and 10% calf serum. Cells were passaged every 3 to 5 days. Cells of passages 5 to 15 were used for the experiments. For splitting, the growth medium was removed and cells were washed once with PBS, before incubation with 3 ml (per 75 cm<sup>2</sup> flask) trypsin/EDTA for around 2 min. Trypsin-reaction was stopped with 7 ml of 10% CS containing DMEM, followed by centrifugation for 4 min at 1,250 rpm. 1.5 x 10<sup>6</sup> cells were seeded per 75 cm<sup>2</sup> flask. Basic cell parameters were routinely checked using a cell viability analyzer (ViCell™, Beckman Coulter, USA).

#### 3.2.1.1.3. Storage

For rat aortic VSMC it is possible to freeze and thaw the cells without significant loss of viability.

Freezing of VSMC was done by harvesting through trypsinization, followed by centrifugation and resuspension in ice-cold freezing medium (containing 10% DMSO). Approximately 1 x 10<sup>6</sup> cells/ml suspension was frozen in cryo-vials. First cells were incubated at -20 °C for one day, then at -80 °C for three days before they were long-term stored in liquid nitrogen at -196 °C.

Thawing of the cells was done by warming the cryo-vials to 37 °C and immediate suspension in warm 20 ml growth medium in 75 cm<sup>2</sup> flasks. The growth medium was changed after 24 h.

#### 3.2.1.1.4. Smooth muscle alpha-actin staining

The alpha-type actin is specific for vascular smooth muscle cells (Gabbiani et al., 1981).

To verify the identity of the cells that we obtained, VSMC were seeded at a density of 2 x 10<sup>5</sup> cells/well on coverslips in 12-well plates. After 24 h they were washed once with ice-cold PBS and then fixed with 1 ml of 1:1 acetone/MeOH



for 5 min on ice. After that the cells were washed twice with ice-cold PBS. Coverslips were incubated with 20 µl of antibody solution (FITC-conjugated smooth muscle alpha-actin antibody diluted 1:250 in PBS containing 1% BSA) for 60 min on 4 °C at dark. Subsequently the coverslips were washed twice with PBS, fixed on a glass slide using mounting medium (Sigma Aldrich, MO, USA) before drying overnight in the dark. Cells were analyzed using a fluorescence microscope (Olympus BX51, Olympus Europe GmbH, Hamburg, Germany) and cell imaging software (cell<sup>^</sup>F software, Europe GmbH, Hamburg, Germany).

### 3.2.2. SDS gel electrophoresis and western blot analysis.

#### 3.2.2.1. Whole cell protein lysate

For cell lysate, cells were grown in 60 mm dishes to ~80% confluency and treated as described. Then cells were washed once with ice-cold PBS and lysed with freshly prepared lysis buffer (100 µl per 6 cm dish; for composition see 3.1.2.) for 5 min on ice. Afterwards the cell debris was scraped off and lysate were cleared by centrifugation at 13,000 rpm for 10 min at 4 °C. 5 µl of the lysate was used for quantification of protein amount by the Bradford method (as described below). 90 µl of the supernatant were diluted 1:3 with 3 x SDS sample buffer (containing 15% 2-mercaptoethanol), and then boiled for 5 min at 95 °C and stored at -20 °C.

#### 3.2.2.2. Protein quantification

The amount of protein was determined using the Bradford method. This method uses the dye Coomassie Brilliant Blue G-250, whose absorbance maximum after binding to proteins is increased from 465 nm to 595 nm. The protein lysate was diluted in ddH<sub>2</sub>O 1:10. 10 µl were transferred into a 96-well plate. Every sample was measured in triplicate. As a calibration curve, different concentrations of BSA in water were used (50-500 µg/ml). 190 µl

diluted Bradford reagent (1:5 dilution in water, Roti® - Quant, Roth) was added to the standards and the samples. Afterwards the plate was incubated for 1 min and measured using a microplate absorbance reader at 595 nm (Tecan Sunrise™ microplate reader). Protein concentrations were calculated using the calibration curve.

### 3.2.2.3. SDS-PAGE

The protein separation was done according to Laemmli with a sodium dodecyl sulphate-polyacrylamide gel electrophoresis (SDS-PAGE).

These gels were prepared using a 30% solution of PAA/0.8% bisacrylamide and a Mini-PROTEAN™ 3 Cell System (BIO-RAD). The concentration of PAA in the resolving gel was 10% in all cases. The protein amount loaded on the gel was 25 µg for all targets and separated by electrophoresis (100 V for 21 min to stack proteins and at 200 V for 36 min to separate proteins).

### 3.2.2.4. Western blotting and detection

The blotting of the separated proteins on a PVDF membrane was done by a tank blotting technique. By applying 100 V for 90 min in a Mini Trans-Blot™ Electrophoretic Transfer Cell System (BIO-RAD) the proteins were transferred. Then membranes were blocked with 5 % fat-free milk powder in 1 X TBS-T for at least 1 h and washed three times with 1 X TBS-T for 10 min, followed by incubation with specific antibodies at 4 °C overnight. The antibodies were diluted as stated above. After washing the membranes three times for 10 min with 1 X TBS-T they were incubated with the respective horseradish-peroxidase conjugated secondary antibodies for 2 h. Subsequently membranes were washed three times with 1 X TBS-T for 10 minutes and incubated with ECL-solution before visualization of the protein bands by detection with a LAS-3000™ (Fujifilm) luminescent image analyzer. The band intensity was specified by densitometric analysis using AIDA software (Raytest).

### 3.2.3. Flow cytometry

Depending on the distribution of cells in the G0/G1-, S-, and G2/M-phase of the cell cycle the content of DNA varies and is characteristic for each phase. Cells in the G0/G1-phase have a diploid set of chromosomes and cells in G2/M-phase have a doubled one. The S-phase cells appear between G0/G1- and G2/M-populations due to the progressive DNA-synthesis.

To analyze the effect of tylophorine on cell cycle distribution flow cytometry (FACSCalibur, BD Biosciences) was used. It is a method to analyze individual cells suspended in a fluid to analyze cell cycle distribution, apoptosis or intra- or extracellular fluorescently labeled proteins. To determine cell cycle stages, apoptosis and DNA-synthesis in VSMC we used the below described methods.

#### 3.2.3.1. Propidium iodide staining

The cell cycle distribution of VSMC and HU VSMC was determined after propidium iodide (PI) staining according to Riccardi and Nicoletti in 2006. PI, is capable of labeling DNA by stoichiometrically binding to nucleic acids. Therefore, the fluorescence emission is proportional to the DNA content of a cell and can be detected by flow cytometry with 562-588 nm filters.

For the PI staining of PDGF-BB-stimulated cells, VSMCs were seeded into 12-well plates ( $1 \times 10^5$  cells/well), serum-starved, pretreated with test compounds or vehicle (DMSO 0.1%) for 30 min, and subsequently stimulated with PDGF-BB (20 ng/ml). After indicated time points, cells were trypsinized, fixed with ice-cold hypotonic fluorochrome solution buffer [0.1% (w/v), sodium citrate 0.1% (v/v), and Triton X-100 in PBS] containing 50 µg/ml PI, and incubated for 2 h at 4°C.

For the PI staining of CS-stimulated cell, VSMC were seeded in 6-well plates ( $5 \times 10^4$  cells/well) and remained in 10% CS-containing DMEM. After 24 h VSMC were treated with test compounds or vehicle (DMSO 0.1%) for the indicated time, and subsequently trypsinized, fixed with ice-cold hypotonic

fluorochrome solution buffer containing 50 µg/ml PI, and incubated for 2 h at 4°C.

All experiments with HUVSMC were performed in the same way. Cells were analyzed by flow cytometry on a FACSCalibur (BD Biosciences, San Jose, CA) by using CellQuest™ Pro software. Experiments were done in triplicate.

### 3.2.3.2. BrdU/7-AAD staining and flow cytometry

In order to analyze the influence of a compound on the cell cycle machinery, cycling cells can be arrested for example in S-phase by aphidicolin, an inhibitor of DNA-polymerase alpha and delta.

To analyze the effect of tylophorine on DNA-synthesis in the S-phase of the cell cycle, a two-colour flow cytometric analysis was used (FITC BrdU Flow Kit (BD Pharmingen, USA). Bromodeoxyuridine (BrdU) is an analogue of the DNA precursor thymidine and is incorporated into newly synthesized DNA by cells progressing through S-phase. The incorporated BrdU is stained with specific anti-BrdU fluorescent antibodies. The levels of cell-associated BrdU are then measured by flow cytometry. Furthermore, the BrdU staining is coupled with a 7-amino-actinomycin D (7-AAD) staining, a dye binding to total DNA similar to propidium iodide. With this combination, the enumeration and characterization of cells that are actively synthesizing DNA and the simultaneous evaluation of cell cycle phase is possible.

For the analysis of PDGF-BB-stimulated VSMCs, cells were seeded in a 6-well plate ( $1 \times 10^5$ /well) and starved in 2 ml starving medium for 24 h. Then cells were stimulated for 4 h with PDGF-BB, treated with aphidicolin (1 µM) for 15 h and then washed twice with PBS. After washing, 2 ml DMEM/well and 10 µM BrdU each well were added as well as 2 µM of aphidicolin for negative control, 0.1% of DMSO for positive control and 1 µM tylophorine as test compound. After 2 h, 4 h, 6 h, 8 h samples were prepared for FACS analysis with BrdU Flow Kit and therefore double stained with BrdU and 7-amino-actinomycin D (7-AAD).

Furthermore VSMC were analyzed without previous synchronization by mitogen starvation. Here VSMC were seeded in a 6-well plate ( $1 \times 10^5$ /well). The next day cells were treated with 1  $\mu$ M tylophorine for 30 min. Then 10  $\mu$ M BrdU was added to each well. After 24 and/or 48 h of treatment samples were prepared for FACS analysis with BrdU Flow Kit and double stained with 7-amino-actinomycin D (7-AAD).

### 3.2.3.3. Annexin V-FITC staining

In apoptotic cells, phosphatidylserine PS is translocated from the inner to the outer leaflet of the plasma membrane, exposing PS to the external environment, whereas in normal cells PS is located on the cytoplasmic side of the cell membrane. Annexin V has a high affinity for PS. To analyze if the compound induces apoptosis an Annexin V-FITC Apoptosis Detection Kit (abcam, Cambridge, USA) was elaborated.

The method is shortly presented:

VSMC were seeded in a 12-well plate ( $1 \times 10^5$  cells/well), starved in 2 ml DMEM for 24 h, then stimulated with PDGF-BB and treated with 1  $\mu$ M tylophorine, 0.1% DMSO as negative or 1 mM H<sub>2</sub>O<sub>2</sub> as positive control for 24 h. Then cell were collected by centrifugation and resuspended in 500  $\mu$ l of 1 X Annexin V Binding Buffer. After that, 5  $\mu$ l of Annexin V-FITC and/or 5  $\mu$ l PI were added and cells were incubated for 5 min at room temperature in the dark. Then VSMC were analyzed for Annexin V-FITC binding by flow cytometry (excitation = 488 nm; emission = 530 nm) using FACSCalibur (BD Biosciences, San Jose, CA) with CellQuest™ Pro software. Experiments were done in three independent experiments.

#### 3.2.3.4. Mitotracker green staining

For the measurement of the total mitochondrial mass per cell a MitoTracker® Green FM (Molecular Probes (Invitrogen)) staining agent was elaborated.

For the mitochondrial staining of CS stimulated cells, VSMC were seeded in 6-well plates ( $2 \times 10^4$  cells/well), remained in 10 % CS containing DMEM. After 24 h VSMC were treated with tylophorine or DMSO 0.1% for the indicated time, and subsequently trypsinized, fixed with ice-cold hypotonic fluorochrome solution buffer containing 200 nM MitoTracker Green® and incubated for 2 h at 4°C.

All experiments with HUVSMC were performed in the same way. Cells were analyzed by flow cytometry on a FACSCalibur (BD Biosciences, San Jose, CA) by using CellQuest™ Pro software. Experiments were done in triplicate.

#### 3.2.4. Proliferation assays

##### 3.2.4.1 Crystal violet staining

The crystal violet staining assay is an easy and cost effective method and delivers useful hints about the anti-proliferative activity of a compound. Crystal violet binds to DNA and stains cell nuclei. The optical density is measured by absorbance at 595 nm. Results represent the overall biomass of cells in a well.

In this assay VSMC were seeded into 96 well plates ( $2 \times 10^4$  cells/ well), serum-starved for 24 h, pretreated with tylophorine or vehicle (DMSO 1%) for 30 min prior to stimulation with PDGF-BB (20 ng/ml). After 48 h cells were washed three times with PBS, immediately fixed and stained with crystal violet staining solution [0.5% (m/v) crystal violet in 20% MeOH] for 15 min at room temperature. Plates were washed with dH<sub>2</sub>O and dried. After that, the dye was resolved in ethanol/sodium citrate solution [50% (v/v) sodium citrate in ethanol]. The optical density was determined using a 96-well plate reader (TECAN Sunrise™, Männedorf, Switzerland).

#### 3.2.4.2. 5-Bromo-2'-deoxyuridine incorporation assay

5-bromo-2'-deoxyuridine (BrdU) incorporation during S-phase of the cell cycle can be used as measurement of DNA synthesis. For this method a cell proliferation kit (Cell proliferation ELISA (Chemiluminescent) - Roche Diagnostics) was employed. VSMCs were seeded into black clear bottom 96-well plates ( $1 \times 10^4$  cells/well), serum-starved for 24 h, pretreated with tylophorine/test compound or vehicle (DMSO 0.1%) for 30 min, and subsequently stimulated with PDGF-BB (20 ng/ml) or 10 % calf serum. After 30 min, 10  $\mu$ M BrdU was added, and cells were further cultivated for 20 h. Then, cells were fixed, washed and incubated with an enzyme-coupled anti-BrdU antibody according to the manufacturer's instructions. To determine the relative light units a 96-well plate reader was used (Tecan GENios Pro; Männedorf, Switzerland). Three independent experiments were always performed.

#### 3.2.4.3. Resazurin conversion assay

Viability of VSMC was assessed by Resazurin conversion. Resazurin measures the metabolic activity of living cells. Viable cells continuously convert resazurin to resorufin, increasing the overall fluorescence and colour of the media surrounding the cells. Therefore the fluorescence is directly proportional to the number of resazurin converting cells and can be taken as a first measure for their proliferative capacity.

VSMC were seeded in transparent 96-well plates ( $1 \times 10^4$  cells/well), serum starved, pretreated with tylophorine or vehicle for 30 min and subsequently stimulated for 48 h with calf serum (10%). Then cells were washed with PBS and incubated in DMEM containing 10  $\mu$ g/ml resazurin for 2 h. Samples were measured by monitoring the increase in fluorescence at a wavelength of 580 nm using an excitation wavelength of 535 nm in a 96-well plate reader (Tecan GENios Pro; Tecan Group Ltd., Männedorf, Switzerland).

### 3.2.5. RNA isolation and real-time qPCR analysis

#### 3.2.5.1. RNA isolation

For the RNA isolation  $8 \times 10^5$  VSMC were grown in 6 cm dishes. Total RNA was isolated using peqGOLD total RNA Kit (PEQLAB Biotechnologie) according to the manufacturer's instructions. VSMC were lysed with 400  $\mu$ l of lysis buffer, scraped from the dish and homogenized. DNA was removed by the supplied DNA removing columns. Then the samples were mixed with 70 % ethanol, shortly vortexed and applied to the RNA-binding columns. The bound RNA on the columns was washed three times and then dried by centrifugation at full speed (10,000 X g, 1 min). Afterwards RNA was eluted from the column in 50  $\mu$ l RNase-free H<sub>2</sub>O and quickly frozen at -80 °C.

The quality of the RNA was controlled on 1% -agarose gel [1.0 g agarose in 100 ml 1 x TBE, SYBR Safe DNA gel stain 10,000 X conc. (Invitrogen, Carlsbad, USA)]. 9  $\mu$ l of RNA solution was mixed with 1  $\mu$ l 10x sample buffer. A peqGold 1 kb DNA ladder (PEQLAB Biotechnologie) was used as control. Samples were separated at 120 V for 60 minutes using 0.5x TBE as running buffer. Bands were visualized by UV transillumination and scanned in a gel documentation system (Biostep).

#### 3.2.5.2. Reverse transcription

For mRNA analysis by qPCR technique, the RNA was converted to a complementary-DNA (cDNA). For this purpose the Superscript™ First-Strand Synthesis System (Invitrogen) was used. 500 ng of the RNA was mixed with 10 ng random hexamers, 1  $\mu$ l 10 mM dNTP mix (deoxyribonucleotides) and filled with DEPC-treated water to a total volume of 10  $\mu$ l. Samples were incubated at 65 °C for 5 min for denaturation of the RNA and left on ice for 1 min. In the meanwhile 2  $\mu$ l of 10x RT buffer, 2  $\mu$ l DTT (0.1 M), 4  $\mu$ l of MgCl<sub>2</sub> (25 mM) and 1  $\mu$ l RNaseOUT inhibitor (40 U/ $\mu$ l) were mixed. 9  $\mu$ l of this reaction mixture was added to each sample and left on room temperature for 2 min. Then 1  $\mu$ l Superscript™ II RT enzyme (50 U/ $\mu$ l) was added and left at 25 °C for further



10 min. Then the samples were incubated at 42 °C for 60 - 90 min before the enzyme was inactivated by heating the samples to 70 °C for 15 min. Before proceeding to amplification of the target cDNA the remaining RNA was digested by 1 µl RNase H. The cDNA was stored at -80 °C.

#### 3.2.5.3. Quantitative real-time PCR

For the quantification of specific mRNA expression level a quantitative real-time polymerase chain reaction (qPCR) was performed.

For this purpose, QuantiTect® Primer assays (Qiagen, Germany) for the different target genes and primers specific for 18S rRNA levels were used from (Invitrogen, USA). Differences in RNA levels were detected by using a LightCycler™ LC480 (Roche Diagnostics) system which detects fluorescence of the dye SYBR® Green. It is a dye that binds to double stranded DNA by intercalating with the minor groove of the DNA double helix. During PCR the DNA amount and the signal of intercalating SYBR® Green increases exponentially, which can be monitored in real-time. The assay was performed particularly employing Lightcycler™ 480 SYBR® Green I Master Mix (Roche Diagnostics, Switzerland). The cDNA of each sample was diluted in RNase-free water 1:10. The reaction mix contained 7.5 µl SYBR® Green I Master Mix, 1.5 µl primer solution and 4 µl PCR-grade water. 13 µl of the mixture was pipetted into each well of a PCR plate and 2 µl of the 1:10 diluted cDNA was added, followed by a brief spin in the centrifuge. The real-time qPCR was performed according to the manufacturer's instructions. Each sample was measured in triplicate. Data were analyzed using LightCycler™ LC480 software and further evaluated in Microsoft Excel.

#### 3.2.6. Transfection of VSMC

In order to transfect VSMC several methods were tested.

### 3.2.6.1. Fugene HD

The transfection of VSMC was performed in 12-well plates, using  $1 \times 10^5$  cells/well. Cells at 80% confluency were either covered by 750  $\mu$ l DMEM containing 10% CS or were mitogen starved for 24 h. First a separate vial was prepared with 25  $\mu$ l serum-free DMEM (HEPES 10 mM) and mixed with 1  $\mu$ g of DNA. Then 1.5  $\mu$ l/vial of Fugene HD was added followed by 15 min incubation. Before pipetting this mixture to the cells, 225  $\mu$ l of 10% CS-containing DMEM was added. Afterwards, the 12-well plate was centrifuged for 5 min at 800 g. Then,  $\text{ZnCl}_2$  was added to a final concentration of 250  $\mu$ M and incubated for 4 h on 37 °C. Finally, cells were washed with PBS and grown in fresh 10% CS containing DMEM over night.

### 3.2.6.2. Amaxa®

Amaxa® Nucleofector® Technology was suggested to be the ideal tool to transfect primary mammalian smooth muscle cells. For this purpose we used the Basic smooth muscle cell Nucleofector® kit [Lonza Group Ltd. (Basel, Switzerland)] and a Nucleofector® device. This technology is based on cell-type-specific solutions and optimized electrical parameters for electroporation.

The transfection of VSMC was done as follows:

VSMC were grown at 37°C and 5%  $\text{CO}_2$  in DMEM containing 2 mM glutamine, 100 U/ml penicillin/100  $\mu$ g/ml streptomycin, and 10% calf serum to 80% confluency in a 75 cm<sup>2</sup> flask. Cells between passages 8 to 12 were used. Growth medium was removed and cells were washed once with PBS, before incubation with 3 ml/75 cm<sup>2</sup> trypsin/EDTA for around 2 min. Trypsin-reaction was stopped with Trypsin neutralization solution (Invitrogen), followed by cell counting in a cell viability analyser (ViCell™, Beckman Coulter, USA).

$1 \times 10^6$  cells were resuspended in 100  $\mu$ l Nucleofector® Solution per sample at room temperature. Then the cell suspension was combined with 5  $\mu$ g DNA (GFP plasmid and NF $\kappa$ B luciferase plasmid), transferred into the supplied cuvette, electroporated with program A33 and added into 500  $\mu$ l pre-warmed

growth medium. This mixture was then transferred into 6-well plates and incubated at 37 °C and 5% CO<sub>2</sub> for 18 hours. Then, transfected cells were treated with compound and/or stimulus before further analysis.

#### 3.2.6.3 Analysis of VSMC transfection

For the analysis of the transfection efficiency we employed a Luciferase Kit (Promega). Every 6-well was lysed with 200 µl of the supplied lysis buffer. 50 µl of the cell lysate was transferred into a black bottom 96-well plate before measurement in a 96-well plate reader (Tecan GENios Pro; Tecan Group Ltd., Männedorf, Switzerland). Samples were measured by monitoring the increase in fluorescence at a wavelength of 520 nm using an excitation wavelength of 485 nm for the green fluorescence protein (GFP) levels. Luminescence of the luciferase was detected with an integration time of 2000 ms.

#### 3.2.7. Transfection of HEK-293 cells

HEK-293 cells were transfected with the calcium phosphate transfection method in a 6-well plate, with a NFκB reporter gene plasmid, p50, p65, eGFP or empty vector. 100.000 HEK-293 cells were seeded in 10% FBS containing DMEM, 2 mM glutamine and 100 U/ml penicillin/100 µg/ml streptomycin.

For tranfections 85 µl of H<sub>2</sub>O, 1 µg of DNA and 12.5 µl of 2 x 2 M CaCl<sub>2</sub> were mixed and added drop wise to 100 µl of a 2 × HBS solution. After incubation for at least 10 min at RT, the mixture was vortexed added drop wise to the cell culture dish and incubated over night. The analysis of HEK-293 transfection was performed as described in 3.2.3.6 for VSMC.

### 3.2.8. Wound healing assay (adapted from Christa Czaloun)

For the wound healing or scratch assay cells were grown to a confluent monolayer, scratched, and the area of the scratch was determined before and after PDGF-BB stimulation. To exclude that proliferation contributes to scratch closure the assay was stopped after 20 h because the VSMC used divided 26 - 28 h after stimulation. VSMC were seeded in 6-well plates ( $0.8 \times 10^6$  cells/ well). To ensure that at 0 h and 20 h the very same area of each scratch is captured perpendicular lines were drawn at the bottom side of the plates. When confluence was reached after 24 h, cells were serum-starved for another 24 h, scratched with a 1000- $\mu$ l pipette tip and after washing with PBS further serum-starved for 24 h. Cells were pretreated with test compounds or vehicle (DMSO 1%) for 30 min and subsequently stimulated with PDGF-BB (10 ng/ml) for 20 h. The scratch area was captured with a light microscope just before PDGF-treatment and 20 h later. The cell re-colonization rate was evaluated by measuring the cell free area of each scratch, using Cell Profiler software (Broad Institute, Cambridge, MA, USA).

### 3.2.9. Saphenous vein model (adapted from Iris Zeller)

This assay was performed by Iris Zeller in the laboratory of Prof. David Bernhard, Allgemeines Krankenhaus (AKH) in Vienna.

For organ culture experiments, remnants of saphenous veins from patients undergoing CABG were collected, opened longitudinally, attached to silicone patches and incubated with culture medium (RPMI 1640, 30% serum, heparin 8 mU/mL, antibiotics) for 2 weeks to induce intimal hyperplasia. The potential inhibition of intimal hyperplasia by tylophorine was tested by the addition of different concentrations of tylophorine, or DMSO to the organ cultures. The medium containing tylophorine or DMSO was replaced by fresh medium every second day. Baseline samples were fixed directly after preparation of fresh tissue and represent the status of the vessel prior to organ culture (adopted from Reisinger U et al., 2009).

### 3.2.10. Statistical analysis

Data are expressed as means  $\pm$  SD, if not stated otherwise. Statistical significance was determined by ANOVA using Tukey post hoc test.

## **4. RESULTS**

## 4. Results

### 4.1. Characterization of Vascular Smooth Muscle Cells

VSMC from rat thoracic aortas of Sprague Dawley rats were provided as described in the materials and methods section. Further, rat VSMC from thoracic aorta of Fischer rats were isolated by myself. To confirm their identity cells were stained with a fluorescent-labeled  $\alpha$ -smooth muscle actin antibody (Fig. 4), a specific marker for vascular smooth muscle cells (Gabbiani G et al, 1981). No contamination with other cell types could be detected.

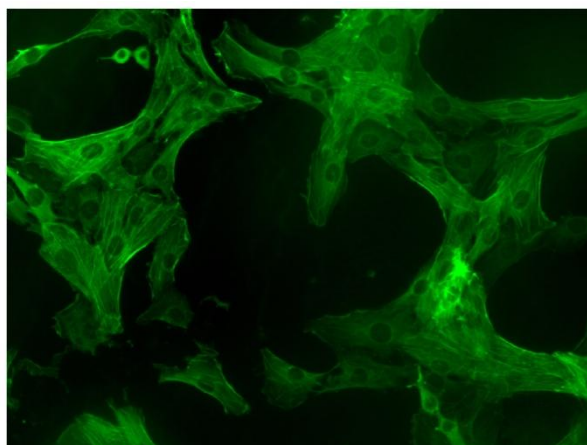


**Figure 4.** Smooth muscle alpha-actin staining of primary rat aortic vascular smooth muscle cells.

### 4.2. Impact of tylophorine on VSMC proliferation

#### 4.2.1. Inhibition of VSMC proliferation (crystal violet staining)

To investigate a potential anti-proliferative activity of tylophorine against VSMC we first used crystal violet to stain the biomass obtained after calf serum (CS) stimulation. VSMC were serum-starved, treated with the indicated concentrations of tylophorine and stimulated with 10% serum for 48 h prior to the addition of crystal violet. Figure 5 shows that tylophorine inhibits

proliferation of VSMC in a concentration dependent manner with highest inhibitory activity at 1000 nM.

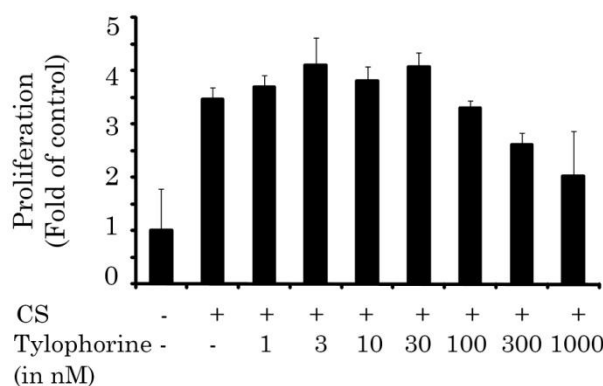


**Figure 5.** Tylophorine inhibits proliferation of serum stimulated VSMC. Serum-starved VSMC were pretreated with the indicated concentrations of tylophorine or DMSO (0.1%) for 30 min. Then, cells were stimulated with 10% serum for 48 h. The obtained biomass was quantified by crystal violet staining and subsequent spectrophotometric analysis. (mean  $\pm$  SD,  $n = 3$ )

This assay is fast, easy and cost effective and delivers first useful but rough hints about the anti-proliferative properties of a compound. In order to confirm growth inhibition by tylophorine with a more precise method, we next assessed the amount of DNA replication in the presence of tylophorine.

#### 4.2.2. Inhibition of VSMC proliferation (DNA-synthesis)

To determine the ability of tylophorine to interfere with DNA replication/synthesis in the cell, we performed a BrdU-incorporation assay. Here, we used PDGF-BB instead of calf serum as stimulus to trigger the proliferation of VSMC. PDGF-BB is the most potent pro-proliferative mitogen for VSMC and its usage limits the range of activated signaling pathways in the cell compared to serum which contains multiple growth factors.



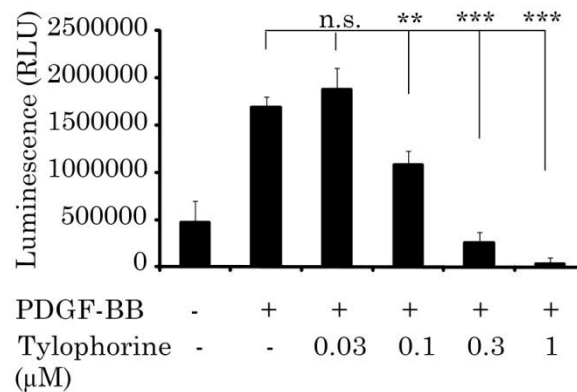


**Figure 6.** Serum-starved VSMC were pretreated with the indicated concentrations of tylophorine or DMSO (0.1%) for 30 min, BrdU (10 μmol/L) was added and cells were stimulated with PDGF-BB (20 ng/ml) for 20 h. Incorporation of BrdU was measured at the end of the stimulation period. (mean  $\pm$  SD,  $n = 3$ , \*\*  $p < 0.01$ , \*\*\*  $p < 0.001$  ANOVA/Tukey).

We added tylophorine in concentrations ranging from 1 nM to 1000 nM to PDGF-BB-activated (20 ng/ml) VSMC. The assessment of DNA synthesis shows that tylophorine potently inhibits PDGF-BB-induced proliferation in a dose-dependent manner with an  $IC_{50}$  of 128.15 nM ( $\pm$  44 nM) and a complete block at 1 μM (Fig. 6).

#### 4.2.3. Accumulation of VSMC in G1-phase

Due to the strong inhibition of DNA-synthesis by tylophorine in VSMC, we further analyzed its effect on the progression of cells through the cell cycle phases. Quiescent VSMC were treated with tylophorine and PDGF-BB for 20 h and then stained with propidium iodide (PI) to allow flow cytometric measurement of the DNA-content of single cells (Fig. 7). PDGF-BB stimulation of VSMC leads to progression through the cell cycle as seen by higher percentages of cells in S-/G2-phase compared to serum-starved cells being in G1-G0 of the cell cycle. Tylophorine-treated (300 nM and 1 μM) VSMC showed

an accumulation of cells in G1-phase of the cell cycle similar to the starved unstimulated cells. A clear subG1-peak indicative for cell death was not observed.

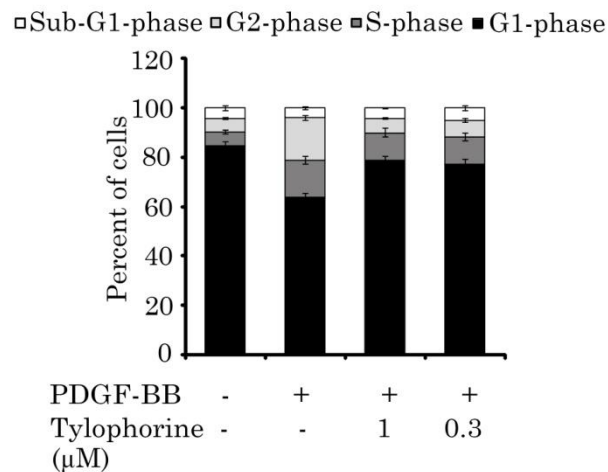


**Figure 7.** VSMC were synchronized by starvation, treated with 1 μM tylophorine or vehicle as indicated and then stimulated for 20 h with PDGF-BB (20 ng/ml). Afterwards VSMC were stained with propidium iodide. DNA contents were measured by flow cytometry. (mean  $\pm$  SD, n = 3).

Drawback of this method is that it is difficult to clearly distinguish between apoptotic and necrotic cells or cell debris due to distortion of the cells during the experimental procedure. Furthermore, it is not possible to distinguish between a true G1-phase or a very early S-phase arrest. Therefore, we went on, first, to prove that tylophorine is not inducing apoptosis and, second, to analyze its ability to stop VSMC in S-phase of the cell cycle.

#### 4.2.4. Tylophorine does not induce apoptosis

To test whether tylophorine is inducing apoptosis in VSMC we used an Annexin V-FITC Apoptosis Detection Kit as described in the material and methods part. In apoptotic cells, phosphatidylserine PS is translocated from the inner to the outer leaflet of the plasma membrane, exposing PS to the

external environment, whereas PS is in normal cells located on the cytoplasmic side of the cell membrane. Annexin V has a high affinity for PS.

Figure 8 depicts the amount of annexin V positive VSMC in a DMSO-, tylophorine- or H<sub>2</sub>O<sub>2</sub>-treated population. The DMSO control contained 5 % of annexin V positive cells, whereas the H<sub>2</sub>O<sub>2</sub> treated cell population, used as positive apoptotic control, showed around 25 % positive VSMC. The amount of annexin V positive cells in the tylophorine-treated cell population is on the level of the negative control. Therefore, treatment of VSMC with 1  $\mu$ M tylophorine does not induce apoptosis.

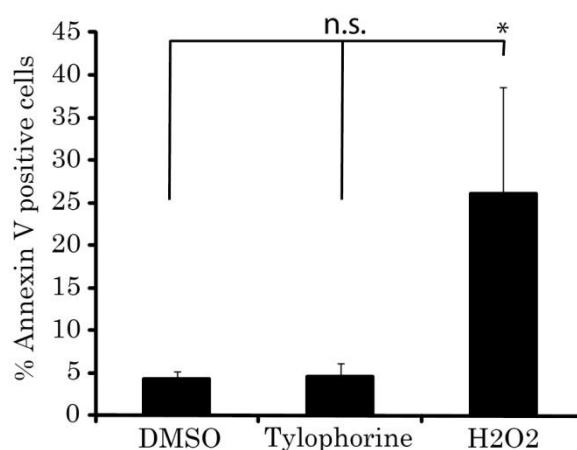


**Figure 8.** VSMC were starved for 24 h, then stimulated with 20 ng/ml PDGF-BB and treated with 1  $\mu$ M tylophorine, 0.1% DMSO as negative or 1 mM H<sub>2</sub>O<sub>2</sub> as positive control for 24 h. VSMC were analyzed for Annexin V-FITC binding by flow cytometry. The amount of annexin V positive cells in the tylophorine-treated cell population is on the level of the negative control (mean  $\pm$  SD,  $n = 3$ , \*  $p < 0.05$ , ANOVA/Tukey).

#### 4.2.5. Tylophorine is not an S-phase, but a true G0/G1-arrestor

To further examine if tylophorine is a true G1- and not an early S-phase-arrestor, VSMC were treated with 1  $\mu$ M aphidicolin, a reversible inhibitor of DNA-polymerase  $\alpha$  and  $\delta$ , which stops the cell cycle in early S-phase (Fig. 9). After removal of aphidicolin, cells were treated with 1% DMSO or aphidicolin or 1  $\mu$ M tylophorine and examined for BrdU incorporation. Continuing

treatment with aphidicolin completely inhibits BrdU incorporation (the percentage of BrdU-incorporating cells is around 1%), whereas treatment with 1  $\mu$ M tylophorine and DMSO allows BrdU incorporation and thus progression through S-phase. Compared to DMSO, tylophorine treated cells pass slower through S-phase as seen by a lag in BrdU incorporation (up to 30% after 6 h).

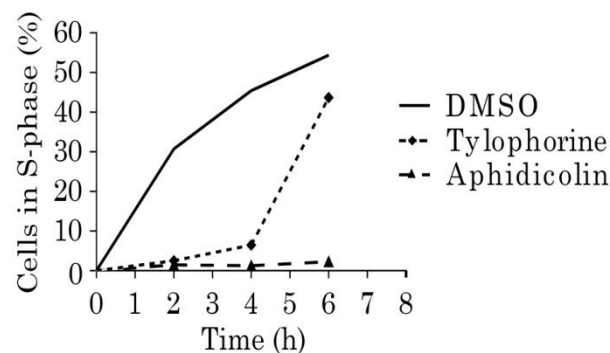


**Figure 9.** Cells were treated with 1  $\mu$ M aphidicolin. After removal of aphidicolin, cells were either treated with 1% DMSO, 1  $\mu$ M aphidicolin or 1  $\mu$ M tylophorine, and examined for BrdU incorporation indicative for a progression into S-phase of the cell cycle. This diagram demonstrates the BrdU incorporation 2 h to 8 h after aphidicolin removal. FACS data presented are representative of those obtained in at least three separate experiments with consistent results.

Overall, these findings indicate that tylophorine dose dependently inhibits VSMC proliferation by arresting starved cells in the G0/G1-phase of the cell cycle, without inducing apoptosis in concentrations up to 1  $\mu$ M.

To consolidate that tylophorine is a true G1-phase arrestor in rat aortic VSMC we investigated the phosphorylation status of the retinoblastoma protein, which is an important regulator of the G1/S-phase transition of the cell cycle. S-phase entry is highly regulated and the hyper-phosphorylation of the retinoblastoma protein is a prerequisite (Sherr CJ and Roberts JM, 1999). Treatment of rat aortic VSMC with PDGF-BB (20 ng/ml) led to a time-dependent increase in phosphorylation of the retinoblastoma protein on residue S807/811 which is blocked by 1  $\mu$ M tylophorine (Fig. 10). These data

underline that tylophorine is a G1-phase-arrestor in PDGF-BB-activated rat aortic VSMC.

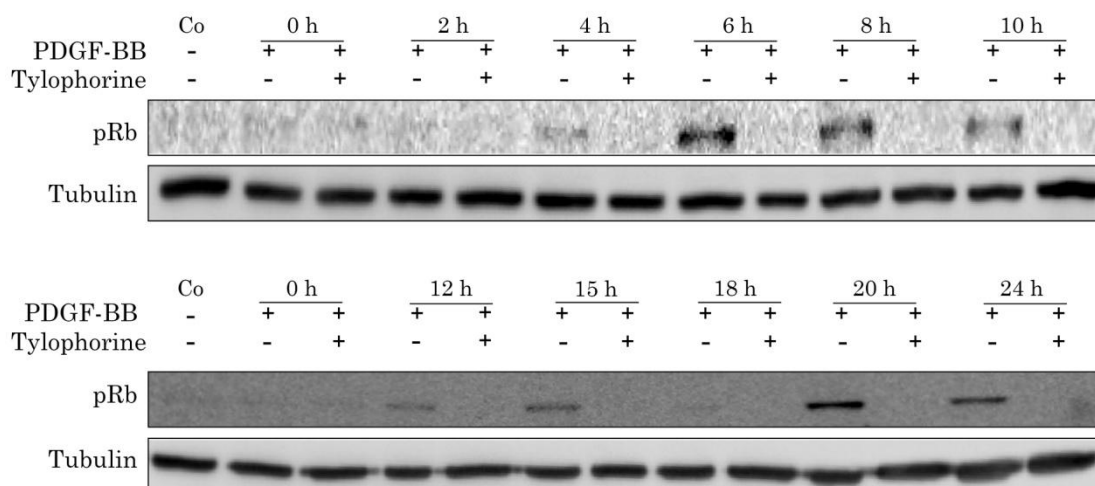


**Figure 10.** As control (Co) mitogen-starved quiescent VSMC were used. VSMC were stimulated with PDGF-BB (20 ng/ml) as indicated in the presence/absence of tylophorine, lysed and subjected to western blot analysis for pRb and tubulin. Western blot data presented are representative of those obtained in at least three separate experiments with consistent results.

### 4.3. Influence of tylophorine on signaling cascades

#### 4.3.1. Early PDGF-BB-induced signaling events

In order to get insight into the underlying mode of action, we next examined important early key signaling molecules leading to proliferation in VSMC upon PDGF-BB stimulation. These include the kinase Akt, the mitogen-activated protein (MAP)-kinases Erk 1/2 (p42/p44), p38MAPK and c-Jun N-terminal kinase (JNK), and the Signal transducer and activator of transcription 3 (STAT3) (Fig. 11).

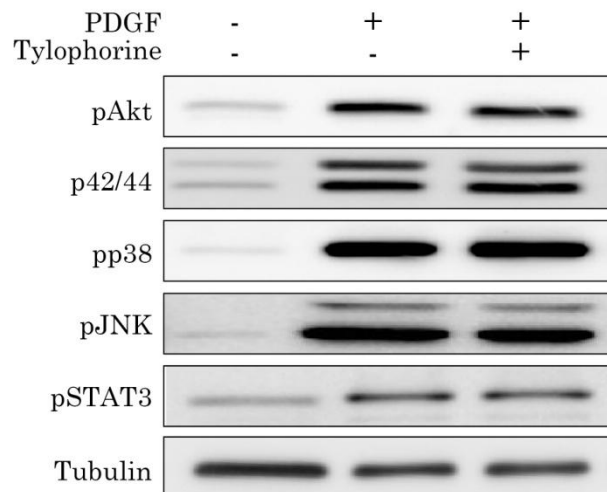


**Figure 11.** Tylophorine has no influence on key molecules of the early PDGF-BB signaling. Quiescent VSMC were stimulated with PDGF-BB (20 ng/ml) for 10 min in the presence/absence of tylophorine (1  $\mu$ M) or vehicle, lysed and subjected to western blot analysis for the depicted proteins. Western blot data presented are representative of those obtained in at least three separate experiments with consistent results.

As seen in figure 11, PDGF-BB (20 ng/ml) treatment for 10 min leads to phosphorylation of the kinase Akt, p42/44, p38, JNK and transcription factor STAT3. Preincubation of cells with 1  $\mu$ M tylophorine for 30 min followed by stimulation with PDGF-BB did not influence the phosphorylation of these early signaling kinases. Therefore tylophorine is not causing a G1-phase arrest via inhibition of these kinases or transcription factors.

#### 4.3.2. Role of NF $\kappa$ B in PDGF-BB signaling

In many cell types the transcription factor Nuclear factor  $\kappa$ B (NF $\kappa$ B) regulates cell cycle progression and proliferation. However, the role of NF $\kappa$ B for the proliferation of VSMC is controversial (Selzman CH et al., 1999; Erl W et al., 1999; Mehrhof FB et al., 2005). Therefore, we needed to verify the influence of PDGF-BB on the activation of NF $\kappa$ B and a possible modulation by tylophorine.

#### 4.3.2.1. NF $\kappa$ B-luciferase reporter gene assay

To investigate a putative influence of tylophorine via the NF $\kappa$ B pathway on the proliferation of VSMC we aimed to perform NF $\kappa$ B-dependent luciferase reporter gene assays. For this reason, transfection of VSMC with plasmids containing an NF $\kappa$ B-dependent reporter gene, were obligatory. Due to general problems with viability of VSMC after transfection we had to try several different transfection agents and methods.

According to literature, primary SMC should be transfectable with plasmids/vectors using Fugene 6 reagent (Elmadbouh I et al., 2004). The transfection was performed as described in materials and methods section. First tests with Fugene 6 showed a low transfection efficiency using a GFP plasmid (< 10% GFP-positive cells). The usage of Fugene HD reagent increased the number of GFP-positive cells. Still, in our primary cells the transfection efficiency with GFP, analyzed by fluorescence microscopy, was too low to perform conclusive experiments. Therefore, we tried a different method using the Amaxa system, as described in materials and methods, which combines liposomal and electroporetic Transfection procedures. However, here the biggest occurring problem was cell death (< 5% viable cells 24 h after transfection).

To check the vectors for the reporter gene luciferase assay and verify that they are not the source of our problems, the transfection was performed in human embryonic kidney (HEK) cells, followed by analysis of fluorescence and luminescence of each sample.

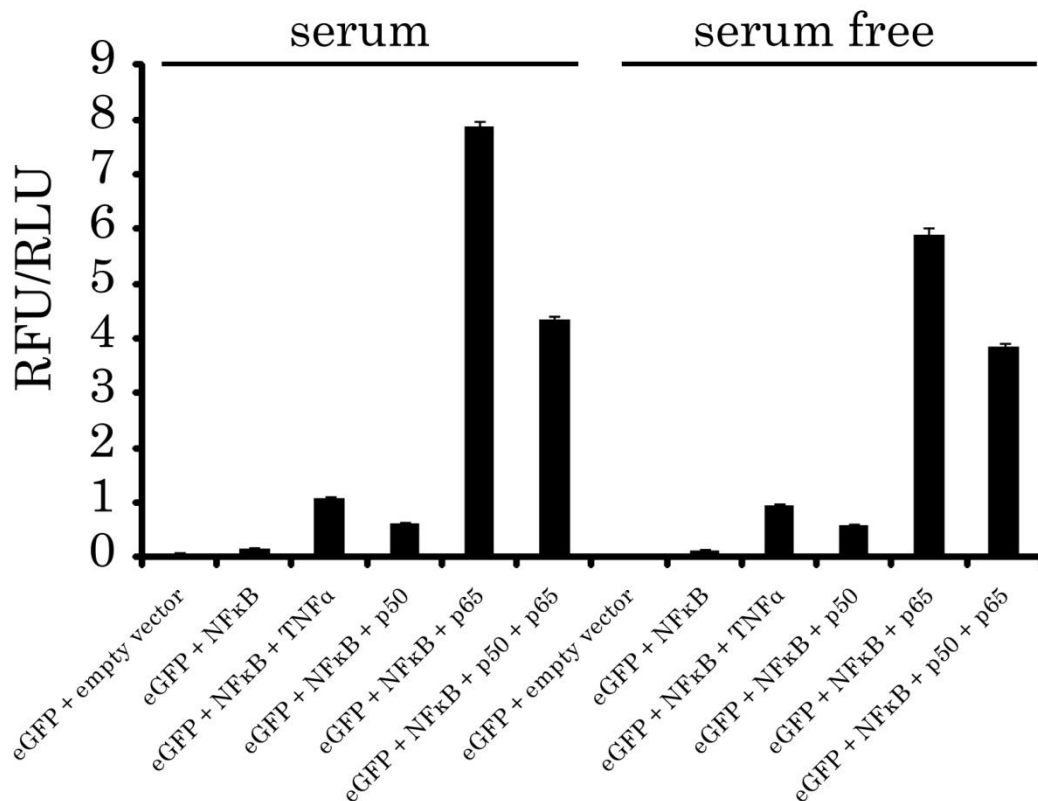


**Figure 12.** HEK cells were transfected, using the calcium phosphate method, with the following vectors for expression: pcDNA3 as empty vector, eGFP, NFκB-Luc, p50 of NFκB (pRSV) and p65 of NFκB (pRSV). Cells transfected with eGFP, NFκB-Luc and p65 show highly increased luciferase activity. The empty vector (pcDNA3) alone has no influence on luciferase activity whereas cotransfection of NFκB and the p50 subunit leads to a minor increase of luminescence. TNFα (2 ng/ml) treatment of NFκB transfected cells slightly increases luciferase activity.

Figure 12 demonstrates that co-transfection of the expression vectors for NFκB and its subunit p65 highly increases luciferase activity of the NFκB-luc plasmid. The GFP expression was used for normalization. The empty vector pcDNA3 alone, which was used for negative control, has no influence on luciferase activity. Co-transfection of NFκB and the p50 subunit leads to a minor increase of luminescence. TNFα (2 ng/ml) treatment of single NFκB-luc transfected cells slightly increases luciferase activity. Therefore, we proved that the plasmids seem to work in a different cell type than VSMC.

Overall, despite major efforts and confirmed functional expression vectors, we were not able to succeed in sufficiently high transfection efficiency in VSMC to perform luciferase reporter gene assays in order to answer the question whether VSMC respond to PDG by activation of the NFκB pathway. Therefore we focused on IκBa levels.



#### 4.3.2.2. Tylophorine has no influence on I $\kappa$ B $\alpha$ levels

To exclude an inhibition of proliferation by tylophorine via inhibition of the transcription factor NF $\kappa$ B we investigated the inhibitor of  $\kappa$ B alpha (I $\kappa$ B $\alpha$ ) levels. I $\kappa$ B $\alpha$  needs to be degraded for NF $\kappa$ B activation (Ferreiro DU and Komives EA, 2010).

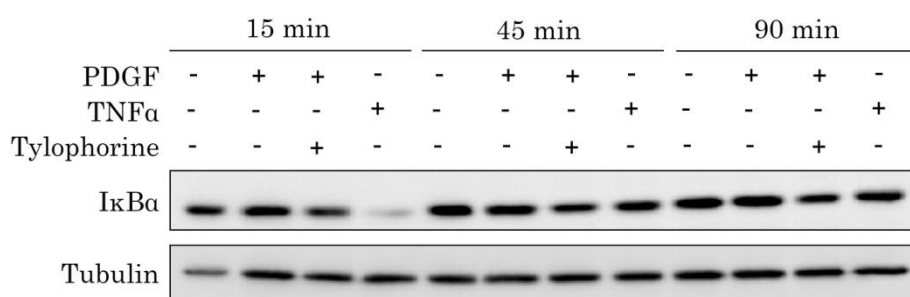


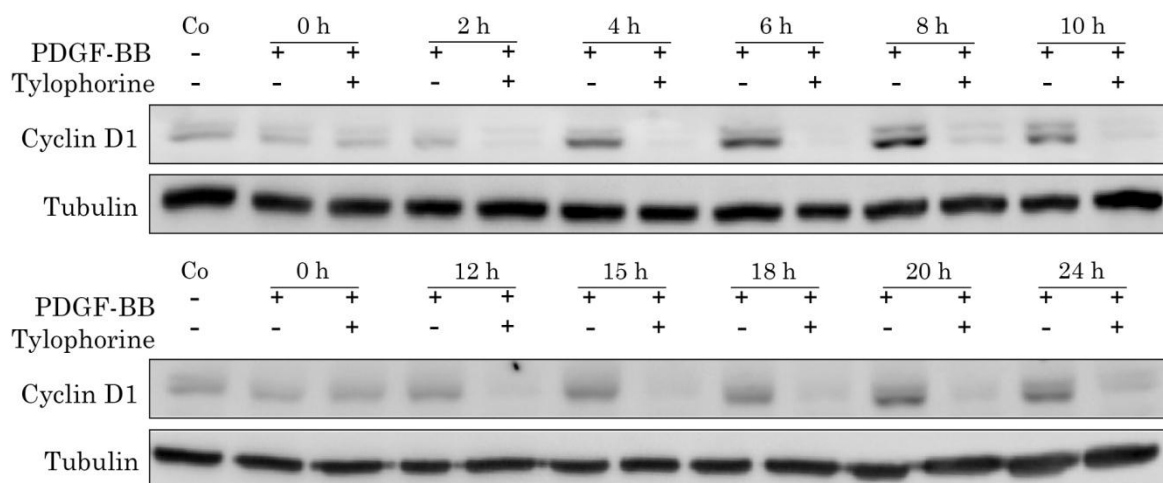
**Figure 13.** VSMC were stimulated with PDGF (20 ng/ml) or TNF $\alpha$  (10 ng/ml) for 15, 45 and 90 min in the presence/absence of 1  $\mu$ M tylophorine, lysed and subjected to western blot analysis. Western blot data presented are representative of those obtained in at least three separate experiments with consistent results.

We show (Fig. 13) that treatment of VSMC with TNF $\alpha$  (10 ng/ml) is leading to degradation of I $\kappa$ B $\alpha$  after 15 min. PDGF-BB is not inducing NF $\kappa$ B activation, demonstrated as an inability of PDGF-BB (20 ng/ml) to degrade I $\kappa$ B $\alpha$ . Furthermore tylophorine has no influence on I $\kappa$ B $\alpha$  levels. Hence, PDGF-BB is not activating NF $\kappa$ B by degradation of I $\kappa$ B $\alpha$  in rat aortic VSMC. Furthermore, tylophorine is not influencing NF $\kappa$ B-activation and therefore not inhibiting the PDGF-BB-induced proliferation of VSMC via this pathway.

#### 4.4. Cyclin D1 is down regulated by tylophorine

Next, we examined the cell cycle-regulatory protein cyclin D1 and its susceptibility to tylophorine. Cyclin D1 is considered to be G1-phase specific, the binding partner of CDK4/6 and essential for the phosphorylation of retinoblastoma protein (Sherr CJ and Roberts JM, 1999). Cyclin D1 up regulation is necessary for the cell to pass from G1- to S-phase of the cell cycle (Sherr CJ, 1995) and lack of cyclin D1 leads to a G1-phase arrest.

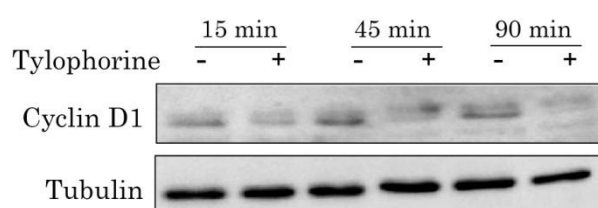
To see an influence of tylophorine on cyclin D1 protein levels we pretreated quiescent VSMC with 1  $\mu$ M tylophorine or vehicle and stimulated them with PDGF-BB (20 ng/ml) for the indicated time. PDGF-BB stimulation led to a time-dependent increase of cyclin D1 levels in control cells. Tylophorine-treated VSMC showed highly reduced cyclin D1 protein levels which are even lower than basal levels in control VSMC (Fig. 14).



**Figure 14.** Quiescent VSMC were stimulated with PDGF-BB (20 ng/ml) for the indicated time (0 h to 24 h) in the presence/absence of tylophorine (1  $\mu$ mol/L) or vehicle, lysed and subjected to western blot analysis. Western blot data presented are representative of those obtained in at least three separate experiments with consistent results.

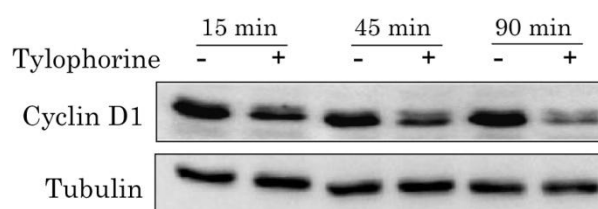
#### 4.5. Influence of mitogens on cyclin D1 expression levels

To check whether the down regulation of cyclin D1 by tylophorine occurs independent of the stimulus or cell cycle phase we investigated the cyclin D1 protein levels of mitogen-starved quiescent (Fig. 15) and calf-serum stimulated rat aortic VSMC (Fig. 16).



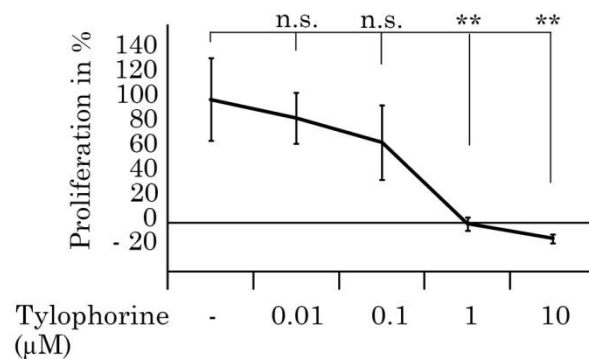
**Figure 15.** VSMC were serum-starved for 24 h and then treated with 1  $\mu$ M tylophorine or vehicle for 15, 45 and 90 min, lysed and subjected to western blot analysis for cyclin D1 and tubulin. Western blot data presented are representative of those obtained in at least three separate experiments with consistent results.

Figure 15 shows that tylophorine leads to down regulation of basal cyclin D1 expression levels in quiescent VSMC already within 15 min. In unsynchronized serum-stimulated VSMC, tylophorine leads to rapid down regulation of cyclin D1 expression levels as well (Fig. 16).



**Figure 16.** VSMC in 10% calf serum containing medium were treated without previous synchronization by starvation with 1  $\mu$ M tylophorine or vehicle for 15, 45 and 90 min, lysed and subjected to western blot analysis for the depicted proteins. Western blot data presented are representative of those obtained in at least three separate experiments with consistent results.

Compared to starved VSMC, serum-stimulated VSMC exhibit higher cyclin D1 levels in control and tylophorine-treated cells. Nevertheless, tylophorine has an inhibitory effect on proliferation in serum-stimulated VSMC as evident in a resazurin conversion assay (Fig. 17) ( $IC_{50} = 468 \text{ nM} \pm 144 \text{ nM}$ ). At  $1 \text{ } \mu\text{M}$  tylophorine proliferation of VSMC in serum is completely inhibited, as expected from the observed reduction of cyclin D1 in these cells.



**Figure 17.** VSMC were pretreated with the indicated concentrations of tylophorine or vehicle for 30 min and stimulated with 10 % calf serum for 48 h. Then cells were washed with PBS and incubated in  $10 \text{ } \mu\text{g/ml}$  resazurin containing DMEM for 2 h. Samples were measured by monitoring the increase in fluorescence at a wavelength of 580 nm using an excitation wavelength of 540 nm in a 96-well plate reader. (mean  $\pm$  SD,  $n = 3$ , n.s. = not significant, \*\*  $p < 0.01$ , ANOVA/Tukey)

#### 4.6. Influence of tylophorine on cyclin A

To demonstrate the specificity of cyclin D1 degradation, we further analyzed the cell cycle-regulatory protein cyclin A and its susceptibility to tylophorine by western blotting. Cyclin A is necessary for S-/G2-phase progression and the binding partner of CDK2 (Voitenleitner C et al., 1997). Here, VSMC were pretreated with  $1 \text{ } \mu\text{M}$  tylophorine or vehicle and stimulated with 10% calf-serum for the indicated time.

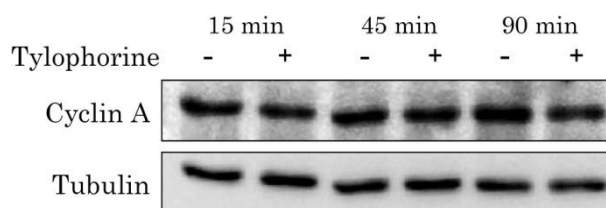


**Figure 18.** VSMC were pretreated with 1  $\mu$ M tylophorine or vehicle and stimulated with 10% calf serum for 15, 45 and 90 min, lysed and subjected to western blot analysis for the depicted proteins. Western blot data presented are representative of those obtained in at least three separate experiments with consistent results.

As seen in figure 18 the protein levels of cyclin A are not changed by tylophorine treatment. Further, starved VSMC which were treated with 1  $\mu$ M tylophorine or vehicle without stimulation do not express cyclin A (Fig. 19).

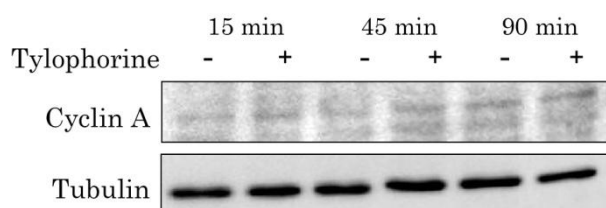


**Figure 19.** VSMC were serum-starved for 24 h and then treated with 1  $\mu$ M tylophorine or vehicle for 15, 45 and 90 min, lysed and subjected to western blot analysis for cyclin A and tubulin. Western blot data presented are representative of those obtained in at least three separate experiments with consistent results.

#### 4.7 No influence of tylophorine on CDK4, but p21 expression levels

Furthermore, we examined the inhibitor of the CDK4-cyclin D1-complex p21. The p21 (CIP/KIP) protein is a cyclin dependent kinase inhibitor which inhibits CDK4-cyclin D1 complexes (Afshari CA et al., 1996). We analyzed the influence of 1  $\mu$ M tylophorine on p21 expression levels by western blotting. VSMC were pretreated with tylophorine or vehicle and stimulated with serum for the indicated time. As demonstrated in figure 20, p21 protein expression levels are down regulated by tylophorine treatment.

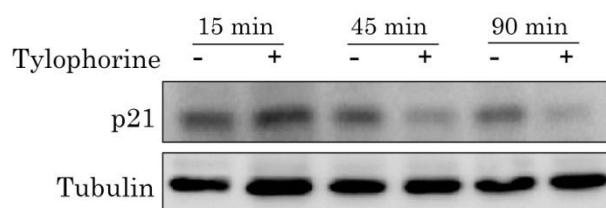


**Figure 20.** Unsynchronized serum-stimulated VSMC were treated with 1  $\mu$ M tylophorine or vehicle for the indicated time, lysed and subjected to western blot analysis for p21 and tubulin. p21 protein expression levels are downregulated by tylophorine treatment. Western blot data presented are representative of those obtained in at least three separate experiments with consistent results.

As two components of the CDK4-cyclin D1-p21 complex are degraded in tylophorine treated cells we analyzed the CDK4 expression levels. As shown in (Fig. 21), CDK4 expression levels are not changed.

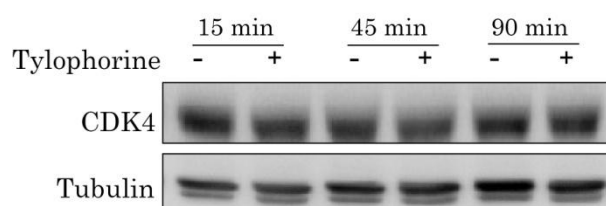


**Figure 21.** VSMC were pretreated with 1  $\mu$ M tylophorine or vehicle and stimulated with 10% serum for the indicated time, lysed and subjected to western blot analysis for CDK4 and tubulin. CDK4 protein expression levels are not changed by tylophorine treatment. Western blot data presented are representative of those obtained in at least three separate experiments with consistent results.

Not just cyclin D1, but also its inhibitory binding partner p21 are down regulated by tylophorine treatment of VSMC. But the expression levels of the kinase CDK4 seem to be unaffected.

#### 4.8. No effect of tylophorine on total p53 expression levels

Due to the fact that p21 is the transcriptional target of the tumor suppressor protein p53 (Jung YS et al., 2010), we determined the total p53 levels after tylophorine treatment. VSMC were stimulated with PDGF-BB (20 ng/ml) as indicated in the presence/absence of 1  $\mu$ M tylophorine. As seen in figure 22 there is no difference in p53 expression levels between control and tylophorine-treated cells, indicating that the induced p21 levels in tylophorine-treated VSMC are not due to altered p53 levels. The activity of p53 is also regulated by posttranslational modifications, such as phosphorylation and acetylation (Brooks CL and Gu W; 2003). The impact of tylophorine on p53 phosphorylation sites is minimal and will get extensive attention in chapter 4.11..

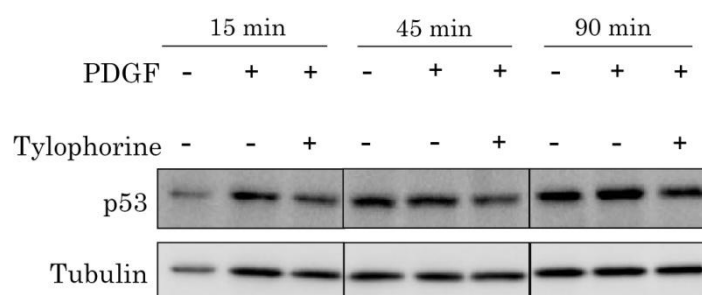


**Figure 22.** VSMC were stimulated with PDGF-BB (20 ng/ml) as indicated in the presence/absence of tylophorine, lysed and subjected to western blot analysis for p53 and tubulin. Western blot data presented are representative of those obtained in at least three separate experiments with consistent results.

#### 4.9. Mechanism of cyclin D1 and p21 degradation

The tylophorine-induced down regulation of cyclin D1 and p21 protein levels in rat aortic VSMC raises the question whether cyclin D1 levels are reduced by inhibition of protein synthesis on the transcriptional or translational level or by increased degradation via the proteasomal pathway.

#### 4.9.1. No effect of tylophorine on cyclin D1 and p21 mRNA levels

To answer this question, we first performed qRT-PCR-analysis (Fig 23). We pretreated quiescent VSMC with 1  $\mu$ M tylophorine and stimulated them for 0.5 h and 2 h with PDGF-BB (20 ng/ml). Then RNA was extracted, transcribed to cDNA and subjected to qRT-PCR analysis as described in materials and methods. The analysis revealed that tylophorine (1  $\mu$ M) has no significant influence on cyclin D1 mRNA levels.

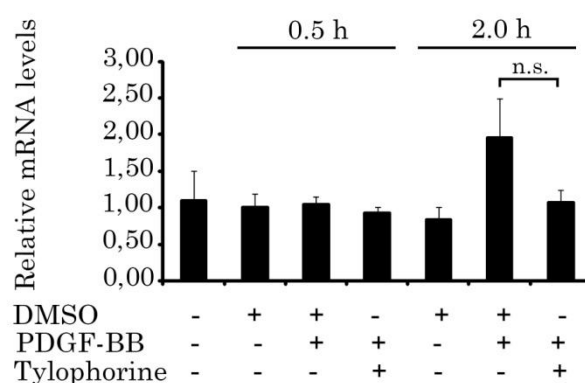


**Figure 23.** Quiescent VSMC were stimulated with PDGF-BB (20 ng/ml) for 30 min or 2 h in the presence/absence of 1  $\mu$ M tylophorine or vehicle. Then RNA was extracted, transcribed to cDNA and subjected to qPCR analysis. Primers for the 18 S rRNA housekeeping gene were used to normalize mRNA levels of cyclin D1 mRNA. (mean  $\pm$  SD,  $n = 3$ , n.s. = not significant, ANOVA/Tukey)

Further qPCR analyses of p21 mRNA levels are depicted in figure 24.



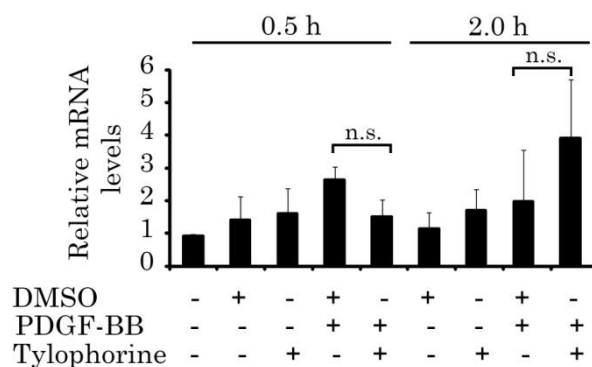


**Figure 24.** Quiescent VSMC were stimulated with PDGF-BB (20 ng/ml) for 30 min or 2 h in the presence/absence of 1  $\mu$ M tylophorine or vehicle. Then RNA was extracted, transcribed to cDNA and subjected to qPCR analysis. Primers for the 18 S rRNA housekeeping gene were used to normalize mRNA levels of p21 mRNA. (mean  $\pm$  SD, n = 3, n.s. = not significant, ANOVA/Tukey)

The p21 mRNA levels seem to be slightly down regulated after 30 min of tylophorine treatment and up regulated after 2 h. But these differences are not significant.

#### 4.9.2. Proteasome-dependent cyclin D1 degradation

In order to investigate the role of the proteasome for cyclin D1 reduction by tylophorine, we employed the known proteasome inhibitor MG132 (Fig. 25). VSMC were pretreated with MG132 (50  $\mu$ M) for 1 h and then treated with 1  $\mu$ M tylophorine or vehicle for 2 h as indicated.

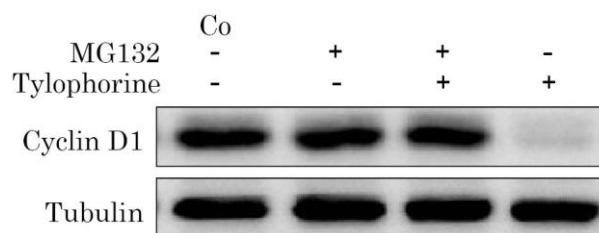


**Figure 25.** VSMC were treated without previous synchronization, with 50  $\mu$ M MG132 for 1 h and 1  $\mu$ M tylophorine or vehicle for 2 h as indicated, lysed and subjected to western blot analysis. Unsynchronized VSMC without any treatment were used as control (Co).

Western blot data presented are representative of those obtained in at least three separate experiments with consistent results.

The immunoblot demonstrates that down regulation of cyclin D1 levels by tylophorine treatment in VSMC is blocked by MG132.

This finding proves that tylophorine leads to down regulation of cyclin D1 via the proteasomal pathway in rat aortic vascular smooth muscle cells, which most likely account for the growth inhibition of tylophorine-treated VSMC.

#### 4.10. Tylophorine has a comparable effect on HUVRMC

In order to exclude species specific effects of tylophorine we aimed to reproduce the anti-proliferative effect of tylophorine on human smooth muscle cells. Consequently we tested tylophorine's activity on primary human umbilical vein smooth muscle cells (HUVRMC).

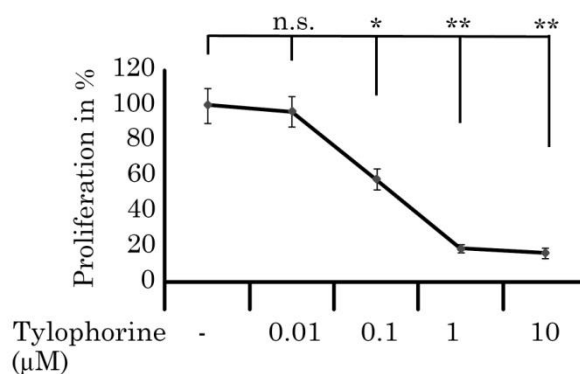


**Figure 26.** HUVEEC were pretreated with the indicated concentrations of typhorine or DMSO (0.1%) for 30 min and stimulated with 10 % calf serum for 48 h. Then cells were washed with PBS and incubated in DMEM containing 10 μg/ml resazurin for 2 h. Samples were measured by monitoring the increase in fluorescence at a wavelength of 580 nm using an excitation wavelength of 540 nm in a 96-well plate reader. (mean  $\pm$  SD,  $n = 3$ , \*  $p < 0.05$ , \*\*  $p < 0.01$ , ANOVA/Tukey)

First we show by a resazurin conversion assay (Fig. 26) that typhorine is able to inhibit the proliferation of HUVEEC dose-dependently ( $IC_{50} = 164 \text{ nM} \pm 49 \text{ nM}$ ). At 1 μM typhorine proliferation is completely blocked.

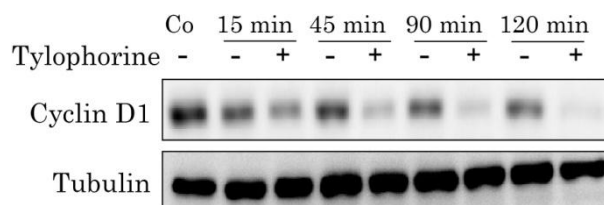


**Figure 27.** HUVEECs were treated with 1 μM typhorine or vehicle for 15, 45, 90, and 120 min, lysed and subjected to western blot analysis. As control (Co) a sample of HUVEEC without any treatment was used. Western blot data presented are representative of those obtained in at least three separate experiments with consistent results.

Second we demonstrate by Immunoblot analysis that typhorine leads to rapid degradation of cyclin D1 (Fig. 27), with first effects seen already after 15 min of treatment. This degradation of cyclin D1 protein levels can also be blocked in HUVEEC by proteasomal inhibition with 50 μM MG132 (Fig. 28).

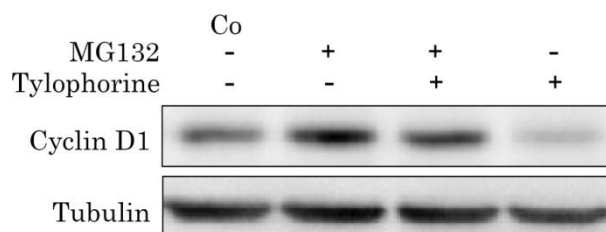


**Figure 28.** HUVMC were treated with 50  $\mu$ M MG132 for 1 h and 1  $\mu$ M *tylophorine* or vehicle for 2 h as indicated, lysed and subjected to western blot analysis. As control (Co), a sample of hUVMC without any treatment was used. Western blot data presented are representative of those obtained in at least three separate experiments with consistent results.

Therefore we conclude that tylophorine leads to inhibition of proliferation and proteasomal degradation of cyclin D1 in human smooth muscle cells as it does in rat aortic VSMC.

#### 4.11. Pepchip kinase array - p53 phosphorylation on serine 9

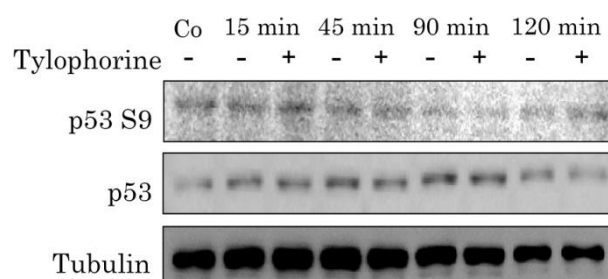
To find the target of tylophorine in the cell we also started an unbiased kinase array approach in parallel. This Pepchip™ kinase array was performed by the cooperation partners in the Netherlands – Pepscan. For this experiment whole cell extracts of tylophorine-treated and vehicle-treated VSMC were used with respect to their ability to lead to phosphorylation of selected peptide sequences, which are specific for a certain protein. (See materials and methods section). The output data of this assay resulted in a list of proteins in which the phosphorylation of a specific amino acid residue was activated or inhibited by our compound as well as the list of suggested kinases responsible for these phosphorylations. The table in section 7.2. shows proteins where the phosphorylation status was modulated by tylophorine. The data analysis revealed a 43 fold induction of p53 phosphorylation on serine 9 presumably via ATM/ATR kinase. This result needed to be confirmed by further immunoblot analyses.

#### 4.11.1. Confirmation of kinase array results

The outcome of the kinase array led to the hypothesis that tylophorine treatment of VSMC induces the phosphorylation of p53 on serine 9 about 43-fold. Unfortunately, the antibodies available for examining phosphorylation of p53 were raised against the human protein. Therefore, we used HUVSMC and specific antibodies against human p53 serine 9 in order to test the impact of tylophorine on phosphorylation of p53 on serine 9 and other phosphorylation sites. Immunoblots for p53 serine 9 phosphorylation sites were performed by our master student Päivi Gruzdaitis.

##### 4.11.1.1. Effect of tylophorine on p53 serine 9

For this, HUVSMC were treated with 1  $\mu$ M tylophorine or vehicle for the depicted time, lysed and subjected to western blot analysis for the p53 phosphorylation at serine 9 and total p53 levels.



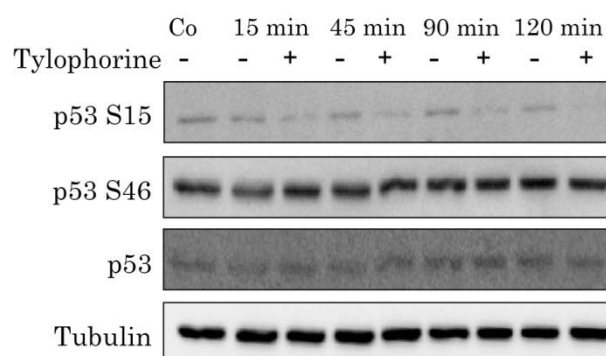
**Figure 29.** HUVSMC were treated with 1  $\mu$ M Tylophorine or vehicle for the depicted time, lysed and subjected to western blot analysis of the p53 phosphorylation site serine 9, total p53 levels and tubulin. Western blot data presented are representative of those obtained in at least three separate experiments with consistent results.

Figure 29 demonstrates that (I) serine 9 phosphorylation of p53 is hardly detectable and (II), at least, not upregulated 43-fold by tylophorine as expected from the kinase array results. Tylophorine seems not to have an influence on

total p53 levels either. Thus, the result of the pepscan kinase array could not be confirmed in our cell system.

#### 4.11.1.2. Effect of tylophorine on other p53 phosphorylation sites

To exclude differences in the phosphorylation status of p53 on several other phosphorylation sites, we performed western blot analysis for the serine sites 15 and 46. HUVSMC were treated with tylophorine or vehicle for the indicated time and subjected to western blot analysis. In figure 30 there seems to be no change in the phosphorylation status of p53 on serine 46 upon tylophorine treatment. However, treatment of HUVSMC with 1  $\mu$ M tylophorine induces a reproducible dephosphorylation of p53 on serine 15.

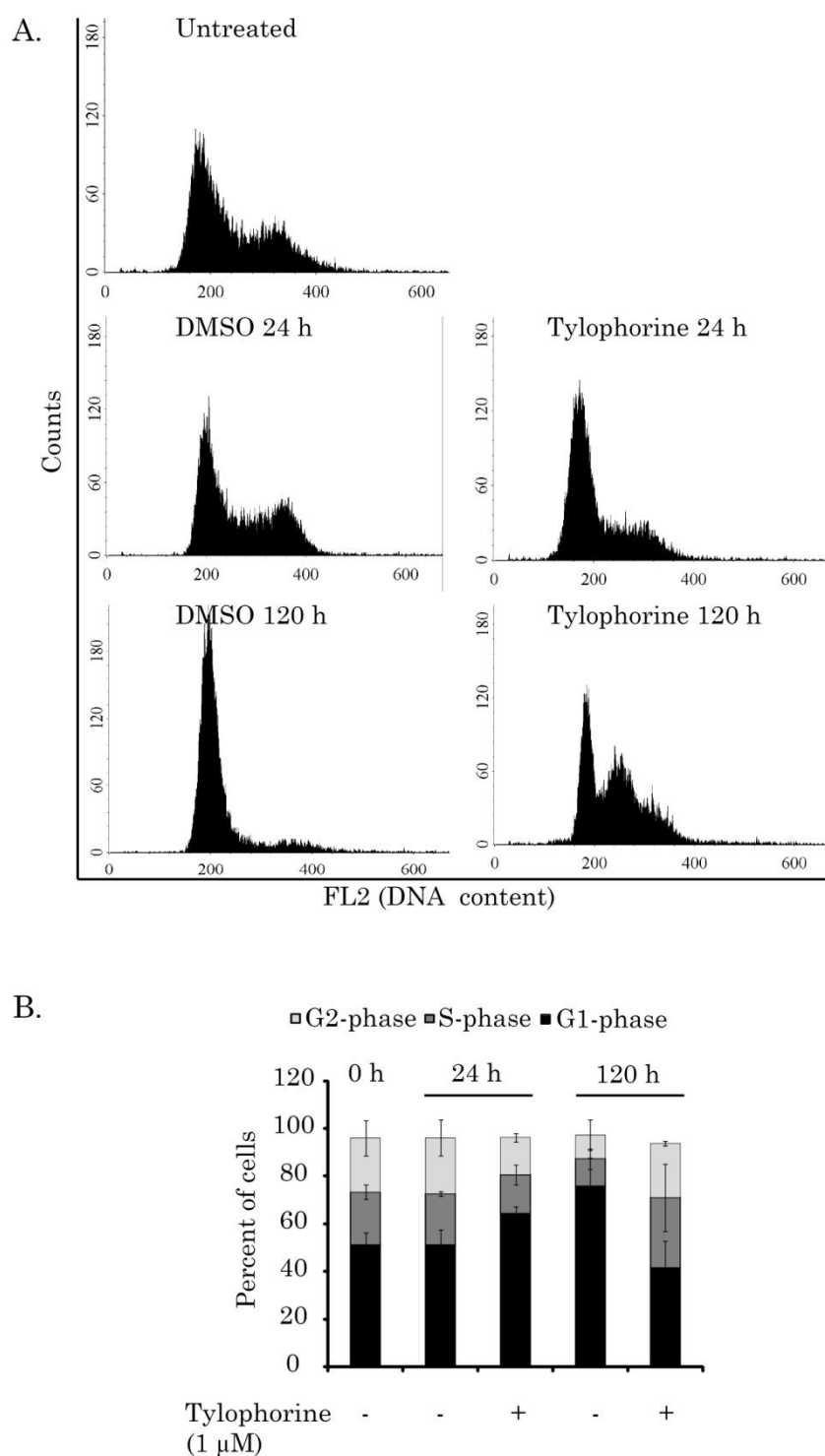


**Figure 30.** HUVSMC were treated with 1  $\mu$ M tylophorine or vehicle for the depicted time, lysed and subjected to western blot analysis of the p53 phosphorylation site serine 15 and 46 as well as total p53 level and tubulin. Western blot data presented are representative of those obtained in at least three separate experiments with consistent results.

#### 4.12. Tylophorine inhibits HUVSMC proliferation

Due to the strong inhibition of HUVSMC proliferation by tylophorine treatment, we further analyzed its effect on the progression of unsynchronized HUVSMC through the cell cycle phases. HUVSMC were treated with

tylophorine for 24 h to 120 h and stained with propidium iodide (PI) to measure the DNA-content of single cells (Fig. 31).



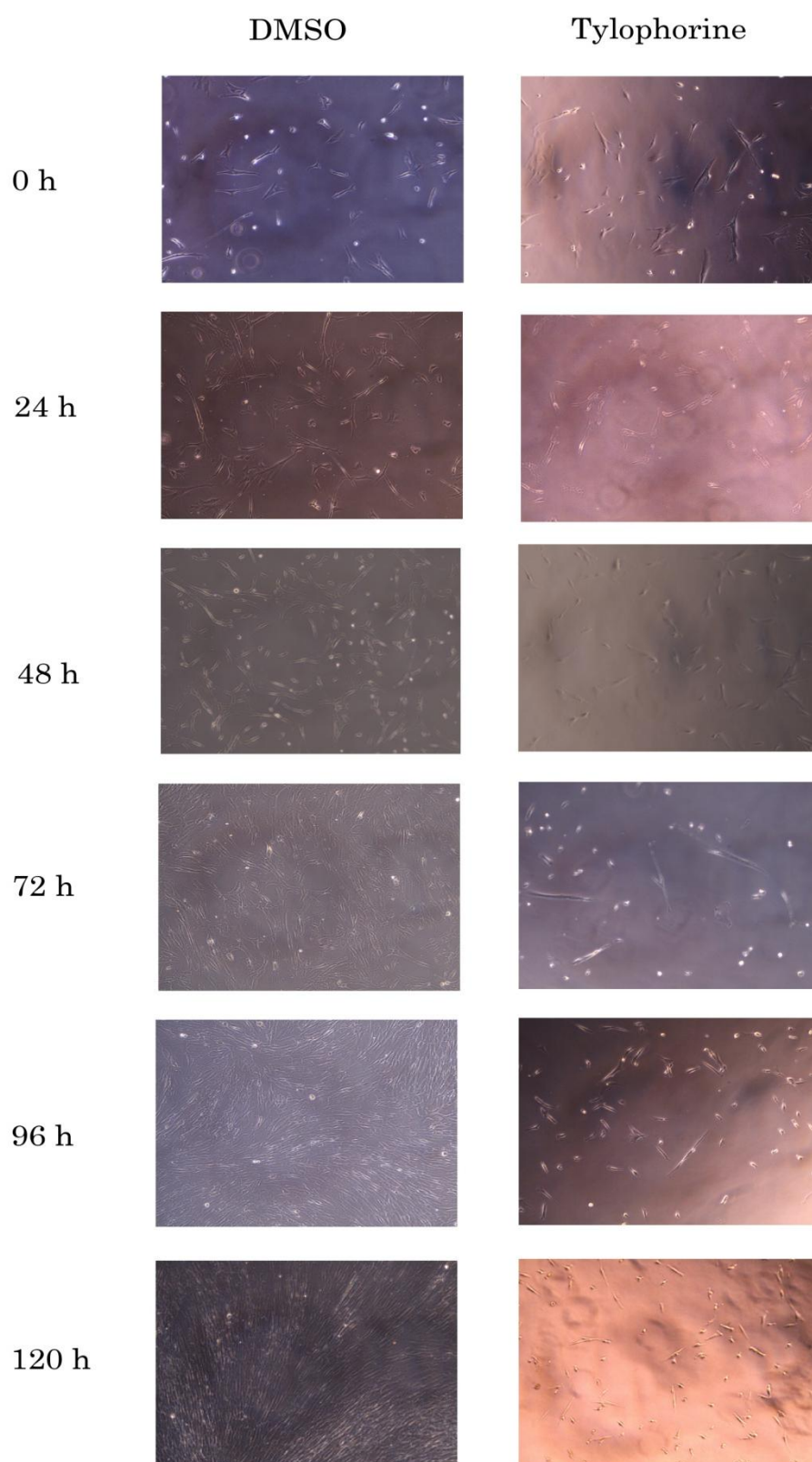
**Figure 31.** A. Representative results of flow cytometric cell cycle analyses of HUVMSC, treated with 1  $\mu$ M tylophorine or vehicle for the indicated time. B. HUVMSC were unsynchronized and treated with 1  $\mu$ M tylophorine or vehicle for the indicated time. Afterwards VSMC were stained with propidium iodide. DNA contents were measured by flow cytometry (mean  $\pm$  SD,  $n = 3$ ).

Figure 31 A. depicts raw flow cytometry results of HUVSMC treated for 24 h or 120 h with 1  $\mu$ M tylophorine or vehicle, whereas figure 31 B. shows the the evaluation of all three independent experiment.

The differences in the cell cycle distribution of tylophorine- or DMSO-treated HUVSMC for 24 h are minor. Tylophorine-treated cells exhibit a broader and higher percentage of cells in G1-phase compared to DMSO-treated cells. After 120 h, tylophorine-treated HUVSMC show a high number of cells in S-phase, and not in G1-phase as seen in and expected from starved rat VSMC. DMSO-treated cells demonstrate a contact inhibition after 120 h and are therefore arrested in G1-phase. Therefore, they are arrested in G1-phase. The cell populations in G1- and G2-phase of the cell cycle in tylophorine-treated cells are similar to the cell populations seen in untreated cells at the 0 h time point. This might indicate that tylophorine-treated cells are slowed down in the progression through S-phase or even “frozen” in this state. But it was obviously visible from microscopic pictures that the cells do not divide at all (Fig. 32). Documented by light-microscopy, there was no increase in density of tylophorine-treated cells over 120 h.

A subG1-peak indicative for cell death was not observed either (Fig. 31 A). Further, we made the observation that side and forward scatter, indicative for size and granularity, were increased by tylophorine treatment. Since, PI stains the whole DNA-content, including mitochondrial DNA of single cells, we hypothesized that tylophorine increases the number of mitochondria per cell. Thus the mitochondrial DNA-content could account for the presumable S-phase peak in the depicted histogram blots.





**Figure 32.** Unsynchronized serum-stimulated VSMC were treated with 1  $\mu$ M tylophorine or vehicle as indicated for 24 to 120 h. Every 24 h representative light-microscopic pictures were taken.

#### 4.13. Tylophorine increases the mitochondrial mass

To analyze changes of the mitochondrial mass in HUVSMC, cells were treated with tylophorine or vehicle for 24 to 120 h and stained with Mitotracker™ green. Figure 33 shows that tylophorine treatment of HUVSMC increased the total mitochondrial mass in the cell over time. Depicted is the ratio of tylophorine- vs DMSO-treated cells. Statistical analysis (ANOVA/Tukey) did not reveal a significant difference between DMSO- and tylophorine treated cells. However, figure 34 is showing, at least, a tendency of a 2-fold higher mitochondrial mass after 120 h of tylophorine treatment.

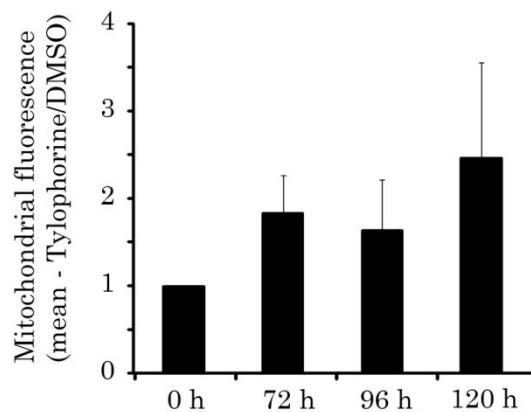


**Figure 34.** Unsynchronized serum-stimulated VSMC were treated with 1  $\mu$ M tylophorine or vehicle as indicated for 0 h, 72 h, 96 h and 120 h. Afterwards VSMC were stained with MitoTracker green and analysed by flow cytometry. (mean  $\pm$  SD, n = 3).

#### 4.14. Effect on “cycling” VSMC

Due to the results of the FACS analysis for HUVSMC, where we observed a slowdown in the progression through S-phase of tylophorine-treated cells, we further tested, if tylophorine can inhibit the cell cycle in G1-phase in unsynchronized serum-stimulated rat VSMC. Therefore, VSMC were treated with tylophorine for 72 h to 120 h and stained with propidium iodide (PI) to measure the DNA-content.

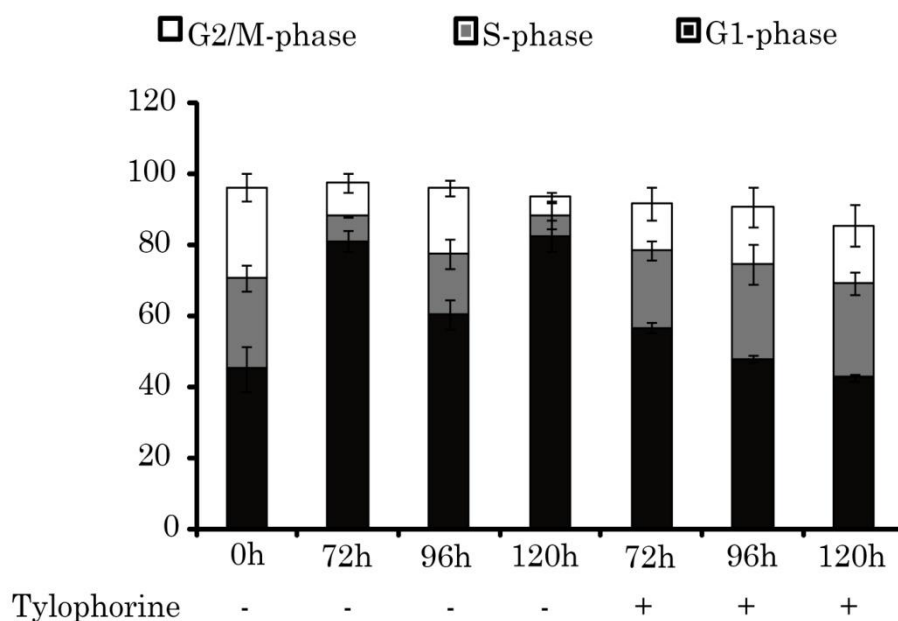


**Figure 34.** Unsynchronized serum-stimulated VSMC were treated with 1  $\mu$ M tylophorine or vehicle as indicated for 72 h, 96 h and 120 h. Afterwards VSMC were stained with propidium iodide. DNA contents were measured by flow cytometry. (mean  $\pm$  SD, n = 3).

Figure 34 demonstrates that tylophorine-treated VSMC showed a comparable distribution of cells in G1-, S- and G2-phase over time as already discovered in HU VSMC. A specific G1-phase arrest is not induced by tylophorine unlike in mitogen-starved and PDGF-BB stimulated VSMC as seen in section 4.2.3. In contrast, cycling VSMC are obviously retarded or stalled in S-phase by tylophorine.

#### 4.15. Migration of VSMC – Wound healing assay

Proliferation and migration contribute to neointima formation. PDGF-BB is not only the most potent proliferative but also the most effective migratory stimulus for VSMC. Here, we examined the influence of tylophorine on VSMC migration via scratch assay (See materials and methods).

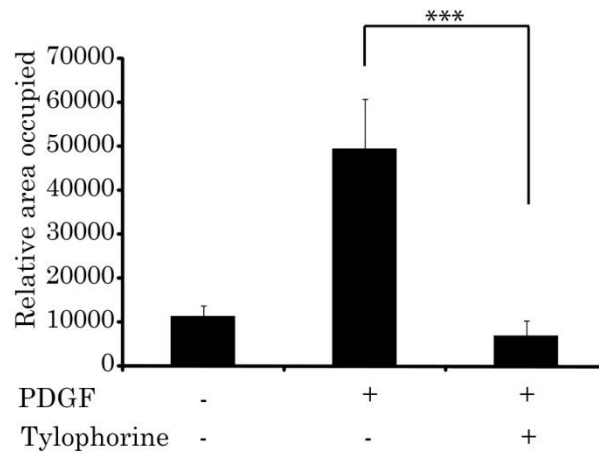


**Figure 35.** VSMC were grown to confluency, starved for 24 h, scratched, then pretreated with 1  $\mu$ M tylophorine or vehicle and then PDGF-BB stimulated (10 ng/ml) for 20 h. The cell migration rate was evaluated by measuring the cell free area of each scratch (mean  $\pm$  SD, n = 3, \*\*\* p < 0.001, ANOVA/Tukey).

Figure 35 demonstrates that tylophorine treatment reduces the PDGF-BB-stimulated migration by 80%. Whether this inhibition is linked to cyclin D1 degradation or other targets needs to be investigated.

#### 4.16. Inhibition of neointimal thickening

In cooperation with the research group of PD Dr. David Bernhard at the AKH Vienna, tylophorine was tested on its ability to inhibit intimal thickening in a human saphenous vein model *in vitro*. The assay was performed as described in the materials and methods section. Tylophorine was used in three different concentrations - 300 nM, 1  $\mu$ M and 3  $\mu$ M.

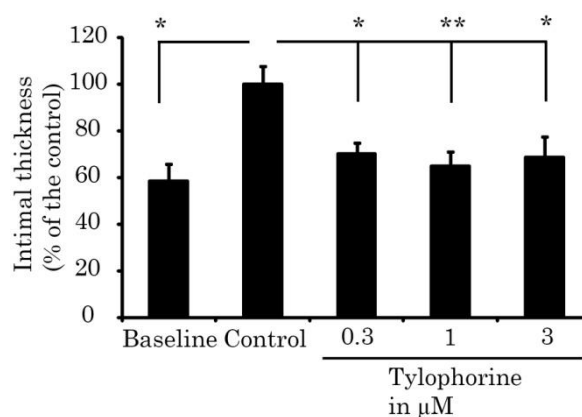


**Figure 36.** Human saphenous veins were induced to develop intimal hyperplasia in organ culture. Tissue samples were incubated with DMSO or various concentrations of tylophorine for 2 weeks. Shown are mean values of intimal thickness (mean  $\pm$  SEM, \*\*  $p < 0.01$ , \*\*\*  $p < 0.001$ , ANOVA/Bonferroni).

As seen in figure 36, tylophorine is able to inhibit intimal thickening significantly in every tested concentration. Therefore, tylophorine seems to be a promising compound in the anti-proliferative in CABG or PCI therapy.

#### 4.17. Plant extracts and natural compounds as anti-proliferative drugs in VSMC

##### 4.17.1. Screening of plant extracts

Natural products represent a rich source for the identification of new lead structures and novel molecular mechanisms. Drugs from nature have always played an important role in human health care. Therefore, we have chosen to lean on the traditional medicinal knowledge to find drugs with new anti-proliferative effects on VSMC.

Around 100 extracts of plants used in traditional Chinese medicine or in Austrian folk medicine with anti-inflammatory properties were tested for their anti-proliferative activity in VSMC (Diploma thesis, Thomas Nakel, 2011). For this, we employed a resazurin conversion assay. The extract with the highest inhibitory activity in this small screening program was from *Peucedanum*

*ostruthium*. Therefore, we chose this extract for further investigation and subjected it to fractionation, aiming for the identification of the active principle.

#### 4.17.2. Impact of *Ostruthium Peucedanum* on VSMC

##### 4.17.2.1. Inhibition of VSMC proliferation

To examine the potential of *Peucedanum ostruthium* rhizome to inhibit the serum-stimulated proliferation of VSMC, we subjected the DCM-extract to calf-serum activated VSMC in concentrations ranging from 3 to 30  $\mu\text{g/ml}$  (Fig. 37). After 30 min pretreatment with the extract, mitogen-starved VSMC were stimulated with 10% calf-serum. Serum-stimulated VSMC were taken as positive and mitogen-starved cells as negative controls. Our resazurin conversion assay analysis revealed that the DCM-extract of *P. ostruthium* inhibits the proliferation of serum-stimulated rat aortic VSMC with an  $\text{IC}_{50}$  of  $24 \mu\text{g/ml} \pm 14 \mu\text{g/ml}$  significantly.

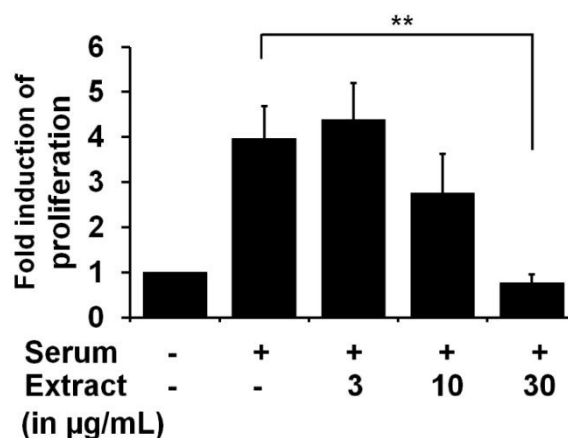
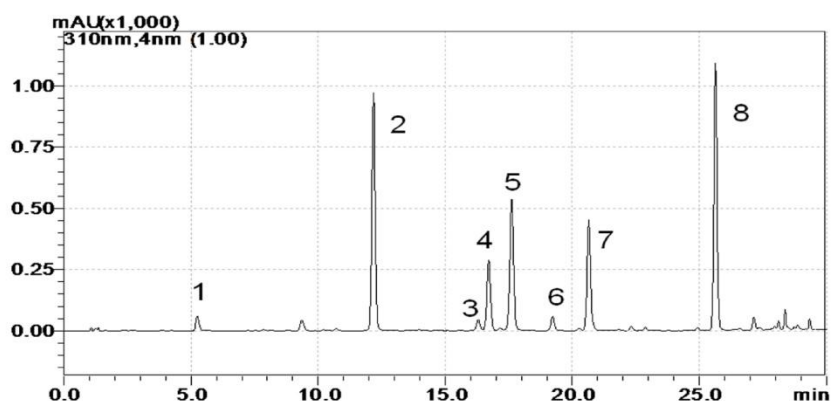


**Figure 37.** *Peucedanum ostruthium* rhizome DCM extract inhibits the proliferation of VSMC. The extract was applied at 3, 10, and 30 µg/mL and after 30 minutes the cells were stimulated with 10% serum for 48 h, followed by quantification of the proliferation by the resazurin conversion method. Final DMSO concentration in all samples was 0.1%. The graph is representative for three independent experiments with consistent results (mean ± SD, \*\* p < 0.01, Anova/Tukey).

#### 4.17.2.2. The extract contains 7 major coumarins

With this promising finding we prove that the DCM-extract of *P. ostruthium* has inhibitory activity on rat aortic VSMC proliferation and therefore we further fractionated and separated the extract by HPLC to elucidate the active compounds (Silvia Vogl, Research group of Prof. Kopp, University of Vienna, Vienna).

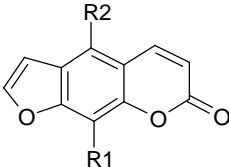
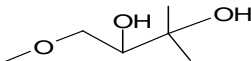
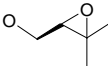
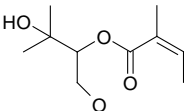
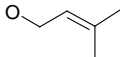
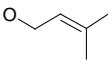
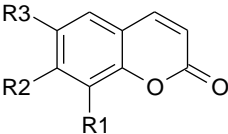
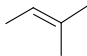
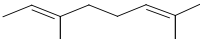
The HPLC investigations led to the identification of seven coumarins in the DCM extract of *Peucedanum ostruthium* rhizomes. As a first separation step we performed preparative HPLC (Fig. 38).



**Figure 38.** HPLC chromatogram (310 nm) of the DCM extract of *Peucedanum ostruthium* rhizome. Peaks identity: 1 - oxypeucedanin hydrate, 2 - oxypeucedanin, 3 - ostruthol, 4 - imperatorin, 5 - osthole, 6 - isoimperatorin, 7 – ostruthin. HPLC-method: Acclaim C-18 reversed phase column from Dionex (2.1 x 150 mm, 3  $\mu$ m); H<sub>2</sub>O + 0.01% acetic acid (A) / MeCN + 0.01% acetic acid (B); gradient 25-37% of B in 6 min, 37-45% of B in 8 min, 45-65% of B in 10 min, 65-95% of B in 1 min, and isocratic at 95% of B for 5 min; temp.: 38 °C; flow: 0.5 mL/min.

With further purification on silica gel eluted with hexane/ ethyl acetate we could isolate seven (furano-) coumarins, oxypeucedanin hydrate, oxypeucedanin, ostruthol, imperatorin, osthole, isoimperatorin and ostruthin (table 2).



| linear furanocoumarins |    | # | compound              | R1   | R2  |   |
|------------------------|---|---|-----------------------|--|---|---|
|                        |   | 1 | oxypeucedanin hydrate | H  |  |   |
|                        |   | 2 | oxypeucedanin         | H  |  |   |
|                        |   | 3 | ostruthol             | H  |  |   |
|                        |   | 4 | imperatorin           |    | H   |   |
|                        |   | 6 | isoimperatorin        | H  |  |   |
|                        |   |   |                       |  |   |   |
| simple coumarins       |  | # | compound              | R1   | R2  | R3  |
|                        |   | 5 | osthole               |  | OMe   | H   |
|                        |   | 7 | ostruthin             | H  | OH  |  |

**Table 2.** Structural classification of the main coumarins in the DCM extract of *Peucedanum ostruthium* rhizomes.

Quantification measurements of the coumarin content in the DCM extract of *Peucedanum ostruthium* rhizome resulted in ostruthin as the main coumarin (41% of the total coumarin content), followed by oxypeucedanin (18%), ostruthol (13%), imperatorin (12%), isoimperatorin (9%), oxypeucedanin hydrate (6%) and osthole composing just 1%. The total coumarin content in this extract made up 78%, whereas the amount on gram dry weight of drug made up only 6%.

## 4.17.2.3. Effect of the major compounds

After the isolation of the major compounds of the *P. ostruthium* extract, we tested each of them for its anti-proliferative activity on serum-stimulated VSMC. Imperatorin, isoimperatorin, ostruthin, ostruthol, osthole, oxypeucedanin and oxypeucedanin hydrate, were subjected to resazurin conversion assay analysis in a concentration of 30  $\mu$ M (Fig. 39).

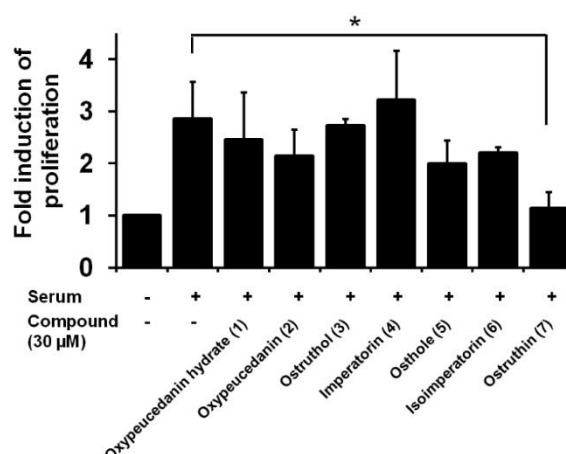


**Figure 39.** Ostruthin is the active compound of the *Peucedanum ostruthium* DCM-extract. The major compounds of the DCM-extract, oxypeucedanin hydrate (1), oxypeucedanin (2), ostruthol (3), imperatorin (4), osthole (5), isoimperatorin (6), ostruthin (7), were tested for an anti-proliferative action on VSMC utilizing the resazurin conversion method. All compounds were tested in a concentration of 30  $\mu$ M. Ostruthin (7) was the only compound significantly inhibiting serum stimulated VSMC proliferation (mean  $\pm$  SD, n = 3, \* p < 0.05; Anova/Tukey).

The result demonstrates that ostruthin is the only compound of this extract which significantly inhibits serum-stimulated VSMC proliferation. Structural similar furanocoumarins to ostruthin, tested in this assay, have no effect on the proliferation of VSMC either.

#### 4.17.2.4. Activity of structural related furano-/coumarins

To validate the effect of ostruthin on VSMC proliferation we further tested several structural similar furano-/coumarins in the resazurin conversion assay (Fig. 40).

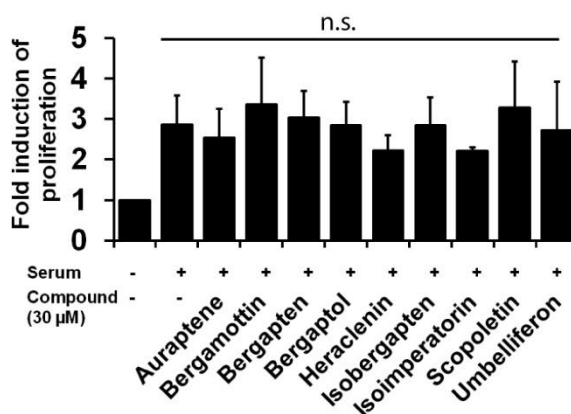


**Figure 40.** Coumarins with structural similarity to ostruthin have no effect on VSMC proliferation. VSMC were pretreated with 30 µM of the indicated compounds or DMSO (0.1%) for 30 min and stimulated with 10 % serum for 48 h. Then cells were washed with PBS and incubated in DMEM containing 10 µg/mL resazurin for 2 h. Samples were measured by monitoring the increase in fluorescence at a wavelength of 580 nm using an excitation wavelength of 540 nm in a 96-well plate reader. Statistical analysis did not reach significance (mean  $\pm$  SD, n = 3, n.s. = not significant, ANOVA/Tukey).

None of these compounds have an inhibitory effect on the proliferation of VSMC. Statistical analysis did not reach significance. Their structure is depicted together with all tested coumarins in table 3 in section 7.2.2.. Therefore, Ostruthin is the compound responsible for the significant inhibitory effect of the *Peucedanum Ostruthium* extract.

#### 4.17.2.5. Ostruthin inhibits DNA-synthesis

To further examine the potential of ostruthin to inhibit VSMC proliferation we subjected it to a BrdU-incorporation assay in concentrations ranging from 1  $\mu$ M to 30  $\mu$ M (Fig. 41).

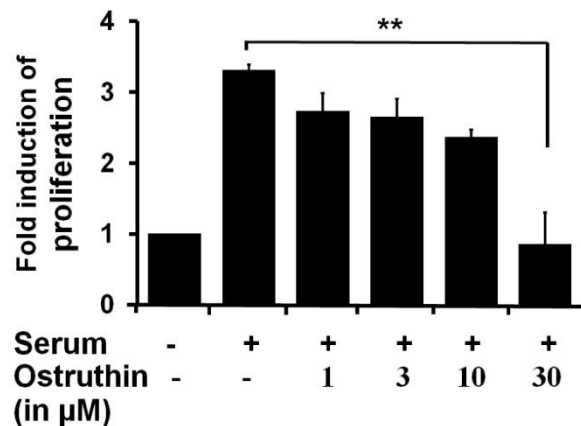


**Figure 41.** Ostruthin is inhibiting the serum-stimulated proliferation of VSMC in a concentration-dependent manner. Serum-starved VSMC were pretreated with the indicated concentrations of ostruthin or DMSO (0.1%) for 30 min, BrdU (10  $\mu$ M) was added and cells were stimulated with 10% serum for 20 h. Incorporation of BrdU was measured at the end of the stimulation period. (SEM, n = 3, \*\* p < 0.01; Anova/Tukey).

The assessment of DNA-synthesis shows that ostruthin potently inhibits serum-induced proliferation in a dose-dependent manner with an  $IC_{50}$  of 17  $\mu$ M  $\pm$  6  $\mu$ M.

In this study, two new important findings have been made. We discovered that the DCM-extract of *Peucedanum ostruthium* inhibits the proliferation of VSMC. Furthermore, we were able to track down the activity of this extract to a single compound, which is responsible for the inhibitory activity on serum-stimulated VSMC proliferation - ostruthin.

## **5. DISCUSSION**

## 5. Discussion

### 5.1. Anti-proliferative activity of tylophorine and its molecular mode of action

In the last years several research groups demonstrated that tylophorine is able to inhibit proliferation in various cancer cell systems (Staerk D et al., 2003; Gao W et al., 2004 and 2007; Wei L et al., 2007; Wu CM et al., 2009). In this study we showed that tylophorine is a cell cycle arrestor in VSMC and HUVMC as well as an inhibitor of neointima thickening in human umbilical vein organ cultures. Here we reveal that tylophorine has a unique mechanism of action, characterized by down regulation of cyclin D1 via a proteasome-dependent pathway leading to cell cycle arrest. We could prove that this mechanism is species- and mitogens-independent by employing rat and human smooth muscle cells, as well as starved, PDGF-BB- and serum-stimulated cells.

First we demonstrated that (-)-R-tylophorine inhibits the proliferation of PDGF-BB and calf-serum stimulated rat aortic VSMC in a dose-dependent manner with an  $IC_{50}$  of  $128.15 \pm 44$  nM for PDGF-BB-, or  $468 \text{ nM} \pm 144$  nM for serum-treated cells. These differences in the  $IC_{50}$  might be due to differences between the employed assay with regard to sensitivity and readout. The  $IC_{50}$  for PDGF-BB treated cells were gained by employing a luminometric BrdU-incorporation assay, which measures DNA synthesis, whereas the  $IC_{50}$  value for calf-serum stimulated VSMC was assessed by a fluorescence-based resazurin conversion assay, which gives a measure for the metabolic activity of the cells. Further, calf-serum contains several growth factors, and therefore elicits a stronger mitogenic response which may be harder to inhibit by tylophorine than that triggered by PDGF-BB alone.

Studies employing the (-)-R-tylophorine are generally scarce. Previous publications demonstrating the anti-proliferative effect of tylophorine on cancer cells (Gao W et al., 2004; Shiah HS et al., 2006) are using the (+)-S-tylophorine or analogues. Just Staerk and colleagues show an effect of (-)-R-tylophorine on human KB-3-1 cells and KB-V1 cancer cells with an  $IC_{50}$  of

around 200 nM. Hence, tylophorine inhibits the proliferation of VSMC in a similar concentration range. This result, together with the fact that tylophorine inhibits human and rat cells, suggests that tylophorine influences elementary mechanisms in the cell.

These mechanisms obviously do not induce apoptosis in the cell. VSMC apoptosis eventually contributes to plaque rupture in an atherosclerotic lesion. An optimal lead structure for anti-restenotic drugs is inhibiting the proliferation of VSMC, but not inducing cell death. With our annexin V staining assay, we could point out, that tylophorine is not inducing apoptosis. The result in figure 8 demonstrates that tylophorine treatment does not increase membrane bound annexin V levels in these cell populations. Though, annexin V is a good marker for the detection of apoptosis, the assay would have performed better, having simultaneous PI staining results and allowing for discrimination between apoptotic and necrotic cells. PI is not passing the healthy plasma membrane. Therefore PI positive cells are an indicator for dead cells. But due to problems with this double staining and an appropriate positive control we had to rely on the annexin V staining results. Experiments using doxorubicin as an apoptosis-inducing agent for VSMC failed due to high toxicity and interferences with the fluorescence detection. Doxorubicin treatment of VSMC did not just lead to cell destruction, but to a color-shift in the measured fluorescence spectrum, which could not be satisfyingly compensated. Thus our focus lay on  $H_2O_2$  which was already published to be probably involved in VSMC apoptosis (Li PF et al., 1997). Indeed,  $H_2O_2$  led to an increase in annexin V positive VSMC and could therefore be employed for the FACS measurement as positive control. Nevertheless, the annexin V positive cell population of tylophorine treated VSMC does not exceed negative control levels. Therefore, an influence of apoptosis or necrosis as an anti-proliferative effect can be excluded.

Further cell cycle analyses of PDGF-BB-stimulated VSMC indicate an accumulation of cells in G1-phase of the cell cycle in the presence of tylophorine. This FACS analyses alone cannot substantiate a G1-phase arrest. The setting of gates and the specifications for the size of cell cycle rely on the

experience of the experimentator. Further, the cells in S-phase of the cell cycle have varying amounts of DNA and hence may be falsely added to G1-phase or G2-/M-phase populations. Therefore, more profound analyses need to be added for consolidation of the results.

The examinations, utilizing the reversible S-phase arrestor aphidicolin, reveal that tylophorine treatment of VSMC still allows slow S-phase progression in PDGF-BB treated cells and exclude an early S-phase arrest upon tylophorine treatment. In addition, consolidation that tylophorine is a G1-phase arrestor in PDGF-BB treated VSMC was gained by analyzing the phosphorylation status of the retinoblastoma protein. Tylophorine completely blocks its phosphorylation, which proves that tylophorine is a G1-phase-arrestor in PDGF-BB-activated rat aortic VSMC, which were mitogen-starved before stimulation.

The outcome for calf-serum stimulated VSMC, which are not starved to quiescence seems to be different. The fact that tylophorine also inhibits the proliferation of cells “cycling” in serum is irrevocable. But, our flow cytometry results do not give indications for a clear G1-phase arrest. It is possible that the S-phase population after 120 h in tylophorine-treated VSMC (Fig. 33) is due to an extreme slow-down of the cell cycle. However, a duplication of cells is not visible, even 120 h after mitogen stimulation. But another fact should be considered. VSMC are in different cell cycle phases at the moment of tylophorine treatment. It is therefore possible, that tylophorine blocks the cell cycle at the G1-/S-phase and the S-/G2-phase transition. This would explain why the cell cycle populations of G0/G1-phase and G2/M-phase are highly similar to the 0 h control level after 120 h. Just the cells which were in the early S-phase of the cell cycle contribute to the visible minor shift of the cell population from G1- to S-phase. Also the increase of mitochondrial mass and its DNA, which is also stained by PI, might contribute to this phenomenon.

To track down the target of tylophorine which is responsible for the inhibition of proliferation in VSMC, we further analyzed the interaction of tylophorine with early PDGF-BB signaling pathways. The PDGF-BB stimulated proliferation of VSMC leads to activation of signaling molecules including the kinase Akt, the mitogen-activated protein (MAP)-kinases Erk 1/2 (p42/p44),



p38MAPK and c-Jun N-terminal kinase (JNK), and the transcription factor Signal transducer and activator of transcription 3 (Heldin CH et al., 1998; Andrae J et al., 2008). Western blot analyses demonstrated that tylophorine is not causing a G1-phase arrest via inhibition of these kinases or STAT3.

There is also another possible signal transduction pathway in the cell, which might be responsible for the induction of proliferation. It is the NFκB signaling cascade. It was previously reported that tylophorine acts as an inhibitor of NFκB in HepG2, PANC-1, and CEM cells (Gao W et al., 2004). However, this report is using the (+)-S-tylophorine. Moreover, the role of the NFκB signaling for the PDGF-triggered proliferation of VSMC is controversial (Selzman CH et al., 1999; Erl W et al., 1999; Mehrhof FB et al., 2005). To examine potential activation of NFκB in our experimental setting, we investigated as a marker, the degradation of IκBα and observed that neither PDGF-BB is inducing degradation of IκBα, nor tylophorine has any effect on it. Taken together, we did not observe any influence of tylophorine on early PDGF-BB-induced signaling steps nor were changes of NFκB activation status detected at the level of IκBα. Our data furthermore support the notion that NFκB signaling pathways are not involved, at least, in PDGF-BB induced proliferation of VSMC.

The progression through the cell cycle, activated by mitogenic stimuli like PDGF-BB, involves sequential activation of cyclin-dependent kinases (Cdks) and their regulatory subunits the cyclins (Vicente A, 2004). We revealed a massive degradation of cyclin D1 in PDGF-BB stimulated VSMC by tylophorine. The tylophorine induced down regulation of cyclin D1 can explain the observed G1-phase arrest, because cyclin D1 up regulation is necessary for the G1- to S-phase progression of the cell cycle. On the contrary, tylophorine treatment did not induce a degradation of cyclin A in VSMC as it was previously shown for cancer cells (Wu CM et al., 2009). We could demonstrate that the down regulation of cyclin D1 expression is occurring not just in PDGF-BB but also in serum stimulated VSMC. Even in mitogen-starved quiescent VSMC, tylophorine is able to reduce cyclin D1 expression below basal levels. Therefore tylophorine inhibits the proliferation of VSMC independent of the

mitogenic stimuli as confirmed by the proliferation stop in PDGF- and CS-stimulated VSMC. These findings lead to the conclusion that the proliferation of rat aortic VSMC is blocked by tylophorine via down regulation of cyclin D1 and a subsequent G1-phase arrest in a stimulus-independent fashion, at least, in cell starved to quiescence prior to mitogen exposure. Tylophorine leads to cyclin D1 degradation also in cycling unsynchronized VSMC. As mentioned above, the expected clear G1 arrest, however, does not occur. Instead, these cells seem to “freeze” the cell cycle at the phase they are in, when they are exposed to tylophorine. There are no indications in the literature yet, whether such behavior can be explained by loss of cyclin D1. This issue needs attention in further investigations, as well as, the possible link between cyclin D1 degradation and the putative increase in mitochondrial mass upon tylophorine treatment. Of note, proliferation has been linked to glycolysis (Warburg effect) (Vander Heiden MG et al., 2009). It is therefore conceivable that an inhibition of proliferation and glycolysis leads to a metabolic shift in the cell, which causes an increase in mitochondrial mass in these VSMC. We also observed a down regulation of p21, a known inhibitor of the cyclinD1-CDK4 complex (Levine AJ, 1997). Its up regulation is commonly accepted in many publications to indicate a cell cycle arrest in G1-/G0-phase (Abbas T and Dutta A, 2009). Association of p21 with cyclin D-CDK4/6 inhibits pRb phosphorylation and induces cell cycle arrest in G1-phase. Furthermore, p21 mediates p53-dependent G1-phase growth arrest (Brugarolas J et al., 1995; Deng C et al., 1995). But p21 is also in low amounts required for normal cell cycle progression by stabilizing and promoting the active cyclin-CDK complex formation (Philipp J et al., 1999; LaBaer J et al., 1997; Besson A and Yong VW, 2000; Weiss RH et al., 2000). Thus tylophorine may induce a stop by interfering with the formation of an active cyclin D1/CDK4 complex by reducing both, cyclin D1 and p21 levels without altering CDK4 levels.

This uncommon activity of tylophorine raised the questions for the mechanism of cyclin D1 and p21 down regulation. A decrease in protein levels of cyclin D1 and p21 could be explained by decreased mRNA levels or an increased degradation of the protein. Here we demonstrate that tylophorine is not influencing cyclin D1 and p21 gene mRNA levels significantly, leading to the

conclusion that tylophorine is not influencing the transcription of these cell cycle regulators.

Our experiments with chemical inhibition (MG132) of the proteasome machinery reveal, that tylophorine leads to down regulation of cyclin D1 via proteasomal pathways in rat aortic VSMC. This mechanism is so far not published for tylophorine or its analogues in other cell systems.

We could also exclude species specific effects of tylophorine by testing the compound on HU VSMC. The anti-proliferative effect is reproducible, even with a highly similar  $IC_{50}$  of around 200 nM which can be observed in rat cells as well as cancer cells. Furthermore, the tylophorine-induced proteasome-dependent degradation of cyclin D1 and p21 is also reproducible.

Moreover, tylophorine is not just active in our cell culture models but also demonstrates high activity in a human saphenous vein model. Here, we demonstrate that tylophorine treatment prevents neointimal thickening.

All the acquired results about the action of tylophorine point out a general mechanism which applies, at least, to rat and human smooth muscle cells. Maybe the mechanism is even conferrable to some cancer cell lines.

The structural related tylophorine analogue DCB-3503 was reported to down regulate cyclin D1 in PANC-1 (Human pancreatic carcinoma, epithelial-like cell line) cells as well (Shiah HS et al., 2006). Furthermore, Wang Y et al. described a cyclin D1, p21, and p53 degradation for HepG2 (human hepatocellular cancer cell line) cells. Although, the cyclin D1 down regulation is the same result as we describe it in our cell system, the additional findings differ. So far, our investigations of tylophorine do not indicate an influence on NF $\kappa$ B pathways or p53 degradation. Anyway, as described already by Gao W and colleagues in 2007, the structural relation between the tylophora alkaloids does not necessarily argue for the same mechanism in the cells.

The unbiased kinase array approach to detect possible targets of tylophorine in SMC could not be reproduced with our cell-based data. The phosphorylation site serine 9 of p53 was not 43-fold upregulated by tylophorine treatment in VSMC as predicted from the assay. The phosphorylation of p53 on the serine 9 position would have suggested that tylophorine induces DNA damage in the

cell (Higashimoto Y et al., 2000). Recent literature introducing FBXO31 up regulation as part of a fast degradation pathway for cyclin D1 after DNA damage could have supported the idea of tylophorine as a DNA damaging compound and explained the observed cyclin D1 degradation (Santra MK et al., 2009). But our experiments did not end up in satisfying and consistent results for FBXO31 (data not shown). With our result for the p53 serine 9 phosphorylation site, namely no highly upregulation upon tylophorine treatment, we can substantiate that tylophorine is no DNA damaging agent. In this context we also investigated other phosphorylation sites of p53 in the presence of tylophorine. The lack of influence on p53 phosphorylation site serine 46 is further another argument against an induction of apoptosis by tylophorine and corroborates our findings of the Annexin V staining assay. According to literature (Mayo LD et al., 2005) this serine phosphorylation site is highly upregulated after induction of apoptosis. Similar indications can be obtained by the investigations of the p53 phosphorylation on serine 15. Our results even show a dephosphorylation by tylophorine on the serine 15 site. According to literature, this dephosphorylation could promote cell survival (Li DW et al., 2006).

How tylophorine induces proteasome-mediated cyclin D1 and p21 degradation is still unclear. For the cyclin D1 turnover exist, besides DNA damage induced degradation, several possibilities.

First, cyclin D1 degradation is dependent on threonine 286 (T286) phosphorylation and regulated by ubiquitin-dependent proteasomal degradation (Diehl et al., 1997). Glycogen synthase kinase 3 $\beta$  (GSK3 $\beta$ ) is capable of phosphorylating cyclin D1 on T286 and inducing its rapid turnover (Diehl JA et al., 1998). Our data does not support an increased phosphorylation of cyclin D1 after tylophorine treatment, at least, for 15 min to 90 min after tylophorine incubation. Immunoblots for shorter tylophorine incubation times did not give conclusive results. Therefore, an up regulation of the phosphorylation on T286 cannot be excluded.

It was also reported, that cyclin D1 degradation occurs independently of GSK3 $\beta$ . A protein kinase Mirk/Dyrk1b seems to be also responsible for the regulation of cyclin D1 stability (Zou Y et al., 2004). It is active at G0 and early

G1 phases of the cell cycle and phosphorylates cyclin D1 on T288. The data published about the phosphorylation site T288 on cyclin D1 is arguable. So far there is no antibody against this phosphorylation site commercially available. Antibodies used in publications are self-made or the provider was not specified. Therefore, the phosphorylation site T288 was not evaluated in our studies.

Furthermore, it was demonstrated that various chemically-induced or environmental stresses induce cyclin D1 degradation in cancer cells via the p38<sup>SAPK2</sup> pathway (Casanovas et al., 2007). The results we obtained for phospho-p38 during the evaluation of the early PDGF signaling indicate that this pathway is not influenced by tylophorine.

A cyclin D1 splice variant, cyclin D1b, has also been reported (Betticher DC et al., 1995; Hosokawa Y et al., 1997; Lu F et al., 2003). It lacks a C-terminal domain where the T286 residue is located. This loss of the regulatory region does not significantly increase the half-life of cyclin D1b. It is constitutively nuclear and has been shown to be a poor activator of CDK4 and RB phosphorylation (Solomon DA et al., 2003). Our antibodies do not discriminate between the two cyclin D1 variants, because they target the amino-acid residues 151 – 170 of a conserved domain. The almost complete degradation of cyclin D1 points out that even this splice-variant gets degraded after tylophorine treatment of the cells.

Second, not just the phosphorylation of cyclin D1 but its ubiquitinylation could also be modulated by tylophorine. The F-box proteins FBX4 and FBXW8 are, besides FBXO31, mediators of cyclin D1 ubiquitinylation (Lin DI et al., 2006; Okabe H et al., 2006). FBX4 recognition of cyclin D1 requires the presence of  $\alpha$ B crystalline and the phosphorylation of T286. Both FBX4 and  $\alpha$ B crystalline are required for the rapid ubiquitin-dependent degradation of T286 phosphorylated cyclin D1 (Lin DI et al., 2006). Also FBXW8 mediates cyclin D1 ubiquitinylation after T286 phosphorylation (Okabe H et al., 2006). All these ubiquitinylations are elements for further investigations.

The literature about the degradation of p21 is scarce. p21 is also found to be degraded in an ubiquitin-independent manner by the proteasome (Chen X et al., 2004; Sheaff RJ et al., 2000). It can be phosphorylated at serine 130 by

CDK2. There is also a p21 turnover independent of ubiquitin E3 ligase activity. It is promoted by Mdm2 (Zhang Z et al., 2004; Jin Y et al. 2003). The exact influence of tylophorine on these pathways cannot be specified so far.

Investigations of the tylophorine analogue DC-3503 point out, that tylophorine reduction might be due to modulation of translational processes (Wang Y et al. 2010). Our data do not exclude this option for tylophorine in VSMC and HUVMSC. The fact that proteasomal inhibition blocks the tylophorine induced cyclin D1 and p21 down regulation just substantiates that tylophorine acts via these degradatory pathways. The reduction of cyclin D1 translation, combined with a short half-life of around 21 min could, still further contributes to the fast down regulation by tylophorine. The specific and detailed mechanism of tylophorine induced cyclin D1 and p21 degradation still needs to be determined.

Taken together, we found that tylophorine, a phenanthroindolizidine alkaloid isolated from *Tylophora indica* (*Asclepiadaceae*), is able to inhibit proliferation of rat aortic vascular smooth muscle cells and human umbilical vein smooth muscle cells by down regulation of cyclin D1 through a proteasome-dependent pathway. Furthermore, we demonstrate that tylophorine treatment prevents neointimal thickening in human saphenous veins.

## 5.2. *Peucedanum ostruthium* and its major coumarins

In the next part of the study, we examined the rhizome extract of *Peucedanum ostruthium*, for its putative anti-proliferative activity in rat aortic VSMC.

*Peucedanum ostruthium*, a traditionally used medicinal plant with anti-inflammatory properties, was a hit of a screening of plant extracts. The Dichloromethane (DCM)-extract of *Peucedanum ostruthium* was therefore interesting for further evaluation.

To find the components responsible for the activity of this extract, we performed a fractionation followed by isolation of the pure compounds (extraction and isolation performed by Mag. Silvia Vogl, University of Vienna). The isolation of all components of this extract was not possible, but we gained the 7 major coumarins. It has been documented that coumarins are major bioactive constituents of extracts from *Peucedanum ostruthium* roots (Hiermann A and Schantl D, 1998; Hiermann A et al., 1996). The anti-proliferative activity of these compounds was tested and resulted in one main active substance of the extract – the coumarin ostruthin. Anti-proliferative action of ostruthin in VSMC was never investigated before, however one study examined the inhibitory action of the structurally similar osthole isolated from *Angelica pubescens* in the smooth muscle cell line A10 (Guh JH et al., 1996). Contradictory to this finding, we did not observe a potent inhibitory action of osthole in our model system utilizing primary rat aorta VSMC. Although, all the substances show structural similarity, just ostruthin was able to inhibit the proliferation of VSMC significantly. Since also the structurally similar linear furanocoumarins have no effect on the proliferation of VSMC, it can be concluded that the prenylgroup in R3-position is necessary for the inhibitory effect (See table 2). Furthermore, ostruthin constitutes around 32% of the total amount of the extract, and it can be recalculated that the 24 µg/mL from the extract (the IC<sub>50</sub> exhibited from the extract is 24 ± 14 µg/mL) contains approximately 26 µM ostruthin. Since ostruthin inhibited VSMC proliferation with IC<sub>50</sub> of 11.07 ± 2.23 µM, its activity can entirely explain the inhibitory properties of the DCM extract. Thus, we describe a new bioactivity of

*Peucedanum ostruthium* and identify ostruthin as major responsible compound.

The mechanism behind ostruthins action on VSMC still remains an unsolved question. First of all, it will be necessary to exclude the induction of apoptosis by ostruthin treatment in VSMC. If ostruthin is not inducing cell death, the specific target of ostruthin in the cell needs to be clarified. Therefore, the ostruthin-induced cell cycle arrest needs to be analyzed by investigation of cyclin and CDK levels or their inhibitors.

In the end, it could be evaluated if ostruthin inhibits the proliferation of endothelial cells to a less extent than VSMC. Then, it could be a promising promising lead for the treatment of vasculo-proliferative disorders, such as restenosis.



## **6. REFERENCES**

## 6. References

- Aase K, Abramsson A, Karlsson L, Betsholtz C, Eriksson U. Expression analysis of PDGF-C in adult and developing mouse tissues. *Mech Dev.* 2002;110:187–191.
- Abbas T and Dutta A. p21 in cancer: intricate networks and multiple activities. *Nat Rev Cancer.* 2009; 9(6):400–414.
- Abedi H, Zachary I. Signalling mechanisms in the regulation of vascular cell migration. *Cardiovasc Res.* 1995;30(4):544-556.
- Afshari CA, Nichols MA, Xiong Y, and Mudryj M. A role for a p21-E2F interaction during senescence arrest of normal human fibroblasts. *Cell Growth Differ.* 1996;7:979-988.
- Alao JP. The regulation of cyclin D1 degradation: roles in cancer development and the potential for therapeutic invention. *Mol Cancer.* 2007;6:24.
- Alt JR, Cleveland JL, Hannink M, Diehl JA. Phosphorylation-dependent regulation of cyclin D1 nuclear export and cyclin D1-dependent cellular transformation. *Genes Dev.* 2000;14:3102–3114.
- Amador V, Ge S, Santamaría P, Pagano M, Guardavaccaro D and Pagano M. APC/CCdc20 controls the ubiquitin-mediated degradation of p21 in prometaphase. *Mol Cell.* 2007;27(3): 462–473.
- Andrae J, Gallini R and Betsholtz C. Role of platelet-derived growth factors in physiology and medicine. *Genes Dev* 2008;22:1276-1312.
- Andrés V. Control of vascular cell proliferation and migration by cyclin-dependent kinase signalling: new perspectives and therapeutic potential. *Cardiovasc Res.* 2004;63(1):11-21.
- Avruch J, Zhang XF and Kyriakis JM. Raf meets Ras: completing the framework of a signal transduction pathway. *Trends Biochem Sci.* 1994;19: 279-283.
- Barone MV and Courtneidge SA. Myc but not Fos rescue of PDGF signaling block caused by kinase-inactive Src. *Nature.* 1995;378:509-512.

- Bergsten E, Uutela M, Li X, Pietras K, Östman A, Heldin CH, Alitalo K, Eriksson U. PDGF-D is a specific, protease-activated ligand for the PDGF- $\beta$ -receptor. *Nat Cell Biol* 2001;3:512–516.
- Besson A, Yong VW. Involvement of p21Waf1/Cip1 in Protein Kinase C Alpha-Induced Cell Cycle Progression. *Mol. Cell. Biol.* 2000;20(13)4580-4590.
- Betticher DC, Thatcher N, Altermatt HJ, Hoban P, Ryder WD, Heighway J. Alternate splicing produces a novel cyclin D1 transcript. *Oncogene*. 1995;11(5):1005-1011.
- Bhutani KK, Sharma GL, Ali M. Plant Based Antiamoebic Drugs; Part I. Antiamoebic activity of phenanthroindolizidine alkaloids; common structural determinants of activity with emetine. *Planta Med.* 1987;53:532–536.
- Bishayee S, Majumdar S, Khire J, Das M. Das, Ligand-induced dimerization of the platelet-derived growth factor receptor. Monomer dimer interconversion occurs independent of receptor phosphorylation, *J. Biol. Chem.* 1989;264:11699-11705.
- Bjorge JD, Jakymiw A and Fujita DJ. Selected glimpses into the activation and function of Src kinase. *Oncogene*. 2000;19:5620-5635.
- Bornfeldt KE, Raines EW, Graves LM, Skinner MP, Krebs EG, Ross R. Platelet-derived growth factor. Distinct signal transduction pathways associated with migration versus proliferation. *Ann N Y Acad Sci.* 1995;766:416-430.
- Bornfeldt KE, Raines EW, Nakano T, Graves LM, Krebs EG, Ross R. Insulin-like growth factor-I and platelet-derived growth factor-BB induce directed migration of human arterial smooth muscle cells via signaling pathways that are distinct from those of proliferation. *J Clin Invest.* 1994;93:1266–1274.
- Bornstein G, Bloom J, Sitry-Shevah D, Nakayama K, Pagano M, Hershko A. Role of the SCFSkp2 Ubiquitin Ligase in the Degradation of p21Cip1 in S Phase. *J Biol Chem.* 2003;278(28):25752-25757.
- Bowman T, Broome MA, Sinibaldi D, Wharton W, Pledger WJ, Sedivy JM, Irby R, Yeatman T, Courtneidge SA, Jove R. Stat3-mediated Myc expression is required for Src transformation and PDGF-induced mitogenesis. *Proc Natl Acad Sci U S A.* 2001;98:7319-7324.

- Bromann PA, Korkaya H and Courtneidge SA. The interplay between Src family kinases and receptor tyrosine kinases. *Oncogene* 2004;23:7957-7968.
- Brooks CL, Gu W. Ubiquitination, phosphorylation and acetylation: the molecular basis for p53 regulation. *Curr Opin Cell Biol.* 2003;15(2):164-171.
- Broome MA and Courtneidge SA. No requirement for src family kinases for PDGF signaling in fibroblasts expressing SV40 large T antigen. *Oncogene.* 2000;19:2867-2869.
- Brugarolas J, Chandrasekaran C, Gordon JI, Beach D, Jacks T and Hannon GJ. Radiation-induced cell cycle arrest compromised by p21 deficiency. *Nature.* 1995;377:552–557.
- Buckley TF, Rapoport H.  $\alpha$ -Amino acids as chiral educts for asymmetric products. Chirally specific synthesis of tylophorine and cryptopleurine. *J Org Chem.* 1983;48:4222–4232.
- Burnett PE, Barrow RK, Cohen NA, Snyder SH, Sabatini DM. RAFT1 phosphorylation of the translational regulators p70 S6 kinase and 4EBP1. *Proc Natl Acad Sci USA.* 1998;95:1432–37.
- Campbell JH, Campbell GR. The role of smooth muscle cells in atherosclerosis. *Curr Opin Lipidol.* 1994;5:323–330.
- Cantley LC. The phosphoinositide 3-kinase pathway. *Science.* 2002;296:1655-1657.
- Casanovas O, Miro F, Estanyol JM, Itarte E, Agell N, Bachs O. Osmotic stress regulates the stability of cyclin D1 in a p38SAPK2-dependent manner. *J Biol Chem.* 2000;275(45):35091-35097.
- Chemler SR. Phenanthroindolizidines and Phenanthroquinolizidines: Promising Alkaloids for Anti-Cancer Therapy. *Curr Bioact Compd.* 2009;5(1):2-19.
- Chen X, Chi Y, Bloecher A, Aebersold R, Clurman BE, Roberts JM. N-acetylation and ubiquitin-independent proteasomal degradation of p21(Cip1). *Mol Cell.* 2004;16(5):839-847.
- Cheng SW, Ting AC and Ho P. Angioplasty and primary stenting of high-grade, long-segment superficial femoral artery disease: is it worthwhile? *Ann. Vasc. Surg.* 2003;17,430–437.

- Chevalier B, Serruys PW, Silber S, Garcia E, Suryapranata H, Hauptmann K, Wijns W, Schuler G, Fath-Ordoubadi F, Worthley S, Thuesen L, Meredith I, Bressers M, Nagai H, Paunovic D. Randomised comparison of Nobori™, biolimus A9-eluting coronary stent with aTaxus®, paclitaxel-eluting coronary stent in patients with stenosis in native coronary arteries: the Nobori 1 trial. *EuroIntervention*. 2007;2:426–434.
- Columbo A. TAXUS-II international study cohort I: slow-release formulation—six month results intent to treat analysis. Presented at Transcatheter Cardiovascular Therapeutics Conference, Washington, DC. 2002;24–28.
- Columbo A. TAXUS-II international study cohort II: moderate-release formulation—six month results intent to treat analysis. Presented at Transcatheter Cardiovascular Therapeutics Conference, Washington, DC. 2002;24–28.
- Cooper Woods T, Marks AR. Drug eluting stents. *Annu Rev Med*. 2004;55:169–178.
- Corjay MH, Thompson MM, Lynch KR, Owens GK. Differential effect of platelet-derived growth factor- versus serum-induced growth on smooth muscle alpha-actin and nonmuscle beta-actin mRNA expression in cultured rat aortic smooth muscle cells. *J Biol Chem*. 1989;264:10501–10506.
- Costa MA, de Wit LE, de Valk V, Serrano P, Wardeh AJ, Serruys PW, Sluiter W. Indirect evidence for a role of a subpopulation of activated neutrophils in the remodelling process after percutaneous coronary intervention. *Eur Heart J*. 2001;22:580–586.
- Costa MA, Sabate M, Kay IP, de Feyter PJ, Kozuma K, Serrano P, de Valk V, Albertal M, Ligthart JM, Disco C, Foley DP, Serruys PW. Threedimensional intravascular ultrasonic volumetric quantification of stent recoil and neointimal formation of two new generation tubular stents. *Am J Cardiol*. 2000;85:135–139.
- Coulombe P, Rodier G, Bonneil E, Thibault P, Meloche S. N-Terminal ubiquitination of extracellular signal-regulated kinase 3 and p21 directs their degradation by the proteasome. *Mol Cell Biol*. 2004;24(14):6140–6150.
- Dalby KN, Morrice N, Caudwell FB, Avruch J and Cohen P. Identification of regulatory phosphorylation sites in mitogen-activated protein kinase

- (MAPK)-activated protein kinase-1a/p90rsk that are inducible by MAPK. *J Biol Chem.* 1998;273:1496-1505.
- De Brabander M, Geuens G, Nuydens R, Willebrords R, De Mey J. Taxol induces the assembly of free microtubules in living cells and blocks the organizing capacity of the centrosomes and kinetochores. *Proc Natl Acad Sci USA.* 1981;78:5608–5612.
- Deng C, Zhang P, Harper JW, Elledge SJ and Leder P. Mice lacking p21CIP1/WAF1 undergo normal development, but are defective in G1 checkpoint control. *Cell.* 1995;82:675–684 .
- Di Mario C, Gil R, Camenzind E, Ozaki Y, von Birgelen C, Umans V, de Jaegere P, de Feyter PJ, Roelandt JR, Serruys PW. Quantitative assessment with intracoronary ultrasound of the mechanisms of restenosis after percutaneous transluminal coronary angioplasty and directional coronary atherectomy. *Am J Cardiol.* 1995;75:772–777.
- Diehl JA, Cheng M, Roussel MF and Sherr CJ. Glycogen synthase kinase-3b regulates cyclin D1 proteolysis and subcellular localization. *Genes Dev.* 1998;12:3499–3511.
- Diehl JA, Zindy F and Sherr CJ. Inhibition of cyclin D1 phosphorylation on threonine-286 prevents its rapid degradation via the ubiquitin–proteasome pathway. *Genes Dev.* 1997;11:957–972.
- Donaldson GR, Atkinson MR, Murray AW. Inhibition of protein synthesis in Ehrlich ascites-tumor cells by the phenanthrene alkaloids tylophorine, tylocrebrine and cryptopleurine. *Biochem Biophys Res Commun* 1968;31:104–109.
- Dong LH, Wen JK, Miao SB, Jia Z, Hu HJ, Sun RH, Wu Y, Han M. Baicalin inhibits PDGF-BB-stimulated vascular smooth muscle cell proliferation through suppressing PDGFR $\beta$ -ERK signaling and increase in p27 accumulation and prevents injury-induced neointimal hyperplasia. *Cell Res.* 2010;20(11):1252-1262.
- Doran AC, Meller N and McNamara CA. Role of smooth muscle cells in the initiation and early progression of atherosclerosis. *Arterioscler Thromb Vasc Biol.* 2008;28:812-819.
- Duchek P, Somogyi K, Jekely G, Beccari S, Rorth P. Guidance of cell migration by the *Drosophila* PDGF/VEGF receptor. *Cell* 2001;107:17–26.

- Dugina VB, Alexandrova AY, Lane K, Bulanova E, Vasiliev JM. The role of the microtubular system in the cell response to HGF/SF. *J Cell Sci.* 1995;108(4):1659–67.
- Dussaillant G, Mintz G, Pichard A, Kent K, Satler L, Popma J, Wong S, Leon M. Small stent size and intimal hyperplasia contribute to restenosis: a volumetric intravascular ultrasound analysis. *J Am Coll Cardiol.* 1995;26:720–724.
- Dzau VJ, Braun-Dullaeus RC and Sedding DG. Vascular proliferation and atherosclerosis: New perspectives and therapeutic strategies. *Nature Medicine.* 2002;8,1249-1256.
- el-Deiry WS, Tokino T, Velculescu VE, Levy DB, Parsons R, Trent JM, Lin D, Mercer WE, Kinzler KW, Vogelstein B. WAF1, a potential mediator of p53 tumor suppression. *Cell.* 1993;75(4):817-825.
- Elledge SJ. Cell cycle checkpoints: preventing an identity crisis. *Science* 1996;274:1664–1671.
- Elmadbouh I, Rossignol P, Meilhac O, Vranckx R, Pichon C, Pouzet B, Midoux P, Michel JB. Optimization of in vitro vascular cell transfection with non-viral vectors for in vivo applications. *J Gene Med.* 2004;6(10):1112-24.
- Erl W, Hansson GK, de Martin R, Draude G, Weber KS, Weber C. Nuclear actor-kappa B regulates induction of apoptosis and inhibitor of apoptosis protein-1 expression in vascular smooth muscle cells. *Circ Res.* 1999;84:668–77.
- Fajadet J, Wijns W, Laarman GJ, Kuck KH, Ormiston J, Münzel T, Popma JJ, Fitzgerald PJ, Bonan R, Kuntz RE; ENDEAVOR II Investigators. Randomized, double-blind, multicenter study of the endeavor zotarolimus-eluting phosphorylcholineencapsulated stent for treatment of native coronary artery lesions: clinical and angiographic results of the ENDEAVOR II trial. *Circulation* 2006;114:798–806.
- Ferreiro DU and Komives EA. Molecular Mechanisms of System Control of NFκB Signaling by IκBα. *Biochemistry.* 2010;49:1560–1567.

- Franke TF, Kaplan DR, Cantley LC, Toker A. Direct regulation of the Akt proto-oncogene product by phosphatidylinositol-3-4-bisphosphate. *Science*. 1997;275:665-8.
- Fredriksson L, Li H, Eriksson U. The PDGF family: four gene products form five dimeric isoforms. *Cytokine Growth F R*. 2004;15:197–204.
- Fresno Vara JA, Casado E, de Castro J, Cejas P, Belda-Iniesta C, González-Barón M. PI3K/Akt signalling pathway and cancer. *Cancer Treat Rev*. 2004;30:193-204.
- Fretto LJ, Snape AJ, Tomlinson JE, Seroogy JJ, Wolf DL, LaRochelle WJ, Giese NA. Mechanism of platelet-derived growth factor (PDGF) AA, AB, and BB binding to  $\alpha$  and  $\beta$  PDGF receptor. *J Biol Chem*. 1993;268:3625-3631.
- Frödin M, Gammeltoft S. Role and regulation of 90 kDa ribosomal S6 kinase (RSK) in signal transduction. *Mol Cell Endocrinol*. 1999;151(1-2):65-77.
- Gabbiani G, Schmid E, Winter S, Chaponnier C, De Chastonay C, Vandekerckhove J, Weber K, Franke WW. Vascular smooth muscle cells differ from other smooth muscle cells: predominance of vimentin filaments and a specific  $\alpha$ -type actin. *Proc Natl Acad Sci U S A*. 1981;78:298–302.
- Gallo R, Padurean A, Jayaraman T, Marx S, Roque M, Adelman S, Chesebro J, Fallon J, Fuster V, Marks A, Badimon JJ. Inhibition of intimal thickening after balloon angioplasty in porcine coronary arteries by targeting regulators of the cell cycle. *Circulation*. 1999;99(16):2164-2170.
- Ganguly T, Sainis KB. Inhibition of cellular immune responses by *Tylophora indica* in experimental models. *Phytomedicine*. 2001;8(5):348-355.
- Gao W, Bussom S, Grill SP, Gullen EA, Hu YC, Huang X, Zhong S, Kaczmarek C, Gutierrez J, Francis S, Baker DC, Yu S, Cheng YC. Structure-activity studies of phenanthroindolizidine alkaloids as potential antitumor agents. *Bioorg Med Chem Lett*. 2007;17,15:4338-4342.
- Gao W, Lam W, Zhong S, Kaczmarek C, Baker DC and Cheng YC. Novel mode of action of tylophorine analogs as antitumor compounds. *Cancer Res*. 2004;64:678-688.
- Gellert E. The indolizidine alkaloids. *J Nat Prod* 1982;45:50–73.



- Gerthoffer WT. Mechanisms of Vascular Smooth Muscle Cell Migration. *Circ Res*. 2007;100:607-621 .
- Gimbrone MA Jr. Vascular endothelium, hemodynamic forces, and atherogenesis. *Am J Pathol*. 1999;155,1–5.
- Gopalakrishnan C, Shankaranarayan D, Kameswaran L, Natarajan S. Pharmacological investigations of tylophorine, the major alkaloid of *tylophora indica*. *Indian J Med Res* 1979;69:513–520.
- Gopalakrishnan C, Shankaranarayan D, Nazimudeen SK, Kameswaran L. Effect of tylophorine, a major alkaloid of *Tylophora indica*, on immunopathological and inflammatory reactions. *Ind J Med Res*. 1980;71:940–948.
- Govindachari TR, Lakshmikantham MV, Pai BR, Rajappa S. Chemical examination of *tylophora asthmatica*--III. The complete structure of tylophorine. *Tetrahedron*. 1960;9:53.
- Griffiths H, Bakhai A, West D, Petrou M, De Souza T, Moat N, Pepper J, Di Mario C. Feasibility and cost of treatment with drug eluting stents of surgical candidates with multi-vessel coronary disease. *Eur J Cardiothorac Surg*. 2004;26(3):528-534.
- Grube E, Sonoda S, Ikeno F, Honda Y, Kar S, Chan C, Gerckens U, Lansky AJ, Fitzgerald PJ. Six- and twelve-month results from first human experience using everolimus-eluting stents with bioabsorbable polymer. *Circulation*. 2004;109:2168–2171.
- Gu Y, Turck CW, Morgan DO. Inhibition of CDK2 activity in vivo by an associated 20K regulatory subunit. *Nature*. 1993;366:707-710.
- Guh JH, Yu SM, Ko FN, Wu TS, Teng CM. Antiproliferative effect in rat vascular smooth muscle cells by osthole, isolated from *Angelica pubescens*. *Eur J Pharmacol*. 1996;298(2):191-197.
- Guo Y, Yang K, Harwalkar J, Nye JM, Mason DR, Garrett MD, Hitomi M, Stacey DW. Phosphorylation of cyclin D1 at Thr 286 during S phase leads to its proteasomal degradation and allows efficient DNA synthesis. *Oncogene*. 2005;24(16):2599-2612.

- Harper JW, Adami GR, Wei N, Keyomarsi K, Elledge SJ. The p21 Cdk-interacting protein Cip1 is a potent inhibitor of G1 cyclin-dependent kinases. *Cell*. 1993;75(4):805-816.
- Harper JW, Elledge SJ, Keyomarsi K, Dynlacht B, Tsai LH, Zhang P, Dobrowolski S, Bai C, Connell-Crowley L, Swindell E. Inhibition of cyclin-dependent kinases by p21. *Mol Biol Cell*. 1995;6(4):387–400.
- Hautmann MB, Madsen CS, Owens GK. A transforming growth factor beta (TGFbeta) control element drives TGFbeta-induced stimulation of smooth muscle alpha-actin gene expression in concert with two CArG elements. *J Biol Chem*. 1997;272:10948–10956.
- Heldin CH, Ernlund A, Rorsman C, Rönnstrand L. Dimerization of B-type platelet-derived growth factor receptors occurs after ligand binding and is closely associated with receptor kinase activation, *J Biol Chem*. 1989;264:8905-8912.
- Heldin CH, Östman A, Rönnstrand L. Signal transduction via platelet-derived growth factor receptors. *Biochim Biophys Acta*. 1998;1378:F79-F113.
- Hedin U, Bottger BA, Luthman J, Johansson S, Thyberg J. A substrate of the cell-attachment sequence of fibronectin (Arg-Gly-Asp-Ser) is sufficient to promote transition of arterial smooth muscle cells from a contractile to a synthetic phenotype. *Dev Biol*. 1989;133:489 –501.
- Hellström M, Kalén M, Lindahl P, Abramsson A, Betsholtz C. Role of PDGF-B and PDGFR-beta in recruitment of vascular smooth muscle cells and pericytes during embryonic blood vessel formation in the mouse. *Development*. 1999;126:3047–55.
- Herren B, Rooney B, Weyer KA, Iberg N, Schmid G, Pech M. Dimerization of extracellular domains of platelet-derived growth factor receptors. *J Biol Chem*. 1993;268:15088-15095.
- Hidalgo M, Rowinsky EK. The rapamycin-sensitive signal transduction pathway as a target for cancer therapy. *Oncogene*. 2000;19(56):6680-6686.
- Hiermann A, Schantl D. Antiphlogistic and antipyretic activity of *Peucedanum ostruthium*. *Planta Med* 1998;64(5):400-403.
- Hiermann A, Schantl D, Schubert-Zsilavecz M, Reiner J. Coumarins from *Peucedanum ostruthium*. *Phytochemistry*. 1996;43(4):881-883.

- Higashimoto Y, Saito S, Tong XH, Hong A, Sakaguchi K, Appella E, Anderson CW. Human p53 is phosphorylated on serines 6 and 9 in response to DNA damage-inducing agents. *J Biol Chem*. 2000;275(30):23199-23203.
- Hirano T, Ishihara K, Hibi M. Roles of STAT3 in mediating the cell growth, differentiation and survival signals relayed through the IL-6 family of cytokine receptors. *Oncogene*. 2000;19(21):2548-2556.
- Hosokawa Y, Gadd M, Smith AP, Koerner FC, Schmidt EV, Arnold A. Cyclin D1 (PRAD1) alternative transcript b: full-length cDNA cloning and expression in breast cancers. *Cancer Lett*. 1997;113(1-2):123-130.
- Hughes AD, Clunn GF, Refson J, Demoliou-Mason C. Platelet-derived growth factor (PDGF): actions and mechanisms in vascular smooth muscle. *Gen Pharmacol*. 1996;27:1079-1089.
- Inui H, Kitami Y, Kondo T, Inagami T. Transduction of mitogenic activity of platelet-derived growth factor (PDGF) AB by PDGF- $\beta$  receptor without participation of PDGF- $\alpha$  receptor in vascular smooth muscle cells. *J Biol Chem*. 1993;268:17045-17050.
- Jayaraman T, Marks AR. Rapamycin- FKBP12 blocks proliferation, induces differentiation, and inhibits cdc2 kinase activity in a myogenic cell line. *J Biol Chem*. 1993;268:25385-25388.
- Jia L, Sun Y. F-box proteins FBXO31 and FBX4 in regulation of cyclin D1 degradation upon DNA damage. *Pigment Cell Melanoma Res*. 2009;22(5):518-519.
- Jin Y, Lee H, Zeng SX, Dai MS, Lu H. MDM2 promotes p21waf1/cip1 proteasomal turnover independently of ubiquitylation. *EMBO J*. 2003;22(23):6365-6377.
- Joukov V, Kaipainen A, Jeltsch M, Pajusola K, Olofsson B, Kumar V, Eriksson U and Alitalo K. Vascular endothelial growth factors Vegf-B and Vegf-C. *J Cell Physiol*. 1997;173:211-215.
- Jung YS, Qian Y, Chen X. Examination of the expanding pathways for the regulation of p21 expression and activity. *Cell Signal*. 2010;22(7):1003-1012.

- Kanakaraj P, Raj S, Khan SA, Bishayee S. Ligand-induced interaction between  $\alpha$ - and  $\beta$ -type platelet derived growth factor (PDGF) receptors: role of receptor heterodimers in kinase activation. *Biochemistry*. 1991;30:1761-1767.
- Kandel ES and Hay N. The regulation and activities of the multifunctional serine/threonine kinase Akt/PKB. *Exp Cell Res*. 1999;253:210-229.
- Kazlauskas A. Platelet derived growth factor. In: William D. Figg, Judah Folkman, editors. *Angiogenesis: An Integrative Approach from Science to Medicine*. 2008.
- Kelman Z. PCNA: structure, functions and interactions. *Oncogene*. 1997;14(6):629-640.
- Kim Y, Starostina NG, Kipreos ET. The CRL4Cdt2 ubiquitin ligase targets the degradation of p21Cip1 to control replication licensing. *Genes Dev*. 2008;22(18):2507-2519.
- Kishi H, Bao J, Kohama K. Inhibitory effects of ML-9, wortmannin, and Y-27632 on the chemotaxis of vascular smooth muscle cells in response to platelet-derived growth factor-BB. *J Biochem*. 2000;128:719–722.
- Klinghoffer RA, Duckworth B, Valius M, Cantley L, Kazlauskas A. Platelet-derived growth factor-dependent activation of phosphatidylinositol 3-kinase is regulated by receptor binding of SH2-domain-containing proteins -which influence ras activity. *Mol Cell Biol*. 1996;16:5909-5914.
- Koepp DM, Harper JW and Elledge EJ. How the cyclin became a cyclin: Regulated proteolysis in the cell cycle. *Cell*. 1999;97,431–434 .
- Kortenjann M, Thomae O and Shaw PE. Inhibition of v-raf-dependent c-fos expression and transformation by a kinase-defective mutant of the mitogenactivated protein kinase Erk2. *Mol Cell Biol*. 1994;14:4815-4824.
- Kraitzer, A., Kloog, Y. & Zilberman, M. Approaches for prevention of restenosis. *J Biomed Mater Res B Appl Biomater*. 2008;85:583-603.
- LaBaer J, Garrett MD, Stevenson LF, Slingerland JM, Sandhu C, Chou HS, Fattaey A, Harlow E. New functional activities for the p21 family of CDK inhibitors. *Genes Dev*. 1997;11(7):847.
- Labinaz M, Pels K, Hoffert C, Aggarwal S, O'Brien ER. Time course and importance of neoadventitial formation in arterial remodeling following

- balloon angioplasty of porcine coronary arteries. *Cardiovasc Res.* 1999;41:255–266.
- Lansky AJ, Costa RA, Mintz GS, Tsuchiya Y, Midei M, Cox DA, O'Shaughnessy C, Applegate RA, Cannon LA, Mooney M, Farah A, Tannenbaum MA, Yakubov S, Kereiakes DJ, Wong SC, Kaplan B, Cristea E, Stone GW, Leon MB, Knopf WD, O'Neill WW. Non-polymer-based paclitaxel-coated coronary stents for the treatment of patients with de novo coronary lesions: angiographic follow-up of the DELIVER clinical trial. *Circulation.* 2004;109(16):1948-1954.
- LaRochelle WJ, May-Siroff M, Robbins KC, Aaronson SA. A novel mechanism regulating growth factor association with the cell surface: identification of a PDGF retention domain. *Genes Dev.* 1991;5:1191– 1199.
- Leon MB, Moses JW, Popma JJ, Kuntz RE, Fitzgerald P, for the SIRIUS Investigators. SIRIUS: a U.S., multicenter, randomized, double blind study of the sirolimus-eluting stent in de novo native coronary lesions. *N Engl J Med.* 2003;349:1315–1323.
- Levine AJ. p53, the cellular gatekeeper for growth and division. *Cell.* 1997;88,323–331.
- Li DW, Liu JP, Schmid PC, Schlosser R, Feng H, Liu WB, Yan Q, Gong L, Sun SM, Deng M, Liu Y. Protein serine/threonine phosphatase-1 dephosphorylates p53 at Ser-15 and Ser-37 to modulate its transcriptional and apoptotic activities. *Oncogene.* 2006;25(21):3006-3022.
- Li PF, Dietz R, von Harsdorf R. Differential effect of hydrogen peroxide and superoxide anion on apoptosis and proliferation of vascular smooth muscle cells. *Circulation.* 1997;96(10):3602-3609.
- Li R, Waga S, Hannon GJ, Beach D, Stillman B. Differential effects by the p21 CDK inhibitor on PCNA-dependent DNA replication and repair. *Nature.* 1994;371:534-537.
- Li X, Van Putten V, Zarinetchi F, Nicks ME, Thaler S, Heasley LE, Nemenoff RA. Suppression of smooth-muscle alpha-actin expression by platelet-derived growth factor in vascular smooth-muscle cells involves Ras and cytosolic phospholipase A2. *Biochem J.* 1997;327(3):709–716.

- Li Y, Jenkins CW, Nichols MA and Xiong Y. Cell cycle expression and p53 regulation of the cyclin-dependent kinase inhibitor p21. *Oncogene*. 1994;9(8):2261-2268.
- Libby P, Ridker PM, Maseri A. Inflammation and atherosclerosis. *Circulation*. 2002;105:1135–1143.
- Libby P, Schwartz D, Brogi E, Tanaka H, Clinton SK. A cascade model for restenosis: a special case of atherosclerosis progression. *Circulation*. 1992;86:47–52.
- Lim CP, Cao X. Serine phosphorylation and negative regulation of Stat3 by JNK. *J Biol Chem*. 1999;274(43):31055-31061.
- Lin DI, Barbash O, Kumar KG, Weber JD, Harper JW, Klein-Szanto AJ, Rustgi A, Fuchs SY, Diehl JA. Phosphorylation-dependent ubiquitination of cyclin D1 by the SCF(FBX4- $\alpha$ B-crystallin) complex. *Mol Cell*. 2006;24(3):355-366.
- Lu F, Gladden AB, Diehl JA. An alternatively spliced cyclin D1 isoform, cyclin D1b, is a nuclear oncogene. *Cancer Res*. 2003;63(21):7056-7061.
- Lundberg MS, Crow MT. Age-related changes in the signaling and function of vascular smooth muscle cells. *Exp Gerontol*. 1999;34:549–57.
- Lusis AJ. Atherosclerosis. *Nature*. 2000;407:233–241.
- Maisel WH. Unanswered questions--drug-eluting stents and the risk of late thrombosis. *N Engl J Med*. 2007;356:981-984.
- Marra DE, Simoncini T, Liao JK. Inhibition of vascular smooth muscle cell proliferation by sodium salicylate mediated by upregulation of p21Waf1 and p27Kip1. *Circulation*. 2000;102:2124–2130.
- Marx SO, Jayaraman T, Go LO, Marks AR. Rapamycin-FKBP inhibits cell cycle regulators of proliferation in vascular smooth muscle cells. *Circ Res*. 1995;76(3):412-417.
- Mayo LD, Seo YR, Jackson MW, Smith ML, Rivera Guzman J, Korgaonkar CK, Donner DB. Phosphorylation of human p53 at serine 46 determines promoter selection and whether apoptosis is attenuated or amplified. *J Biol Chem*. 2005;280(28):25953-25959.

- Mehrhof FB, Schmidt-Ullrich R, Dietz R, Scheidereit C. Regulation of vascular smooth muscle cell proliferation: role of NF-kappaB revisited. *Circ Res*. 2005;13,96(9):958-964.
- Mintz G, Popma J, Pichard A, Kent K, Satler L, Wong C, Hong M, Kovach J, Leon M. Arterial remodeling after coronary angioplasty: a serial intravascular ultrasound study. *Circulation*. 1996;94:35–43.
- Mita MM, Mita A, Rowinsky EK. The molecular target of rapamycin (mTOR) as a therapeutic target against cancer. *Cancer Biol Ther*. 2003;2(4):169-177.
- Morice MC, Serruys PW, Sousa JE, Fajadet J, Ban Hayashi E, Perin M, Colombo A, Schuler G, Barragan P, Guagliumi G, Molnàr F, Falotico R; RAVEL Study Group. Randomized Study with the Sirolimus-Coated Bx Velocity Balloon-Expandable Stent in the Treatment of Patients with de Novo Native Coronary Artery Lesions. A randomized comparison of a sirolimus-eluting stent with a standard stent for coronary revascularization. *N Engl J Med*. 2002;346(23):1773-1780.
- Mosse PR, Campbell GR, Wang ZL, Campbell JH. Smooth muscle phenotypic expression in human carotid arteries. I. Comparison of cells from diffuse intimal thickenings adjacent to atheromatous plaques with those of the media. *Lab Invest*. 1985;53:556-562.
- Murphy LO and Blenis J. MAPK signal specificity: the right place at the right time. *Trends Biochem Sci*. 2006;31:268-275.
- Murphy LO, MacKeigan JP and Blenis J. A network of immediate early gene products propagates subtle differences in mitogen-activated protein kinase signal amplitude and duration. *Mol Cell Biol*. 2004;24:144-153.
- Nakayama M, Amano M, Katsumi A, Kaneko T, Kawabata S, Takefuji M, Kaibuchi K. Rho-kinase and myosin II activities are required for cell type and environment specific migration. *Genes Cells*. 2005;10:107–117.
- Noda A, Ning Y, Venable SF, Pereira-Smith OM, Smith JR. Cloning of senescent cell-derived inhibitors of DNA synthesis using an expression screen. *Exp Cell Res*. 1994;211(1):90–98.
- Okabe H, Lee SH, Phuchareon J, Albertson DG, McCormick F, Tetsu O. A Critical Role for FBXW8 and MAPK in Cyclin D1 Degradation and Cancer Cell Proliferation. *PLoS ONE*. 2006;1:e128.

- Oku T, Ikeda S, Sasaki H, Fukuda K, Morioka H, Ohtsuka E, Yoshikawa H, Tsurimoto T. Functional sites of human PCNA which interact with p21 (Cip1/Waf1), DNA polymerase delta and replication factor C. *Genes Cells*. 1998;3(6):357-369.
- Orr-Urtreger A, Lonai P. Platelet-derived growth factor-A and its receptor are expressed in separate, but adjacent cell layers of the mouse embryo. *Development*. 1992;115:1045–1058.
- Östman A, Andersson M, Betsholtz C, Westermark B, Heldin CH. Identification of a cell retention signal in the B-chain of platelet-derived growth factor and in the long splice version of the A-chain. *Cell Regulat*. 1991;2:503–512.
- Pardee AB. G1 events and regulation of cell proliferation. *Science*. 1989;240:603-608.
- Pawson T, Scott JD. Signaling through scaffold, anchoring, and adaptor proteins. *Science*. 1997;278:2075-2080.
- Perez-Roger I, Kim SH, Griffiths B, Sewing A, Land H. Cyclins D1 and D2 mediate Myc-induced proliferation via sequestration of p27(Kip1) and p21(Cip1) *EMBO J*. 1999;18(19):5310-5320.
- Philipp J, Vo K, Gurley KE, Seidel K, and Kemp SJ. Tumor suppression by p27(kip1) and p21(Cip1) during chemically induced skin carcinogenesis. *Oncogene*. 1999;18(33):4689–4698.
- Pidkovka NA, Cherepanova OA, Yoshida T, Alexander MR, Deaton RA, Thomas JA, Leitinger N, Owens GK. Oxidized phospholipids induce phenotypic switching of vascular smooth muscle cells in vivo and in vitro. *Circ Res*. 2007;101:792–801.
- Poon M, Marx SO, Gallo R, Badimon JJ, Taubman MB, Marks AR. Rapamycin inhibits vascular smooth muscle cell migration. *J. Clin. Invest*. 1996;98:2277–2283.
- Prelich G, Stillman B. Coordinated leading and lagging strand synthesis during SV40 DNA replication in vitro requires PCNA. *Cell*. 1988;53(1):117-126.



- Rathnagiriswaran AN, Venkatachalam K. The chemical examination of tylophora asthmatica and isolation of the alkaloids tylophorine and tylophorinine. *Indian J Med Res.* 1935;22:433.
- Reisinger U, Schwaiger S, Zeller I, Messner B, Stigler R, Wiedemann D, Mayr T, Seger C, Schachner T, Dirsch VM, Vollmar AM, Bonatti JO, Stuppner H, Laufer G, Bernhard D. Leoligin, the major lignan from Edelweiss, inhibits intimal hyperplasia of venous bypass grafts. *Cardiovasc Res.* 2009; 82(3):542–549.
- Reusch P, Wagdy H, Reusch R, Wilson E, Ives HE. Mechanical strain increases smooth muscle and decreases nonmuscle myosin expression in rat vascular smooth muscle cells. *Circ Res.* 1996;79:1046–1053.
- Riccardi C, Nicoletti I. Analysis of apoptosis by propidium iodide staining and flow cytometry. *Nat Protoc.* 2006;1(3):1458-1461.
- Rivard A, Andre's V. Vascular smooth muscle cell proliferation in the pathogenesis of atherosclerotic cardiovascular diseases. *Histol Histopathol.* 2000;15:557–571.
- Roche S, Koegl M, Barone MV, Roussel MF and Courtneidge SA. DNA synthesis induced by some but not all growth factors requires Src family protein tyrosine kinases. *Mol Cell Biol.* 1995;15:1102-1109.
- Rodriguez-Viciana P, Marte BM, Warne PH, Downward J. Phosphatidylinositol 3' kinase: one of the effectors of Ras. *Philos Trans R Soc Lond B Biol Sci.* 1996;351(1336):225-231.
- Rosania GR, Swanson JA. Microtubules can modulate pseudopod activity from a distance inside macrophages. *Cell Motil. Cytoskelet.* 1996;34:230–245.
- Rosette C, Karin M. Cytoskeletal control of gene expression: depolymerization of microtubules activates NF-kappa B. *J. Cell Biol.* 1995;128:1111–1119.
- Rosner D, McCarthy N, Bennett M. Rapamycin inhibits human in stent restenosis vascular smooth muscle cells independently of pRB phosphorylation and p53. *Cardiovasc Res.* 2005;66(3):601-610.
- Ross R. Atherosclerosis - an inflammatory disease. *N Engl J Med.* 1999;340:115-126.

- Rowinsky EK, Donehower RC, Jones RJ, et al. Microtubule changes and cytotoxicity in leukemic cell lines treated with taxol. *Cancer Res.* 1988;48:4093–4100.
- Sabers CJ, Martin MM, Brunn GJ, Williams JM, Dumont FJ, Wiederrecht G, Abraham RT. Isolation of a protein target of the FKBP12-rapamycin complex in mammalian cells. *J Biol Chem.* 1995;270(2):815-822.
- Santra MK, Wajapeyee N, Green MR. F-box protein FBXO31 mediates cyclin D1 degradation to induce G1 arrest after DNA damage. *Nature.* 2009;459(7247):722-725.
- Scherberich A, Campos-Toimil M, Ronde P, Takeda K, Beretz A. Migration of human vascular smooth muscle cells involves serum-dependent repeated cytosolic calcium transients. *J Cell Sci.* 2000;113:653–662.
- Schiff PB, Fant J, Horwitz SB. Promotion of microtubule assembly in vitro by taxol. *Nature.* 1979;277:665–667.
- Schiff PB, Horwitz SB. Taxol stabilizes microtubules in mouse fibroblast cells. *Proc Natl Acad Sci USA.* 1980;77:1561–1565.
- Schillinger M, Exner M, Mlekusch W, Haumer M, Sabeti S, Ahmadi R, Schwarzwinger I, Wagner O, Minar E. Restenosis after femoropopliteal PTA and elective stent implantation: predictive value of monocyte counts. *J Endovasc Ther.* 2003;10:557–565.
- Schwartz RS, Topol EJ, Serruys PW, Sangiorgi G, Holmes DR Jr. Artery size, neointima, and remodeling: time for some standards. *J Am Coll Cardiol.* 1998;32:2087–2094.
- Seifert RA, Hart CE, Phillips PE, Forstrom JW, Ross R, Murray MJ, Bowen-Pope DF. Two different subunits associate to create isoform-specific platelet-derived growth factor receptors. *J Biol Chem.* 1989;264:8771-8778.
- Selzman CH, Shames BD, Reznikov LL, Miller SA, Meng X, Barton HA, Werman A, Harken AH, Dinarello CA, Banerjee A. Liposomal delivery of purified inhibitory-kappaBalpha inhibits tumor necrosis factor-alpha-induced human vascular smooth muscle proliferation. *Circ Res.* 1999;84:867–875.
- Sheaff RJ, Singer JD, Swanger J, Smitherman M, Roberts JM, Clurman BE. Proteasomal turnover of p21Cip1 does not require p21Cip1 ubiquitination. *Mol Cell.* 2000;5(2):403-410.

- Sherr CJ. Cancer cell cycles. *Science*. 1996;274(5293):1672-1674.
- Sherr CJ. D-type cyclins. *Trends Biochem Sci*. 1995;20(5):187-190.
- Sherr CJ. Mammalian G1 cyclins and cell cycle progression. *Proc Assoc Am Physicians*. 1995;107(2):181-186.
- Sherr CJ, Roberts JM. CDK inhibitors: positive and negative regulators of G1-phase progression. *Genes Dev*. 1999;13(12):1501-1512.
- Sherr CJ, Roberts JM. Inhibitors of mammalian G1 cyclin-dependent kinases. *Genes Dev*. 1995;9(10):1149-1163.
- Shiah HS, Gao W, Baker DC, Cheng YC. Inhibition of cell growth and nuclear factor-kappaB activity in pancreatic cancer cell lines by a tylophorine analogue, DCB-3503. *Mol Cancer Ther*. 2006;5(10):2484-2493.
- Shivpuri DN, Singhal SC, Prakash D. Treatment of asthma with an alcoholic extract of *Tylophora indica*: a crossover, double-blind study. *Ann Allergy*. 1972;30:407-412.
- Solomon DA, Wang Y, Fox SR, Lambeck TC, Giesting S, Lan Z, Senderowicz AM, Conti CJ, Knudsen ES. Cyclin D1 splice variants. Differential effects on localization, RB phosphorylation, and cellular transformation. *J Biol Chem*. 2003;278(32):30339-30347.
- Songyang Z, Shoelson SE, Chaudhuri M, Gish G, Pawson T, Haser WG, King F, Roberts T, Ratnofsky S, Lechleider RJ, Neel BG, Birge RB, Fajardof JE, Chouf MM, Hanafusaf H, Schaffhausen B and Cantley LC. SH2 domains recognize specific phosphopeptide sequences. *Cell*. 1993;72(5):767-778.
- Sousa JE, Costa MA, Sousa AG, Abizaid AC, Seixas AC, Abizaid AS, Feres F, Mattos LA, Falotico R, Jaeger J, Popma JJ, Serruys PW. Two-year angiographic and intravascular ultrasound follow-up after implantation of sirolimus-eluting stents in human coronary arteries. *Circulation*. 2003;107:381-383.
- Staab ME, Srivatsa SS, Lerman A, Sangiorgi G, Jeong MH, Edwards WD, Holmes DR Jr, Schwartz RS. Arterial remodeling after experimental percutaneous injury is highly dependent on adventitial injury and histopathology. *Int J Cardiol*. 1997;58:31-40.

- Staerk D, Lykkeberg AK, Christensen J, Budnik BA, Abe F and Jaroszewski JW. In vitro cytotoxic activity of phenanthroindolizidine alkaloids from *Cynanchum vincetoxicum* and *Tylophora tanakae* against drug-sensitive and multidrug-resistant cancer cells. *J Nat Prod.* 2002;65:1299-1302.
- Stambolic V, Woodgett JR. Mitogen inactivation of glycogen synthase kinase-3 $\beta$  in intact cells via serine 9 phosphorylation. *Biochem J.* 1994;303:701-704.
- Su B, Mitra S, Gregg H, Flavahan S, Chotani MA, Clark KR, Goldschmidt-Clermont PJ, Flavahan NA. Redox regulation of vascular smooth muscle cell differentiation. *Circ Res.* 2001;89:39–46.
- Takenawa T, Suetsugu S. The WASP-WAVE protein network: connecting the membrane to the cytoskeleton. *Nat Rev Mol Cell Biol.* 2007;8(1):37-48.
- Tallquist M and Kazlauskas A. PDGF signaling in cells and mice. *Cytokine Growth F R.* 2004;15:205.
- Tanabe K, Serruys PW, Grube E, Smits PC, Selbach G, van der Giessen WJ, Staberock M, de Feyter P, Müller R, Regar E, Degertekin M, Ligthart JM, Disco C, Backx B, Russell ME. TAXUS III Trial: in-stent restenosis treated with stent-based delivery of paclitaxel incorporated in a slow-release polymer formulation. *Circulation.* 2003;107(4):559-564.
- Tedgui A, Mallat Z. Cytokines in atherosclerosis: pathogenic and regulatory pathways. *Physiol Rev.* 2006;86(2):515-581.
- Thyberg J, Hultgardh-Nilsson A. Fibronectin and the basement membrane components laminin and collagen type IV influence the phenotypic properties of subcultured rat aortic smooth muscle cells differently. *Cell Tissue Res.* 1994;276:263–271.
- Tien Y, Autieri M. Cytokine expression and AIF-1-mediated activation of Rac2 in vascular smooth muscle cells: a role for Rac2 in VSMC activation. *Am J Physiol Cell Physiol.* 2006;292:C841–C849.
- Twamley-Stein GM, Pepperkok R, Ansorge W and Courtneidge SA. The Src family tyrosine kinases are required for platelet-derived growth factor-mediated signal transduction in NIH 3T3 cells. *Proc Natl Acad Sci U S A.* 1993;90:7696-7700.

- Uutela M, Laurén J, Bergsten E, Li X, Horelli-Kuitunen N, Eriksson U, Alitalo K. Chromosomal location, exon structure, and vascular expression patterns of the human PDGFC and PDGFD genes. *Circulation*. 2001;103:2242–2247.
- Vander Heiden MG, Cantley LC, Thompson CB. Understanding the Warburg effect: the metabolic requirements of cell proliferation. *Science*. 2009;324(5930):1029-1033.
- Vicente A. Control of vascular cell proliferation and migration by cyclin-dependent kinase signalling: new perspectives and therapeutic potential. *Cardiovasc Res*. 2004;63,11–21.
- Vicente-Manzanares M, Webb DJ, Horwitz AR. Cell migration at a glance. *J Cell Sci*. 2005;118:4917–4919.
- Virmani R, Liistro F, Stankovic G, Di Mario C, Montorfano M, Farb A, Kolodgie FD, Colombo A. Mechanism of late in-stent restenosis after implantation of a paclitaxel derivate-eluting polymer stent system in humans. *Circulation*. 2002;106:2649–2651.
- Voitenleitner C, Fanning E, Nasheuer HP. Phosphorylation of DNA polymerase alpha-primase by cyclin A-dependent kinases regulates initiation of DNA replication in vitro. *Oncogene*. 1997;14(13):1611-1615.
- Waga S, Hannon GJ, Beach D, Stillman B. The p21 inhibitor of cyclin-dependent kinases controls DNA replication by interaction with PCNA. *Nature*. 1994;369:574-578.
- Wang W, Nacusi L, Sheaff RJ, Liu X. Ubiquitination of p21Cip1/WAF1 by SCFSkp2: substrate requirement and ubiquitination site selection. *Biochemistry*. 2005;44(44):14553-14564.
- Wang Y, Gao W, Svitkin YV, Chen AP, Cheng YC. DCB-3503, a tylophorine analog, inhibits protein synthesis through a novel mechanism. *PLoS One*. 2010;5(7):e11607.
- Webb DJ, Parsons JT, Horwitz AF. Adhesion assembly, disassembly and turnover in migrating cells— over and over and over again. *Nat Cell Biol*. 2002;4:E97–E100.
- Wei L, Shi Q, Bastow KF, Brossi A, Morris-Natschke SL, Nakagawa-Goto K, Wu TS, Pan SL, Teng CM and Lee KH. Antitumor agents 253. Design,

- synthesis, and antitumor evaluation of novel 9-substituted phenanthrene-based tylophorine derivatives as potential anticancer agents. *J Med Chem.* 2007;50:3674-3680.
- Weiss RH, Joo A, Randour C. p21Waf1/Cip1 Is an Assembly Factor Required for Platelet-derived Growth Factor-induced Vascular Smooth Muscle Cell Proliferation. *J Biol Chem.* 2000;275(14):10285–10290.
- Worth NF, Rolfe BE, Song J, Campbell GR. Vascular smooth muscle cell phenotypic modulation in culture is associated with reorganization of contractile and cytoskeletal proteins. *Cell Motil Cytoskel.* 2001;49:130-145.
- Wu CM, Yang CW, Lee YZ, Chuang TH, Wu PL, Chao YS and Lee SJ. Tylophorine arrests carcinoma cells at G1 phase by downregulating cyclin A2 expression. *Biochem Bioph Res Co.* 2009;386,140-145.
- Xiong Y, Hannon GJ, Zhang H, Casso D, Kobayashi R, Beach D. p21 is a universal inhibitor of cyclin kinases. *Nature.* 1993;366:701-704.
- Xiong Y, Zhang H and Beach D. D type cyclins associate with multiple protein kinases and the DNA replication and repair factor PCNA. *Cell.* 1992;71(3):505-514.
- Yamazaki Y, Takani K, Atoda H, Morita T. Snake venom vascular endothelial growth factors (VEGFs) exhibit potent activity through their specific recognition of KDR (VEGF receptor 2). *J Biol Chem.* 2003;278:51985–1988.
- Yang CW, Chen WL, Wu PL, Tseng HY, Lee SJ. Anti-inflammatory mechanisms of phenanthroindolizidine alkaloids. *Mol Pharmacol.* 2006;69(3):749-758.
- Yu H, Jove R. The STATs of cancer--new molecular targets come of age. *Nat Rev Cancer.* 2004;4(2):97-105.
- Yu ZK, Gervais JL, Zhang H. Human CUL-1 associates with the SKP1/SKP2 complex and regulates p21(CIP1/WAF1) and cyclin D proteins. *Proc Natl Acad Sci U S A.* 1998;95(19):11324-11329.
- Zargham R. Preventing restenosis after angioplasty: a multistage approach. *Clin Sci.* 2008;114,3-4:257-264.
- Zhang H, Hannon GH and Beach D. p21-containing cyclin kinases exist in both active and inactive states. *Gene Dev.* 1994;8:1750-1758.

Zhang Z, Wang H, Li M, Agrawal S, Chen X, Zhang R. MDM2 is a negative regulator of p21WAF1/CIP1, independent of p53. J Biol Chem. 2004;279(16):16000-16006.

Zou Y, Ewton DZ, Deng X, Mercer SE, Friedman E. Mirk/dyrk1B kinase destabilizes cyclin D1 by phosphorylation at threonine 288. J Biol Chem. 2004;279(26):27790-27798.

## **7. APPENDIX**



## 7. Appendix

### 7.1. Abbreviations

#### A

Akt Protein kinase B

#### B

BSA Bovine serum albumin

BMS Bare metal stents

#### C

CABG Coronary artery bypass grafting

CDK Cyclin dependent kinase

cDNA Complementary DNA

CKI Cyclin dependent kinase inhibitor

CS Calf serum

CVD Cardiovascular disease

#### D

DCM Dichloromethane

ddH<sub>2</sub>O Double distilled water

DEPC Diethylpyrocarbonate

DES Drug eluting stents

DMEM Dulbecco's modified Eagle's medium

DMSO Dimethyl sulfoxide

DNA Desoxyribonucleic acid

dNTP Deoxyribonucleotide triphosphate

DTT Dithiothreitol

#### E

EC Endothelial cells

ECL Enhanced chemiluminescence

EDTA Ethylenediaminetetraacetic acid

ERK Extracellular signal-regulated kinase

## F

FACS Fluorescence-activated cell sorter

FITC Fluorescein isothiocyanate

FBXO31 F-box only protein 31

FBX4 F-box only protein 4

## G

GFP Green fluorescence protein

GSK-3 $\beta$  Glycogen synthase kinase 3  $\beta$

GPCRs G protein-coupled receptors

## H

HBSS Hank's balanced salt solution

HEPES 2-(4-(2-Hydroxyethyl)-1-piperazinyl)-  
ethansulfonsäure

HUVSMC Human umbilical vein smooth muscle cells

## I

I $\kappa$ B $\alpha$  NF-kappa-B inhibitor alpha

## J

JNK c-Jun N-terminal kinase

## K

kDA kilo Dalton

## L

LDL Low density lipoprotein

## M

MAPK Mitogen activated protein kinase

|               |  |
|---------------|--|
| mc            | Monoclonal                                     |
| MG132         | Z-Leu-Leu-Leu-aldehyde                         |
| mRNA          | Messenger RNA                                  |
| mTOR          | Mammalian target of rapamycin                  |
| <b>N</b>      |  |
| NF $\kappa$ B | Nuclear factor- $\kappa$ B                     |
| <b>P</b>      |  |
| PAA           | Polyacrylamide                                 |
| PBS           | Phosphate buffered saline                      |
| Pc            | Polyclonal                                     |
| PCR           | Polymerase chain reaction                      |
| PDGF          | Platelet-derived growth factor                 |
| PI3K          | Phosphatidylinositol 3-kinase                  |
| PMSF          | Phenylmethylsulphonyl fluoride                 |
| PTCA          | percutaneous transluminal coronary angioplasty |
| PVDF          | Polyvinylidene difluoride                      |
| <b>Q</b>      |  |
| qPCR          | Quantitative real-time PCR                     |
| <b>R</b>      |  |
| RNA           | Ribonucleic acid                               |
| RT            | Reverse transcription                          |
| RTKs          | Receptor tyrosine kinases                      |
| RT-PCR        | Real time PCR                                  |
| <b>S</b>      |  |
| SDS           | Sodium dodecyl sulphate                        |
| SDS-PAGE      | Sodium dodecyl sulphate polyacrylamide gel     |

|          |  |
|----------|--|
|          | electrophoresis                          |
| SMCs     | Smooth muscle cells                      |
| <b>T</b> |  |
| TBS-T    | Tris-buffered saline containing Tween 20 |
| TEMED    | N,N,N',N'-tetramethylethylene diamine    |
| <b>U</b> |  |
| U        | Units                                    |
| <b>V</b> |  |
| VSMC     | Vascular smooth muscle cells             |

## 7.2. Supplementary data

### 7.2.1. Pepscan results

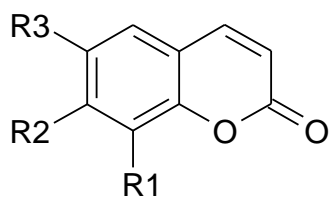
| PROTEIN   | PSITE | Upstream kinase  | Fold activation |
|---|-------|--|-----------------|
| p53   | S9    | ATM +<br>Casein_kinase_1,_alpha_1                        | 43.70           |
| SMAD5   | Y128  | nd   | 3.57            |
| STAT5B  | Y679  | c-Src  | 2.35            |
| Metabotropic<br>glutamate receptor 1                          | T695  | Protein_kinase_C_alpha                                   | 2.09            |
| Erythropoietin<br>receptor                                    | Y368  | Janus_kinase_2   | 2.08            |
| 6-phosphofructo-2-<br>kinase/fructose-2,6-<br>biphosphatase 2 | T475  | Protein_kinase_C_alpha                                   | 1.87            |
| p47-phox  | S348  | Casein_kinase_II,_alpha_2 +<br>Casein_kinase_II,_beta    | 1.78            |
| RGS2  | S46   | Protein_kinase__cGMP-<br>dependent_type_I                | 1.78            |
| SPIB transcription<br>factor                                  | S146  | Casein_kinase_II,_alpha_1 +<br>Casein_kinase_II,_alpha_2 | 1.77            |
| Regulator of G<br>protein signaling 19                        | S151  | ERK2   | 1.72            |
| Synuclein alpha   | Y136  | SYK  | 1.62            |
| Transcription factor<br>IIA, 1                                | S280  | Casein_kinase_II,_alpha_2 +<br>Transcription_factor_IID  | 1.62            |
| Stomatin  | S10   | -  | 1.59            |
| Formyl peptide<br>receptor 1                                  | S328  | G_protein_dependent_receptor_k<br>inase_2                | 1.56            |
| AFX 1   | S196  | AKT1   | 1.56            |

|   |      |  |      |
|---|------|--|------|
| HLA-A   | S359 | Protein_kinase_C_alpha   | 1.55 |
| Polo like kinase  | T210 | -  | 1.55 |
| FAS associated factor 1                                 | S289 | Casein_kinase_II,_alpha_1  | 1.53 |
| CTD phosphatase, subunit 1                              | S575 | Casein_kinase_II,_alpha_2 + Casein_kinase_II,_beta   | 1.48 |
| TBK1  | S172 | -  | 1.45 |
| ERK5  | T218 | -  | 1.42 |
| Protein phosphatase inhibitor 2                         | S87  | Casein_kinase_II,_alpha_1 + Casein_kinase_II,_alpha_2                                      | 1.42 |
| E2F transcription factor 1                              | S403 | Cyclin_dependent_kinase_7 + TFIIH_62_kDa_subunit   | 1.42 |
| ZAP70   | Y319 | ZAP70  | 1.41 |
| Syntrophin alpha 1                                      | S193 | MAPK12   | 1.39 |
| Ribosomal S6 kinase 1                                   | S230 | 3_Phosphoinositide_dependent_protein_kinase_1 + Pyruvate_dehydrogenase_kinase,_isoenzyme_1 | 1.37 |
| Phosphatidylinositol 3-kinase, regulatory gamma subunit | Y341 | -  | 1.35 |
| Eukaryotic translation initiation factor 4E             | S209 | Protein_kinase_C,_beta_1 + Protein_kinase_C,_gamma   | 1.34 |
| p21-activated kinase 7                                  | S573 | p21_activated_kinase_7   | 1.33 |
| LNK   | Y273 | Lck + ZAP70  | 1.33 |
| SHP2  | S591 | Protein_kinase_C,_beta_1 + Protein_kinase_C,_eta   | 1.31 |

**Table 1.** Pepscan results. Depicted are protein and their phosphorylation site (PSITE) as well as the upstream regulatory kinase. The fold activation is demonstrating the upregulation of phosphorylation by tylophorine and PDGF-BB treatment of VSMC compared to DMSO and PDGF-BB treated cells.

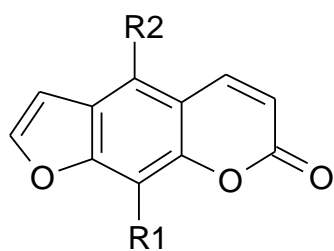
## 7.2.2. Chemical structures of coumarins

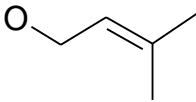
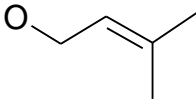
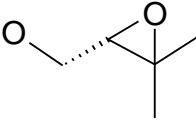
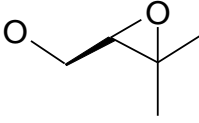
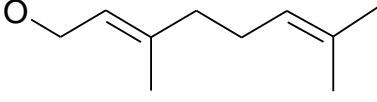
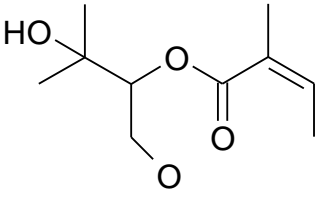
## Simple coumarins



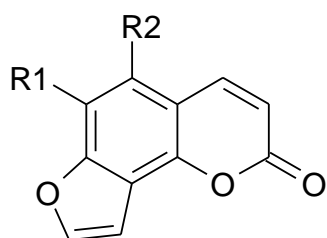
|               | R1 | R2  | R3  |
|---------------|----|-----|-----|
| coumarin      | H  | H   | H   |
| umbelliferone | H  | OH  | H   |
| scopoletin    | H  | OH  | OMe |
| osthole       |    | OMe | H   |
| auraptene     | H  |     | H   |
| ostruthin     | H  | OH  |     |

## Linear furanocoumarins



|                | R1  | R2   |
|----------------|---|--|
| bergaptol      | H   | OH   |
| bergapten      | H   | OMe  |
| isopimpinellin | OMe   | OMe  |
| isoimperatorin | H   |    |
| imperatorin    |  | H  |
| heraclenin     |  | H  |
| oxypeucedanin  | H   |  |
| bergamottin    | H   |  |
| ostruthol      | H   |  |



**Angular furanocoumarins**

|              | R1 | R2  |
|--------------|----|-----|
| isobergapten | H  | OMe |

**Table 3.** Structural classification of all tested coumarins

### 7.3. Publications

Joa H, Vogl S, Atanasov AG, Zehl M, Nakel T, Fakhrudin N, Heiss EH, Picker P, Schmiderer C, Novak J, Franz C, Saukel J Reznicek G, Kopp B and Dirsch VM. Identification of ostruthin from *Peucedanum ostruthium* rhizomes as an inhibitor of vascular smooth muscle cell proliferation. (in submission)

Joa H, Gruzdaitis P, Zeller I, Proksch P, Bernhard D, Atanasov AG, Heiss EH, Dirsch VM. Tylophorine inhibits VSMC proliferation and intimal hyperplasia of venous bypass grafts. (in preparation)

### 7.4. Poster Presentations

Joa H, Heiss E, Atanasov AG, Proksch P, Dirsch VM. Tylophorine inhibits PDGF-induced vascular smooth muscle cell proliferation. 50. Jahrestagung der DGPT, Mainz (Germany), 2009.

Joa H, Heiss E, Atanasov AG, Proksch P, Dirsch VM. Growth factor-induced vascular smooth muscle cell proliferation is inhibited by Tylophorine. 21. Wissenschaftliche Tagung der ÖPhG, Wien, 2009.

Joa H, Heiss E, Atanasov AG, Proksch P, Dirsch VM. Vascular smooth muscle cell proliferation is inhibited by tylophorine by down regulation of Cyclin D1. 51st Annual Meeting of the Deutsche-Gesellschaft-für-Experimentelle-und-Klinische-Pharmakologie-und-Toxikologie. Mainz (Germany), 2010.

## 7.5. Curriculum Vitae

### Personal information

|                         |   |
|-------------------------|---|
| Present address         | Romanogasse 29/3/2<br>1200 Vienna<br>Austria      |
| Date and place of birth | November 7th, 1980<br>Bad Neustadt/Saale, Germany |
| Nationality             | German  |

### Education

|                          |  |
|--------------------------|--|
| February 2008 – present  | Doctoral thesis at the Department of<br>Pharmacognosy, University of Vienna                  |
| May 2007                 | Graduation (Diplom in Biology)   |
| August 2006 – May 2007   | Diploma thesis at the Institute of<br>Pharmacology and Toxicology,<br>University of Würzburg |
| October 2001 – June 2006 | Study of Biology with focus on<br>Pharmaceutical Biology,<br>Pharmacology and Neurobiology   |

## 7.6. Acknowledgements/Danksagung

Vielen Dank an meine Betreuerin Prof. Verena Dirsch die mir die Chance gegeben hat, meine Doktorarbeit in Ihrer Gruppe durchzuführen und mit wertvollen Ratschlägen für das Gelingen der Arbeit beigetragen hat. Außerdem möchte ich mich dafür bedanken, dass Sie sich trotz Ihres engen Terminplanes sehr viel Zeit für unsere Besprechungen genommen hat.

Ein weiterer Dank gilt Prof. Peter Proksch aus Düsseldorf für die Bereitstellung von Tylophorine, sowie PD David Bernhard vom AKH für die Kooperation bei der Durchführung der Organkulturen.

Weiterhin danke ich Dr. Elke Heiss, die mich in den letzten Jahren mit praktischen Tipps, Korrekturen und Ratschlägen aller Art unterstützt hat.

Bei Dr. Atanas Atanasov bedanke ich mich für seine Unterstützung und Hilfe, aber auch ganz besonders für den wertvollen Beistand bei der Erweiterung des cineastischen Horizonts.

Auch möchte ich den Ehemaligen unserer Arbeitsgruppe danken. Dazu gehören Andrea Schwaiberger, Christoph Schmitt, Cornelia Schreiner, Mario Kumerz, Irene Sroka und Renate Baumgartner. Besonderer Dank gilt hierbei Irene, die mir in meinen Anfangstagen die wichtigsten Zellkulturtechniken näher brachte. Außerdem danke ich Conny, mit der ich lange Zeit das Büro teilen durfte und wir immer erfrischende Gespräche führten.

Hortenzia Beres, Daniel Schachner, Elisabeth Geiger und Judith Benedic möchte ich für Ihre Unterstützung im Laboralltag Dank sagen.

Andrea Szabo und Martin Groiss gilt der Dank für die Zusammenarbeit bei der Bewältigung bürokratischer Papierwelten.

Angela Ladurner, Tina Oberan, Matthias Kramer und Nanang Fakhrudin danke ich herzlich für die netten Tipps, interessanten Gespräche und schönen Teestunden. Auch allen anderen die daran beteiligt waren, ein herzliches Dankeschön. Es wäre alleine doch langweilig gewesen. Einen besonderen Dank noch an Angela und Tina die in den letzten Monaten immer wieder ein offenes Ohr für Fragen aller Art hatten.

Bei Oliver Donath bedanke ich mich für den Beistand bei der Durchführung wissenschaftlich grundlegender und dennoch schmackhafter Nebenprojekte.

Ich möchte auch ganz herzlich meiner Masterandin Päivi Gruzdaitis, dem Diplomanden Thomas Nakel, Iris Zeller vom AKH, sowie Sylvia Vogl aus der Nachbarspange danken, die experimentell zu dieser Arbeit beigetragen haben.

Natürlich möchte ich mich auch bei allen anderen Kollegen des Departments bedanken, mit denen ich Seminare oder Journal clubs verbringen durfte.

Außerdem danke ich meinen Eltern, die den Grundstein für meinen Weg gelegt haben und mich immer unterstützten solange sie konnten. Es ist sehr schade und traurig, dass Ihr dieses glückliche Ende der Arbeit nicht mehr erleben dürft.

Meinen Schwestern danke ich dafür, dass ich bei Ihnen nette Tage und Urlaube verbringen durfte um mich vom Laboralltag zu erholen.

Zu guter letzt möchte ich Dr. Franziska Walter von ganzem Herzen für die liebevolle Unterstützung und den Beistand in den letzten Jahren danken.